Elucidating the potential of IgA antibodies for cancer immunotherapy

Inaugural-Dissertation

to obtain the academic degree

Doctor rerum naturalium (Dr. rer. nat.)

submitted to the Department of Biology, Chemistry and Pharmacy

of Freie Universität Berlin

by

Felix Andreas Wolfgang Hart

from Kassel, Germany

Berlin 2016

The dissertation was prepared between September 2011 and April 2016 in the laboratories of the Research and Development department (Director Dr. Antje Danielczyk) of Glycotope GmbH in Berlin.

1. Reviewer Prof. Dr. Oliver Daumke
2. Reviewer Prof. Dr. Stephan Hinderlich

Date of disputation 27th June 2016

Acknowledgements

I would like to thank Dr. Steffen Goletz for the opportunity to work on my project at Glycotope GmbH in Berlin. It was a great experience to work in many different laboratories within the lifecycle of the project. I would like to acknowledge Dr. Antje Danielczyk for great supervision and numerous discussions about the project. Moreover, I thank Dr. Renate Stahn for asking many constructive questions.

Next, I would like to thank Prof. Dr. Oliver Daumke for being supervisor and first reviewer of my dissertation. Moreover, I thank Prof. Dr. Stephan Hinderlich not only for being second reviewer but also for introducing me to Glycotope.

I would like to thank all colleagues at Glycotope for their help, inspiring working environment and great atmosphere in and outside of the laboratories. A special thanks to the groups “Platform Development and Lead Discovery” and “Clone Development” for helping me to initiate the project. Also, I would like to thank my colleagues from the group “DSP Antibodies” for integrating me in their meetings and work space. I also thank the groups “USP Development” and “PTM Analytics” for collaborations on the IgA project. Moreover, I thank the groups “Bioassays and Preclinical Studies” and “DSP Glycoproteins” for their help, hosting me in their laboratories and constant feedback on my project.

Finally I thank my family and friends for all their support!

Table of Contents

1 Introduction

The human immune system has to face multiple pathological conditions like injuries, pathogen invasion or cancer. In ancient Egypt, the first scientific documentation of human disease and injuries including suggestions for their treatment was prepared. The Edwin Smith Surgical Papyrus dates back to 3000 BC to 2500 BC and probably includes the first documentation of tumors (Breasted 1930). Hippocrates later introduced the terms cancer and carcinoma for ulcerated malignant tumors and malignant tumors, respectively (Hajdu 2011, Vagelpohl 2014). The cellular origin of cancer was demonstrated by Rudolf Virchow (Virchow 1863). In 1911, Peyton Rous discovered that viral infections can lead to avian cancer and in 1914 Theodor Boveri proposed that mutations in chromosomes could cause cancer (Rous 1911; Boveri 1914; DeVita & Rosenberg 2012). The fatal outcome when distant organs are affected by the disease was described by Aulus Celsus (Celsus & Spencer 1935). The central dogma of biology – from deoxyribonucleic acid (DNA) to ribonucleic acid (RNA) to protein synthesis – was based on findings revealing that information is transmitted by DNA and not proteins, solving the structure of DNA and deciphering the genetic code (Avery 1944; Franklin & Gosling 1953; Watson & Crick 1953; Wilkins et al. 1953; Nirenberg & Matthaei 1961). Understanding these fundamental biological processes facilitated the study of human diseases and allowed detailed insight into cellular processes on a molecular level. The discovery of restriction enzymes in 1970 (Smith & Welcox 1970) provided a technique to prove that genes encoding immunoglobulins are rearranged within certain cells and hence explain how the immune system builds its large repertoire of molecules with different specificities. These molecules are known as antibodies and enable the human body to combat multifaceted pathological conditions (Murphy 2011).

1.1 The human immune system and immunoglobulin A antibodies

1.1.1 Innate and adaptive immunity – from rapid responses to flexibility and memory

The human body constantly needs to keep a fragile balance between recognizing, excluding and eliminating pathogens while sparing normal and healthy tissue. The immune system is responsible for keeping this balance and comprises two mayor parts, the innate and adaptive immune system (Murphy 2011). The innate immune system reacts fast and recognizes

conserved pathogen-associated molecular patterns (PAMP). It includes epithelial cell barriers as well as cellular and non-cellular components. Innate immunity is mediated by dendritic cells, monocytes, macrophages, granulocytes and natural killer (NK) cells. The complement cascade is a major non-cellular component which recognizes pathogens and mediates their destruction. In contrast, the adaptive immune system takes its time to react and depends on signals of the innate immune system. However, within hours or days it yields highly specific responses which can result in lifelong protection through memory mechanisms. The major components of adaptive immunity are B and T lymphocytes (B and T cells), which are characterized by the surface expression of molecules with specificity to one antigen. In case of T cells, the T cell receptor (TCR) can bind to antigens derived from proteolytic digestion of larger structures that are presented on the surface of other cells. The B cell receptor (BCR) is composed of a surface-bound antibody which is responsible for specific antigen binding and a heterodimer composed of disulfide-linked Igα and Igβ which is responsible for signal transduction upon antigen binding. The signal transduction results in B cell activation which in turn starts to proliferate and terminally differentiates into antibody secreting plasma cells. During B cell activation and proliferation, somatic hypermutation results in the production of affinity matured antibodies (Reth 1992; Murphy 2011). While mature naïve B cells express IgM and IgD antibodies on their surface, upon differentiation into plasma cells other classes of antibodies with the same specificity as their preceding counterpart can be secreted as well. During a process known as class switch recombination, gene segments are exchanged resulting in the production of IgG, IgA or IgE antibodies. All antibodies can be either expressed bound to the membrane or as secretory version by alternative RNA splicing. In terminally differentiated plasma cells, most of the antibody is produced as secretory form. A subset of activated T and B cells does not differentiate into effector and plasma cells, respectively, but instead into long-lived memory cells. These cells reside in the body and can be activated upon additional challenge with an antigen resulting in long-time memory against an antigen of a pathogen. Memory T and B cells thereby ensure fast responses upon additional encounter with a pathogen (Murphy 2011).

Some of the cellular components of the innate immunity can be involved in adaptive immune responses through the participation of antibodies. They express receptors specific for the part of the antibody which is not involved in antigen binding. Crosslinking of these receptors by antibody-opsonized pathogens can result in multiple effector functions against pathogens. Class switch recombination increases the functional diversity of antibodies by utilizing different constant, non-antigen binding regions. These regions bind to different receptors on

effector cells which can elicit different functionalities (Ravetch 1997; Clark & Kupper 2005; Murphy 2011).

1.1.2 Structure of IgA in comparison to IgG antibodies

Immunoglobulin (Ig) A is the predominant immunoglobulin in mucosal secretions, where it serves as first line of defense and protects against pathogens that are ingested or inhaled (Woof & Kerr 2004; Kerr 1990). In human serum, IgA is the second most prevalent antibody, with a comparable rate of synthesis like IgG. However, due to faster catabolism, the serum concentration of IgA (0.6-3.8 mg/mL) is smaller than of IgG (6-14 mg/mL). Serum IgA is mainly monomeric, while secretory IgA (SIgA) is dimeric and can be associated with additional polypeptides, the joining (J) chain and secretory component (SC) (Murphy 2011; Woof & Kerr 2006; Kerr 1990; Brandtzaeg & Prydz 1984; Tomasi et al. 1965). Per day an adult produces about 66 mg IgA antibodies per kilogram, which is more than all other isotypes combined (Monteiro & Van De Winkel 2003).

Structurally, antibody monomer units consist of two fragment antigen binding (Fab) domains including the variable antigen binding part and the constant fragment crystallizable (Fc) domain, which binds to different receptors including those of immune effector cells and other components of the immune system (Figure 1). The variable domain contains hypervariable complementarity-determining regions (CDRs), which determines the specificity of an antibody to its target. The CDRs lie within four framework regions, which are human for humanized or human antibodies. Mouse-human chimeric antibodies derived from immunized animals contain human constant domains and their variable domain, including the framework regions, are murine (Murphy 2011).

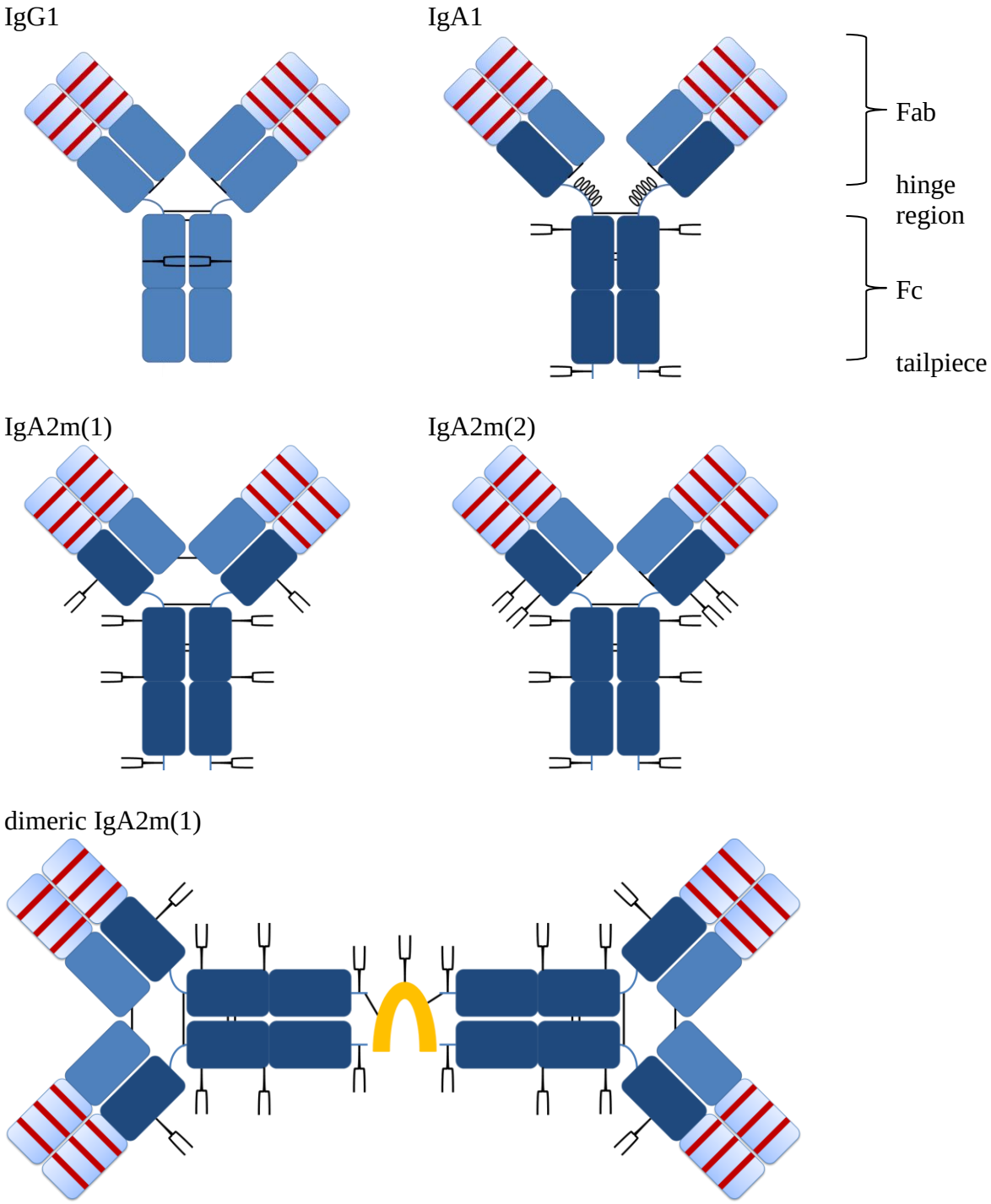

Figure 1 Schematic illustration of IgG1 and IgA antibodies. IgG Cγ and common Cκ light chain domains (both blue) and IgA Cα domains (dark blue) are indicated. Variable domains (light blue) including complementary-determining regions (CDRs, red bars) of heavy and light chains are indicated. N-glycosylation sites (*Y*) with their different orientation towards the inside or outside of the molecules are indicated for IgG or IgA, respectively. Antibodies might possess N-glycosylation sites within their variable domain which is not shown here. The tailpiece for IgA antibodies is shown which is not present for IgG antibodies. Inter-chain disulfide bonds (black lines) of heavy and light chains are indicated and differ between isotypes and allotypes. For IgA1, O-glycosylation sites (*0*) within the extended hinge region are shown. IgA2m(1) forms disulfide bonds between the two light chains. Dimeric IgA2m(1) including inter-chain disulfide bonds between the J chain (orange) and two IgA monomer units is shown. The J chain stabilizes IgA dimers but other interactions between IgA monomer units (not shown) can result in the formation of dimers lacking the J chain. Adopted from Woof and Burton (Woof & Burton 2004).

Like IgG, IgA monomers consist of two light chains (LC, kappa or lambda) and two heavy chains (HC). The alpha HC contains a variable region (VH) and three constant regions, Cα1, Cα2 and Cα3. In humans there are two alpha HC genes, encoding IgA1 or IgA2 subclasses (Kerr 1990; Woof & Russell 2011). Both, IgA1 and IgA2 HC contain an 18 amino acid C-terminal tailpiece with penultimate Cys residue, which is found on IgM antibodies as well. There is one allotype for IgA1, whereas three allotypes for IgA2 were described: IgA2m(1), IgA2m(2) and IgA2(n) (Rifai et al. 2000; Chintalacharuvu et al. 1994). Of note, IgA2m(1) lacks disulfide bonds between HCs and LCs which is found in other isotypes, instead the two LCs are linked by disulfide bonds and HC-LC interactions are non-covalent (Woof & Kerr 2006). IgA1 possesses a 23 amino acid hinge region, while the hinge region of IgA2 is 10 amino acids in length. The extended hinge region is rich in proline, serine and threonine and carries two to five, in some cases up to six, O-glycosylations (Novak et al. 2001; Pouria et al. 2004). The most favored O-glycosylation sites are: Thr228, Ser230, Ser323 (Mattu et al. 1998). Each O-glycosylation at a serine or threonine in the hinge region can be composed of N-acetylgalactosamine, galactose and sialic acid in a heterogenic mixture (Woof & Russell 2011; Pouria et al. 2004; Allen et al. 1999). The extended T-shape structure of IgA1, compared to the Y-shape of other Igs like IgG1 or IgA2 (IgA2 can be present in a compact T-shape as well), could be caused by the O-glycosylated extended hinge region and allow IgA1 to reach more distant antigens simultaneously (Boehm et al. 1999; Furtado et al. 2004; Van Egmond et al. 2001; Woof & Kerr 2006). A potential role of the hinge glycans towards a more rigid conformation was proposed and investigated with synthetic peptides (Narimatsu et al. 2010). The expression of proteases which target the IgA1 hinge region has been linked to bacterial pathogenicity (Van Egmond et al. 2001; Monteiro & Van De Winkel 2003). Apart from the O-glycosylation, IgA1 has two N-glycosylation sites: Asn263 in Cα2 and Asn459 in the tailpiece at the C terminus. For IgA2m(1) there are two additional N-glycosylation sites, Asn166 in Cα1 and Asn337 in Cα2. Asn211 is a fifth N-glycosylation site present in Cα1 of IgA2m(2). Most of the N-glycans are biantennary complex-type structures with a minority of triantennary and tetraantennary glycans as well as oligomannose structures (Woof & Russell 2011; Arnold et al. 2007). For recombinant IgA1, N-glycosylation sites for Cα2 and tailpiece possess mainly biantennary and triantennary glycans, respectively (Field et al. 1994; Mattu et al. 1998). In contrast to IgG1 where glycans are orientated towards the inside between the two Cγ2 domains, molecular modeling for IgA1 revealed a glycan orientation towards the outside of the molecule (Mattu et al. 1998). Compared to IgG, IgA glycosylation is characterized by more complete processing, potentially because of better accessibility of the glycans for

glycosyltransferases within the Golgi. The degree of sialylation is much higher for IgA than for IgG, 90% and 10%, respectively (Mattu et al. 1998). A putative role of IgA glycosylations is protection against self-aggregation (Hiki et al. 1999).

Investigations of secretory IgA1 and IgA2 (association of IgA dimers with J chain and SC) revealed less processed glycan structures containing terminal GlcNAc and mannose, which differ from serum IgA glycans. These structures might serve as binding epitopes for pathogens and thereby secretory IgA (SIgA) possibly links innate and adaptive immunity by glycan epitope-mediated and specific Fab binding, respectively (Royle et al. 2003). Moreover, the J chain and SC possesses N-glycosylations that could serve as binding sites for bacterial adhesins and lectins (Royle et al. 2003; Brandtzaeg 2009).

Differences in glycosylation of serum and secretory IgA could be caused by differing glycosidase and glycosyltransferase expression profiles of serum IgA producing plasma cells in the bone marrow, spleen or liver as compared to local dimeric IgA producing plasma cells at mucosal sites (Royle et al. 2003). Different clearance mechanisms in the serum and at mucosal sites could also be responsible for the accumulation of specific glycosylated IgA antibodies.

For IgG antibodies, the Fc glycosylation is important for effective Fc gamma receptor (FcγR) binding and biofunctionality, affinity to FcγRs is decreased by deglycosylation as well as alterations in the glycan structures (Jefferis 2009; Ferrara et al. 2011; Umaña et al. 1999). In case of IgA, deletion of glycosylation motifs in the Cα2 and tailpiece region of recombinant IgA1 had no effect on binding to its main receptor, FcαRI (Chapter 1.1.4) (Mattu et al. 1998).

While IgG antibodies are only present as monomers, IgA antibodies can form dimers and higher order polymers by themselves or in complex with additional components. Mucosal plasma cells co-express the J chain, a 15 kDa polypeptide which associates with IgA dimers. A disulfide bridge is formed between J chain and Cys residues of each IgA antibody. The J chain has one N-glycosylation site and contains three intra-chain disulfide bonds. Two additional disulfide bonds are formed between the J chain and two IgA monomer units within the tailpiece (Figure 1). The same polypeptide associates with pentameric IgM antibodies. A second polypeptide associates with SIgA, the SC is about 80 kDa in size and the extracellular part of the polymeric Immunoglobulin receptor (pIgR) (Chapter 1.1.3). During epithelial cell transcytosis mediated by the pIgR, the SC is cleaved off at the apical site to release SIgA, which consist of two IgA monomers, one J chain and one SC (Van Egmond et al. 2001; Woof & Kerr 2006).

1.1.3 Production sites of IgA antibodies and transcytosis of secretory IgA

In humans, serum and secreted mucosal IgA antibodies can be distinguished. They differ in several characteristics and their production sites. In human serum, IgA1 is more prevalent than IgA2 with concentrations of about 3 mg/mL and 0.5 mg/mL, respectively. The majority of serum IgA is monomeric (about 90%). Like IgG antibodies, serum IgA is produced in the bone marrow and peripheral lymphoid organs (Monteiro & Van De Winkel 2003; Woof & Kerr 2006; Murphy 2011).

In mucosal tissue, dimeric, J chain-containing IgA antibodies are produced by local plasma cells and transported by epithelial cells from the basolateral to the apical site. IgA-producing plasma cells mainly derive form mucosa-associated lymphoid tissue. In contrast to other secretory sites, the migration of activated B cells form the gut-associated lymphoid tissue (GALT), to lamina propria (LP) is well defined. Within GALT, IgA class switch takes place in germinal centers (GCs) (Brandtzaeg & Johansen 2005; Sutherland & Fagarasan 2012). In the human LP, 80% to 90% of B cells produce polymeric IgA. Precursor IgA-producing cells are primed in Peyer's patches (PPs) and mesenteric lymph nodes (MLNs) before they home into the LP. Through another route, primed B cells can also migrate directly from solitary lymphoid follicles to the LP. Solitary lymphoid follicles together with PPs constitute GALT, where GCs are formed after antigen stimulation. Several cytokines are presumed to promote B cell differentiation into IgA producing cells. Interleukin-10 (IL-10) and transforming growth factor-β (TGF-β) play a central role in this process (Brandtzaeg et al. 2001; Brandtzaeg & Johansen 2005; Pabst 2012).

After antigen sampling by microfold (M) cells in PPs, the production of IgA can be induced T cell-dependent or -independent. Dendritic cells (DCs) take up antigens and then activate naïve T cells into effector T cells, which in turn activate B cells in GCs, promote their class switch recombination (CSR) and differentiation in IgA-producing plasma cells. In solitary lymphoid follicles, DCs activate B cells directly and promote, with the support of stromal cells, the differentiation in IgA-producing cells in GCs. In the LP, a local class switch from IgM- to IgA-producing B cells as well as the switch from IgA1 to IgA2 expression has been described as well (Pabst 2012).

In 1965, first evidence was found that serum and secretory IgA differ in size and a specific mechanism for the transport of polymeric non-serum IgA through the epithelial barrier into mucosal sites was proposed (Tomasi et al. 1965). This mechanism is called transcytosis and was shown to be mediated by the polymeric immunoglobulin receptor (pIgR) which is

expressed by epithelial cells and mediates transcytosis of IgM antibodies as well (Brandtzaeg & Prydz 1984; Johansen & Kaetzel 2011). The pIgR consist of five Ig-like domains on the extracellular site, a single-spanning transmembrane domain and a cytoplasmatic C-terminal domain of 103 amino acids (Mostov 1994). A mechanism similar to antibody-antigen binding was proposed for the fifth Ig-like domain, which is important for IgA-binding (Coyne et al. 1994). On dimeric IgA, the binding site for pIgR is located in the Cα3 domains and dimerization is probably necessary for higher binding affinity and successful transcytosis. The role of the J chain in pIgR binding remains to be elucidated (Hexham et al. 1999). The SC is the IgA-binding domain of the pIgR and consists of the five Ig-like domains. Upon release on the apical site, the SC bound to dimeric IgA is cleaved off from the receptor to release SIgA into mucosal tissue (Van Egmond et al. 2001; Woof & Kerr 2006). The SC protects SIgA from degradation by proteases and containes pathogen binding sites (Royle et al. 2003). The abundance of IgA1 and IgA2 differs between mucosal sites. While IgA2 is more prevalent in the colon, in other secretory sites IgA1 is mainly found. Comparable amounts of both isotypes are present in the small intestine (Brandtzaeg & Johansen 2005; Pabst 2012).

1.1.4 Fc alpha receptor I – activator and inhibitor of cellular responses

The major receptor binding IgA is Fc alpha receptor I (FcαRI), which is also called cluster of differentiation (CD) 89. It is expressed on neutrophils, eosinophils, monocytes, macrophages, intestinal dendritic cells and Kupffer cells (Monteiro & Van De Winkel 2003). Due to differences in glycosylation, the size of FcαRI varies between 55 kDa and 100 kDa (Van Egmond et al. 2001). On the extracellular site, it possesses two 206-amino acids Ig-like domains (EC1 and EC2), of which N-terminal EC1 binds IgA within the Cα2/Cα3 boundary (Figure 2). In contrast, FcγRs bind IgG within the Cγ2 domain in close proximity to the hinge region with their membrane-proximate extracellular Ig-like domain (EC2). The differences in structural binding orientation might allow a stoichiometry for FcαRI and IgA binding of 2:1 as compared to a 1:1 stoichiometry for FcγRIII and IgG (Herr, White, et al. 2003; Herr, Ballister, et al. 2003; Woof & Burton 2004). On the IgA HC, three Leu residues in the Cα2 and 16 residues in Cα3 are involved in FcαRI binding (Bakema & van Egmond 2011). FcαRI contains a transmembrane region and a cytoplasmatic tail with 19 and 41 amino acids in length, respectively (Morton & Brandtzaeg 2001; Pleass et al. 1999; Bakema & van Egmond 2011). Six potential N-glycosylation sites and at least one O-glycosylation site have been described for FcαRI (Monteiro et al. 1990; Monteiro et al. 1992; Morton & Brandtzaeg 2001).

Deglycosylation of Asn58 increased the binding of FcαRI to IgA, while deglycosylation of the other N-glycosylation sites (Asn44, Asn120, Asn156, Asn165 and Asn177) had no effect. Interestingly, sialylated glycans of Asn58 hindered binding to IgA, neuraminidase treatment resulted in increased binding (Xue et al. 2010).

The signal transduction of FcαRI is mediated by the common FcR γ chain, which is also involved in signal transduction of IgG receptors (FcγRs). Upon IgA-mediated crosslinking of FcαRI, intracellular immunoreceptor tyrosine-based activation motif (ITAM)-dependent signals are initiated, which result in phosphorylation of different kinases and activation of inflammatory responses (Figure 2). FcαRI interacts with common FcR γ chain homodimers containing ITAMs, which subsequently become phosphorylated and promote signaling events (Woof 2002). For the association with the FcR γ chain homodimers the transmembrane domain of FcαRI is important. Their interaction is stabilized by positively and negatively charged amino acids in the transmembrane domain and the FcR γ chain, respectively. ITAMs become phosphorylated by Src kinase Lyn and subsequently recruit B lymphocyte kinase (Blk), Syk, phospholipase (PLC)-γ, Shc and growth factor receptor-bound protein 2 (Grb2). Depending on the effector cell, this activation can lead to multiple cellular functionalities including antibody-dependent cellular phagocytosis (ADCP), antibody-dependent cellular cytotoxicity (ADCC), respiratory burst, degranulation, cytokine release and antigen-presentation (Chapter 1.2.1) (Van Egmond et al. 2001; Bakema & van Egmond 2011).

However, upon monovalent binding (e.g. by serum IgA, which is not present as immune complex), the ITAMs of FcR γ chains can also mediate inhibitory signals through FcαRI, called inhibitory ITAM (ITAMi) (Monteiro & Van De Winkel 2003; Ben Mkaddem et al. 2013). Therefore, FcαRI-FcR γ chains complexes associate with inhibitory Src homology 2 (SH2) domain-containing phosphatase-1 (SHP-1), which results in partial phosphorylation of the ITAMs (Figure 2). Other activating receptors co-locate within lipid rafts with the FcαRI-FcR γ chains ITAMi complex, resulting in internalization and formation of so called inhibisomes. Therefore, this IgA receptor can circumvent excessive immune responses by inhibiting other activating receptors (Pfirsch-Maisonnas et al. 2011; Ivashkiv 2011).

Thus, the main IgA receptor FcαRI is capable to mediate activating as well as inhibitory signals depending on immune complex-mediated crosslinking or monovalent binding, respectively (Figure 2).

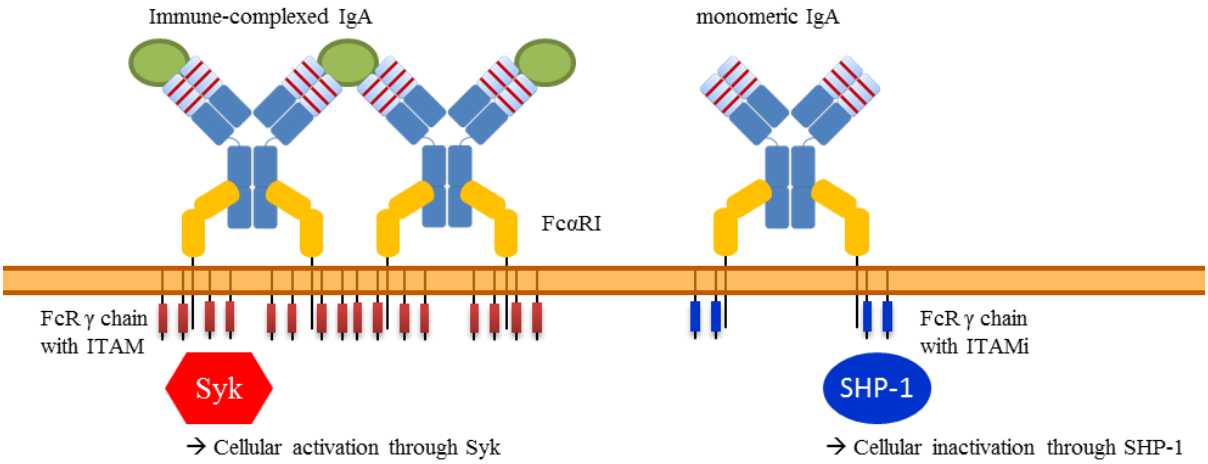

Figure 2 Intracellular signaling of FcαRI upon immune-complexed or monovalent IgA binding. The boundary of IgA Cα2 and Cα3 domains is involved in FcαRI binding. In contrast to FcγRs extracellular domain (EC) 2 domains binding IgG antibodies, the N-terminal domain EC1 of the two extracellular domains of FcαRI binds IgA antibodies. Moreover, binding stoichiometry is 2:1 for FcαRI:IgA as compared to 1:1 for FcγRs:IgG. **(a)** In case of IgA immune complexes, crosslinking of multiple receptors results in cellular activation and thereby causes inflammatory responses. Signal transduction is mediated by phosphorylated immunoreceptor tyrosine-based activation motifs (ITAM, indicated in red) of the common Fc receptor γ chain and Syk. **(b)** Upon monovalent binding of IgA antibodies cellular inactivation is mediated by partially phosphorylated inhibitory ITAM (ITAMi, indicated in blue) of the common Fc receptor γ chain and the phosphatase SHP-1. Adopted from Bakema and van Egmond (Bakema & van Egmond 2011).

Different isoforms of FcαRI have been described, for example FcαRIb can be expressed soluble or membrane attached on granulocytes and is reduced in size. It is incapable to interact with FcR γ chains and does not induce intracellular signaling (van Dijk et al. 1996; Bakema & van Egmond 2011). Shedding of FcαRI can be induced by IgA binding to monocytic cell lines (van Zandbergen et al. 1999). Soluble as well as membrane-bound FcαRIb could regulate inflammatory responses of IgA antibodies because they compete with full-length FcαRI for antibody binding. The *FCAR* gene encodes the FcαRI and several single-nucleotide polymorphisms (SNPs) in untranslated or translated regions have been described (Narita et al. 2001; Woof & Kerr 2006; Bakema & van Egmond 2011). Base exchange from AGC (Ser) to GGC (Gly) in codon 248 results in a functional change of FcαRI-mediated signaling. S248G exchange enhances responses to IgA binding and results in increased cytokine release. This phenotypic change might have implications for autoimmune diseases (Wu et al. 2007; Bournazos et al. 2009).

1.1.5 Other IgA-binding receptors

Apart from FcαRI and pIgR, other receptors have been identified that bind IgA antibodies (Bakema & van Egmond 2011).

The Fcα/μR is a 70 kDa type I transmembrane glycoprotein expressed on mature B lymphocytes and macrophages, which binds IgA and IgM antibodies. Expression of Fcα/μR was also shown on secondary lymphoid tissues. Binding of either IgM or IgA inhibits the binding of the other isotype to Fcα/μR. It mediates phagocytosis of IgM-coated bacteria, which might indicate its role in early immune responses (Shibuya et al. 2000; Sakamoto et al. 2001). Binding to this receptor requires polymerization of IgM and IgA. The regions important for binding are Cμ3/Cμ4 and Cα3 for IgM and IgA, respectively (Ghumra et al. 2009). While it seems to play a role in immune responses, the exact function of Fcα/μR is not known yet (Woof & Russell 2011).

In the liver, asialoglycoprotein receptor (ASGP-R) is expressed on hepatocytes. ASGP-R binds to desialylated glycoproteins possessing terminal galactose residues. It is important for the maintenance of homeostasis through the regulation of IgA catabolism (Monteiro & Van De Winkel 2003). The role of IgA1 O-glycosylation or IgA1 and IgA2 N-glycosylation in the binding of ASGP-R is controversial. While in an earlier study IgA1, but not IgA2 binding to ASGP-R was shown, Rifai et al. found that IgA2 is more rapidly cleared in a galactose-dependent manner (Stockert et al. 1982; Rifai et al. 2000). Deletion of the IgA1 hinge region, including its O-glycosylation sites, resulted in increased clearance and indicates that O-glycosylations are no binding sites for ASGP-R. IgA2 possesses at least two additional N-glycosylation sites compared to IgA1, which could be binding sites for ASGP-R when being desialylated and therefore explain the faster clearance of IgA2. Binding to ASGP-R could be reduced by over-sialylation of IgA (Basset et al. 1999). Apart from ASGP-R-dependent clearance, other routes for IgA elimination must be present. The faster clearance of IgA2 compared to IgA1 might be an explanation for lower serum levels of IgA2 (Rifai et al. 2000).

The transferrin receptor (TfR), which is also known as CD71, selectively binds IgA1 which was shown for T cells and cultured renal mesangial cells (Monteiro & Van De Winkel 2003). The IgA1-TfR interaction can be inhibited by transferrin and binding of IgA1 to T cells depends on their proliferation and is mediated by TfR (Moura et al. 2001). O-glycosylation-dependent binding of IgA1 to T cells might be related to the TfR (Rudd et al. 1994; Swenson et al. 1998; Monteiro & Van De Winkel 2003).

Other receptors for IgA are not as well described. For example the secretory component receptor (SCR) binds SIgA but not serum IgA. SCR is 15 kDa in size and expressed on eosinophils. Upon crosslinking of SCR, eosinophils are activated and release eosinophil cationic protein and eosinophil peroxidase. This mechanism might play a role in immune responses at secretory sites (Lamkhioued et al. 1995). M cells within PP sample antigens from the luminal site for delivery in GALT. A receptor for binding IgA2 or hinge-deleted IgA1 was found in mice. The presence of IgA on the apical site of human M cells suggests the presence of a human homologue. The binding site within IgA is located at Cα1 and Cα2, which might explain why only hinge-deleted IgA1 is capable of binding to this receptor (Mantis et al. 2002).

1.1.6 Biological function of IgA antibodies

The detailed biological role of IgA antibodies exceeding mucosal defense remains to be elucidated. In mucosal vaccination settings for influenza viruses, rotavirus, poliovirus, *Salmonella* or Cholera, the mechanism of protection often includes IgA responses (Lycke 2012). While IgA deficiency is related to an increased risk for diseases like allergy, autoimmunity and infections, it normally does not result in serious pathologies. In IgA deficiency, elevated levels of antibodies of other isotypes indicate a compensation of IgA functionalities (Van Egmond et al. 2001).

The best known biological functions of IgA antibodies relates to secretory IgA (SIgA) which serves as fist line of defense (Woof & Kerr 2004; Van Egmond et al. 2001) (Figure 3). At mucosal sites SIgA protects epithelial cells from bacterial invasion by agglutination and hindering host-pathogen interactions, a process called immune exclusion. Bacterial products are neutralized in the luminal site by SIgA antibodies. Due to the hydrophilic nature of SIgA, IgA-coated bacteria are prevented from mucosal surface binding. Glycans on IgA, J chain and SC as well as their amino acid sequences are responsible for the hydrophilic nature. Another function of SIgA is the transport of basolateral antigens in the lumen by transcytosis (Chapter 1.1.3). In epithelial cells, IgA can bind viruses or virus antigens intracellularly and thereby protect form viral infections (Van Egmond et al. 2001).

Additional functions within mucosal surfaces have been described. Retro-transport of luminal antigens across the epithelial barrier to GALT residing DC is mediated by IgA antibodies (Favre et al. 2005). Moreover, the homeostasis within mucosal sites might be attributed to the help of SIgA. Under homeostatic conditions, retro-transport of IgA-antigen complexes to DCs

presumably results in the suppression of inflammatory response and thus prevents pathogen-induced excessive inflammatory responses. Also, IgA antibodies were described to facilitate the retention of non-pathogenic bacteria within biofilms that line epithelial surfaces (Mantis et al. 2011). Together, these IgA-mediated functions do not trigger inflammation, rendering them as non-inflammatory biological functions.

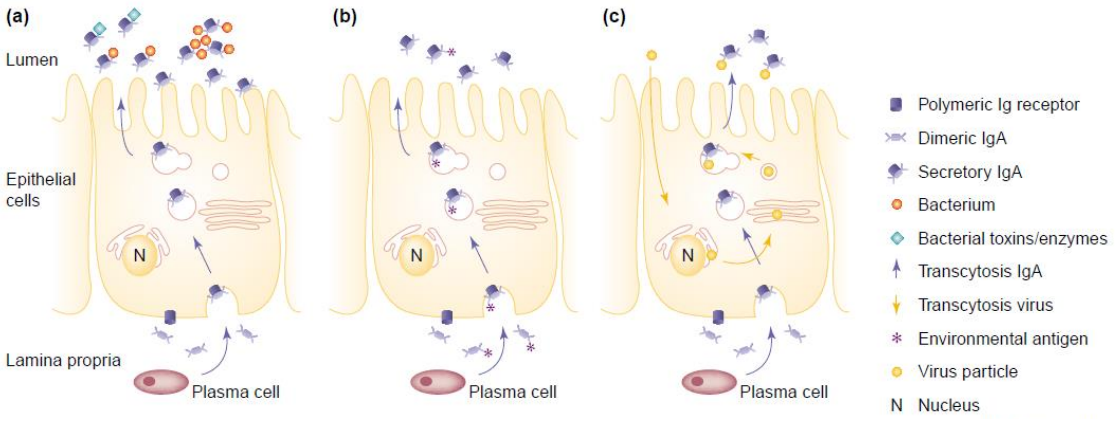

Figure 3 Non-inflammatory biological functions of secretory IgA (SIgA) at mucosal sites. In the lamina propria (LP), dimeric IgA is produced by local plasma cells. **(a)** After transcytosis SIgA is released on the luminal site where it inactivates bacteria or bacterial toxins and prevents epithelial penetration. This process is referred to as immune exclusion. **(b)** In the LP, dimeric IgA can mediate the cleaning of antigens. After antigen binding, dimeric IgA-antigen complexes can be transported to the luminal site through transcytosis. **(c)** In virus infected epithelial cells, transported IgA can inactivate viruses and mediate luminal release or prevent virus assembly intracellularly. Figure from van Egmond et al. (Van Egmond et al. 2001).

In contrast to representing a first line of defense and mediating homeostasis at mucosal sites, IgA antibodies serve as second line of defense within the serum. FcαRI crosslinking by IgA results in inflammatory activation of effector cells such as granulocytes, monocytes or macrophages (Chapter 1.1.4, Figure 2). For example, Kupffer cells in the liver can phagocyte IgA-coated pathogens present in circulation (Van Egmond et al. 2001). Inflammatory signals mediated by FcαRI induce cellular responses like phagocytosis, respiratory burst and release of cytokines (Monteiro & Van De Winkel 2003; Van Egmond et al. 2001).

As mentioned, IgA antibodies can inhibit inflammatory responses through ITAMi and SHP-1 (Chapter 1.1.4). Therefore, IgA antibodies have neutralizing and inflammatory functions, but at the same time also represent inflammatory regulators to prevent excessive immune responses (Bakema & van Egmond 2011). Taken together, these diverse functions could be harnessed to use tumor-specific IgA antibodies for cancer immunotherapy. In circulation therapeutic IgA antibodies could stay inactive, while at tumor sites with high antigen expression IgA antibodies could mediate crosslinking of FcαRI on effector cells resulting in inflammatory responses.

IgA antibodies are also involved in pathological conditions. Alterations in the O-glycosylation of IgA1 are related to IgA nephropathy (IgAN). In IgAN, reduction of galactosylation of IgA1 hinge O-glycans results in the formation of binding sites for auto-antibodies. As a consequence, immune complexes are formed which deposit in the kidney and result in inflammatory responses and disease (Odani et al. 2000; Oortwijn et al. 2006; Hiki et al. 1999; Xue et al. 2013).

1.2 Antibodies for cancer therapy

During cancer development, normal cells acquire certain characteristics which results in uncontrolled proliferation. The six hallmarks for tumorigenesis and later metastasis are self-sufficiency of growth signals, insensitivity to anti-growth signals, evading apoptosis, limitless replicative potential, sustained angiogenesis and tissue invasion and metastasis (Hanahan & Weinberg 2000). The combination of all these capabilities of a cell results in the development of cancer. The main factors are mutational changes of cancer initiating cells but their surrounding including healthy cells plays an important role for the formation of a tumor-promoting microenvironment. Loosing functional tumor suppressor genes and gaining activated oncogenes of cells forms the basis for the development of a tumor. Additional hallmarks of equal importance have been proposed: reprogramming of energy metabolism and evading immune destruction (Hanahan & Weinberg 2000; Hanahan & Weinberg 2011; Hanahan & Coussens 2012). This cellular transformation results in changes on the surface on a molecular basis. Molecules which are overexpressed or exclusively expressed on the surface of these cells are called tumor-associated antigens. Antibodies which specifically bind to such structures can be administered in tumor therapy. They recognize the antigens and activate the immune system or cause direct cytotoxic effects (Scott, Wolchok, et al. 2012).

The number of antibodies developed for clinical application in tumor therapy is increasing. Various tumor-associated surface antigens offer the potential to specifically target tumor cells using antibodies to attract components of the immune system. In addition, administered antibodies can conduct direct Fab-mediated effector functions to diminish uncontrolled proliferation of cancer cells. Today, monoclonal IgG isotype antibodies have improved current cancer therapy regiments (Weiner et al. 2010). Hybridoma technology and molecular cloning founded the basis for monoclonal antibody (mAb) development (Köhler & Milstein 1975). Several tumor-associated targets like CD20 and epidermal growth factors have been clinically validated for the treatment of hematological and solid cancers, respectively, and

more novel targets are emerging (Weiner et al. 2010). However, these magic bullets still lack some of their magic. For example, epidermal growth factor receptor (EGFR) targeting antibodies cetuximab (Erbitux) and panitumumab (Vectibix) are used for the treatment of colorectal and head and neck cancer. Clinical response rates for these mAbs are in the range of 10% to 15% when used as single agent (Trivedi et al. 2014). Since the first approval of a monoclonal antibody for cancer therapy in 1998 (anti-CD20, rituximab), research pursued to further improve current formats by for example finding the best tumor-associated target, engaging multiple targets at a time or conjugating cytotoxic agents to mAbs. In other approaches, the protein backbone is modified to improve serum half-life, effector cell receptor binding or to increase avidity (Leget & Czuczman 1998; Beck et al. 2010; Weiner et al. 2010).

1.2.1 Effector mechanisms of antibodies against tumor-associated antigens

All antibodies approved for cancer therapy today are of the IgG isotype (Beck et al. 2010). Depending on the target molecule on the surface of a tumor cell, signals might be triggered by antibodies upon antigen binding. These signals can result in decreased cell proliferation, induction of apoptosis, shedding of targets or receptor down-modulation by internalization. In addition, binding of the antibody can block interaction with agonistic ligands (Deans et al. 2002; Patel et al. 2007; Dechant et al. 2007). Since the Fc domain is not involved in these effector mechanisms against cancer cells, they can be referred to as Fab-mediated (Figure 4a).

On the surface of effector cells of the immune system, several receptors for the Fc domain of antibodies are expressed. The main human leukocyte receptors for IgG are FcγRI (CD64), FcγRII (CD32) and FcγRIII (CD16), which bind IgG within the Cγ2 domain. As described before (Chapter 1.1.4), FcαRI (CD89) is the main human leucocyte receptor for IgA antibodies. Effector mechanisms involving receptor binding to antibodies are called Fc-mediated. While most of these receptors contain ITAMs for signaling, CD16b isoform present on neutrophils has no intracellular domain and is linked to the membrane by glycophosphatidylinositol (GPI). In addition, CD32b isoform possesses an immunoreceptor tyrosine-based inhibition motif (ITIM) and therefore contributes to cellular inactivation (Nimmerjahn & Ravetch 2006).

CD16a is present on natural killer (NK) cells and mediates antibody-dependent cellular cytotoxicity (ADCC) when being crosslinked by IgG antibodies on the surface of a target cell. ADCC represents an important effector mechanism of antibodies for cancer therapy (Weiner

et al. 2010). During this process, activated NK cells release perforin and granzymes which results in tumor cell lysis. Through the interaction of antibodies with Ig receptors on neutrophils, tumor cells can be lysed by degranulation of cytotoxic components from neutrophils (Woof & Burton 2004; Nimmerjahn & Ravetch 2006). Tumor-specific recombinant IgA antibodies were effective in mediating ADCC against cancer cell lines using granulocytes as effector cells (Dechant et al. 2007; Lohse et al. 2011). Due to the large number of granulocytes in human blood, recruiting this cell population is an interesting strategy for targeting cancer cells (Murphy 2011; Valerius et al. 1997; Huls et al. 1999).

Another important Fc-mediated effector function of antibodies is antibody-mediated cellular phagocytosis (ADCP). Tumor cells which are coated with antibodies can be recognized by FcRs on macrophages or other phagocytic cells, which subsequently engulf the tumor cell for lysosomal degradation. Macrophages are known to infiltrate the tumor microenvironment and therefore ADCP mediated by this cell population constitutes another important mode of action of therapeutic antibodies (Akewanlop et al. 2001; Dhodapkar et al. 2002; Weiner et al. 2010; Golay et al. 2013).

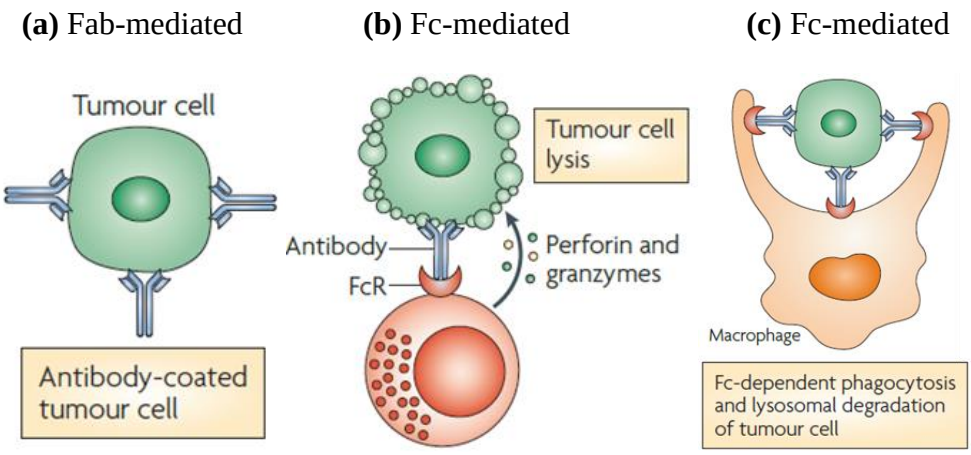

Figure 4 Selected effector mechanisms of antibodies for cancer immunotherapy. (a) Antibodies coating a tumor cell can prevent its proliferation. **(b)** Through interaction with Fc receptors, antibodies can mediate tumor cell lysis through effector cells of the immune system (red), e.g. natural killer cells or neutrophils. **(c)** Through interaction with Fc receptors on phagocytic cells like macrophages, antibody-coated tumor cells are engulfed followed by lysosomal degradation. Adopted from Weiner et al. (Weiner et al. 2010).

Upon antigen binding by IgG antibodies on a target cell, complement component 1q (C1q) binds to the Fc domain of therapeutic antibodies and activates downstream complement proteins through the classical pathway. For the initiation of this process crosslinking with two or more IgG antibodies is necessary. The complement cascade then results in the formation of

a membrane attack complex (MAC), which causes target cell lysis through pores and is referred to as complement-dependent cytotoxicity (CDC) (Weiner et al. 2010; Murphy 2011).

Therefore, antibodies can mediate the attack of tumor cells by marking them for components of the immune system. Depending on the antibody isotype, interaction with certain cells of the immune system expressing receptors for the corresponding antibody Fc domains can result in tumor cell lysis or phagocytosis. In contrast, for Fab-mediated effector functions similar effects can be expected for different isotypes with comparable binding characteristics (Dechant et al. 2007; Murphy 2011).

To elucidate the therapeutic potential of recombinant antibodies, different effector mechanisms have to be evaluated (Figure 4). Depending on the target or the epitope on a given target and the antibody format different mechanisms of action might contribute to the antibodies' functionality.

1.2.2 Selected antigens targeted for cancer immunotherapy

The number of potential targets for tumor therapy is large and counting (Weiner et al. 2010; Scott, Allison, et al. 2012). Several factors influence target selection: tumor specificity, high density on tumor cells and homogeneous abundance within tumors. Specificity is important, if an antigen is expressed on tumors and healthy tissue, one has to be aware of potential on-target toxicities. In some cases antigens can be present on healthy tissue but without being accessible from circulation which renders an intravenous administered therapeutic antibody as specific. Antigens which are only present on a subset of tumor cells while being highly specific might also not be suitable for cancer therapy because only antigen-positive cells of the tumor could be targeted (Scott, Wolchok, et al. 2012). To increase the chance of clinical benefit, target expression on tumors is confirmed prior to treatment (Pirker et al. 2012; Carvajal-Hausdorf et al. 2015). In order to elucidate the potential of IgA isotype antibodies for cancer therapy, antibodies directed against five heterogeneous targets were investigated (Table 1). These could reveal whether IgA antibodies may increase the therapeutic options for patients who do not sufficiently benefit from IgG antibody therapy. An introduction of tumor-associated antigens selected for this study follows.

Table 1 Overview of tumor-associated antigens relevant for this study.

Target	Type of target	Function	Approved antibodies	References
Her2	Epidermal growth factor receptor	Cell survival signaling	Herceptin, Perjeta, Kadcyla[+]	(Hudis 2007; Baselga & Swain 2009)
EGFR	Epidermal growth factor receptor	Cell survival signaling	Erbitux, Vectibix	(Krawczyk & Kowalski 2014)
TA-MUC1	Mucin glyco-protein	Cellular protection by hydration capacity, maintain pluripotency and self-renewal of embryonic stem cells	None	(Danielczyk et al. 2006; Nath & Mukherjee 2014)
TF	Carbohydrate	Putative cancer stem cell marker	None	(Karsten & Goletz 2013)
CD20	Hematopoietic differentiation marker	Potentially involved in ion transport	Rituxan/Mabthera, Azerra, Gazyvaro, Zevalin[*], Bexxar[*]	(Boross & Leusen 2012; Lim et al. 2010; Golay et al. 2013)

Her2: ErbB2 receptor; EGFR: epidermal growth factor receptor; TA-MUC1: tumor-associated mucin 1; TF: Thomsen-Friedenreich; CD: cluster of differentiation; + antibody-drug conjugate; * labeled with radioactive isotopes

1.2.2.1 ErbB2 receptor; Her2

ErbB2 is also known as Her2 and belongs to the family of ErbB receptor tyrosine kinases. Today, four receptors of this family are known, ErbB1 (or EGFR; Chapter 1.2.2.2), ErbB2, ErbB3 and ErbB4 (Figure 5). Upon ligand binding, the cytoplasmic catalytic function is activated and results in homodimerization or heterodimerization of these receptors and self-phosphorylation on tyrosine residues (Yarden & Sliwkowski 2001). Together with their ligands, receptor tyrosine kinases are involved in many cellular processes like cell proliferation, survival, migration or differentiation (Yarden 2001). In case of Her2, no extracellular ligand is known and it is considered to be constitutively available for dimerization (Baselga & Swain 2009). One of the most potent mitogenic signaling heterodimer consists of Her2 and Her3 (Baselga & Swain 2009). Her2 is 185 kDa in size and encoded by the *Her-2/neu* proto-oncogene, which is overexpressed and/or amplified in 25% to 30% of human breast and ovarian cancer patients. In breast and gastric cancer, Her2 overexpression is linked to poorer prognosis for patients (Slamon et al. 1987; Jaehne et al. 1992). Herceptin (trastuzumab) is a humanized monoclonal antibody which binds the

extracellular juxtamembrane domain (domain IV) of Her2 (Hudis 2007; Phillips et al. 2014). It is approved for Her2 overexpressing breast cancer, metastatic gastric or gastroesophageal junction adenocarcinoma (Herceptin prescribing information, revised 10/2010, http://www.accessdata.fda.gov). Apart from Fc-mediated effector functions like ADCC, binding of trastuzumab to Her2 prevents its activating signaling. Another antibody developed for the treatment of Her2-positve cancers is Perjeta (pertuzumab), which binds dimerization domain II (Baselga & Swain 2009). Given that Her2 is a clinically validated target, it is an interesting model to evaluate the potential of novel antibody isotypes for cancer therapy.

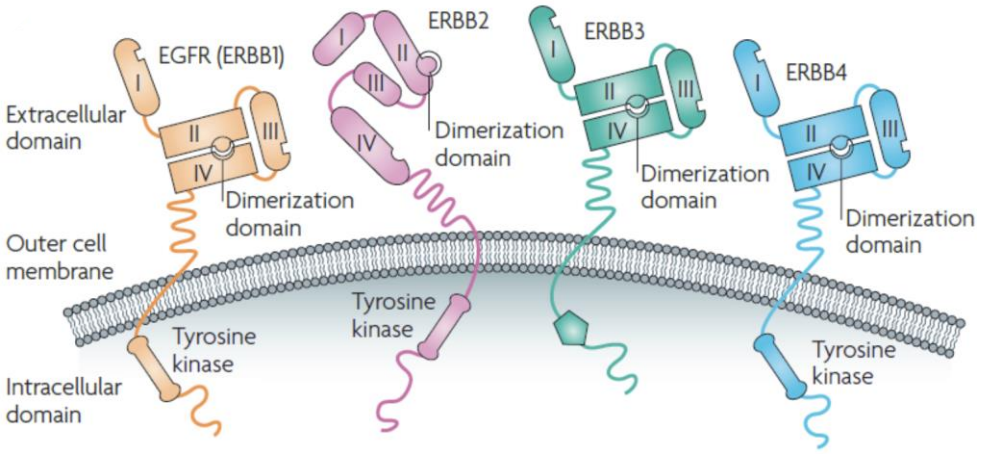

Figure 5 Illustration of epidermal growth factor receptors. The four members of epidermal growth factor receptors are illustrated with their intracellular and extracellular domains. Her2 (ERBB2) is constitutively present in a conformation available for dimerization while the other members need to undergo conformational changes to make the dimerization domain accessible for dimerization and subsequent intracellular signaling. Figure from Baselga and Swain (Baselga & Swain 2009).

1.2.2.2 Epidermal growth factor receptor

Like Her2, epidermal growth factor receptor (EGFR; also known as Her1 or ErbB1) is a type I transmembrane tyrosine kinase receptor (Figure 5). EGFR, Her2 and Her4 possess active tyrosine kinase domains, while Her3 cannot bind adenosine triphosphate and has no intrinsic tyrosine kinase activity (Baselga & Swain 2009). Ligands for EGFR include epidermal growth factor (EGF), transforming growth factor-alpha (TGF-alpha) and other ligands which all possess an EGF-like domain that is responsible for receptor binding. Like Her2, EGFR is composed of four extracellular domains, domains I and III are responsible for ligand binding and domains II and IV are involved in dimerization and interaction with other membrane proteins (Schlessinger 2002). In the current model for EGFR activation, EGFR remains in a tethered configuration in the absence of bound ligand. Upon ligand binding, the receptor is

extended and dimerization domain II becomes available for interaction with other receptors. In contrast, Her2 is considered to be constantly in a conformation which is available for dimerization. Once receptor dimers are formed, on the intracellular site receptor tyrosine kinases form asymmetric dimers, which results in kinase activation (Baselga & Swain 2009; Lemmon et al. 2014). Overexpression of EGFR in epithelial malignancies is correlated with poorer patient survival and different monoclonal antibodies were developed against this tumor-associated antigen. These include Erbitux (cetuximab), the first regulatory approved anti-EGFR antibody, and Vectibix (panitumumab). Cetuximab, a chimeric IgG1 antibody, competes with natural ligands for binding and thereby interferes with downstream signaling. Moreover, cetuximab causes receptor down-modulation though internalization (Trivedi et al. 2014). Other effector functions of cetuximab are Fc-mediated, ADCC and CDC rely on immune effector cell binding and binding of complement components to the Fc domain, respectively (Derer et al. 2012). Several other anti-EGFR antibodies are in clinical development or have been approved (Peipp et al. 2009). In retrospective clinical trial data analysis, it was shown that response to EGFR-directed antibodies as well as small-molecule tyrosine kinase inhibitors depends on inter-patient heterogeneity regarding *KRAS* mutations (Karapetis et al. 2008; Amado et al. 2008; Khambata-Ford et al. 2007; Loupakis et al. 2009), EGFR ligand expression (Khambata-Ford et al. 2007) and FcγRIIIa or FcγRIIa polymorphisms (Zhang et al. 2007; Bibeau et al. 2009; Peipp et al. 2009). Best response can be expected for patients without activating *KRAS* mutation, high EGFR ligand expression and higher affinity FcγR allotypes. *KRAS* mutations, *BRAF* mutations or *PTEN* loss can result in constitutive activation of EGFR downstream signaling, resulting in proliferation, survival or mobility of cells (Roock et al. 2011; Peipp et al. 2009). Like Her2, EGFR is a clinically validated target and therefore it is interesting to investigate other isotypes with this target.

1.2.2.3 Tumor-associated mucin 1

High molecular weight mucin membrane proteins like mucin 1 (MUC1), MUC4 or MUC16 are highly glycosylated and upon pathological transformation of a cancer cell, mucins are overexpressed and their glycans become altered. In normal tissue, mucins are present in mucus gels to protect epithelial surfaces by their hydration capacity. Transmembrane mucins are found on the apical surface of glandular and ductal epithelia (Mall 2008). Due to differences in length and glycosylation degree, MUC1 is between 250 kDa and 500 kDa in size and consists of an N-terminal signal sequence, a large extracellular domain of 20 or 21

amino acids variable number tandem repeats and a Sea urchin sperm protein, enterokinase, and agrin (SEA) domain, a transmembrane domain and a 69 amino acids C-terminal cytoplasmatic tail (Bafna et al. 2010; Nath & Mukherjee 2014). After translation, the single polypeptide of MUC1 is cleaved within the SEA domain to yield a longer N-terminal extracellular subunit (MUC1-N) and a shorter C-terminal subunit (MUC1-C), which are linked by stable hydrogen bonds. The extracellular domain contains variable number tandem repeats which are polymorphic in sequence and rich in serine, proline and threonine residues (PTS domain) (Nath & Mukherjee 2014). The serine and threonine residues of the tandem repeat domain are highly O-glycosylated and make up more than 50% of the molecular weight. Those glycans consist of galactose, N-acetylgalactosamine, N-acetylglucosamine, fucose and/or sialic acid (Hang & Bertozzi 2005). MUC1-C contains one N-glycosylation site in the extracellular domain and MUC1-N contains 4 N-glycosylation sites in the SEA domain. Within the cytoplasmatic tail, tyrosine, threonine and serine residues can be phosphorylated by growth factor receptors or kinases (Nath & Mukherjee 2014).

In most cancers MUC1 (also refered to as CD227) is overexpressed, truncated and underglycosylated, which results in the presentation of novel tumor-specific antigens (Danielczyk et al. 2006; Mall 2008; Nath & Mukherjee 2014). Tumor-associated MUC1 (TA-MUC1) is characterized by shorter O-glycans, a lower number of glycosylated sites in the extracellular domain and loss of the apical localization on cancer cells (Nath & Mukherjee 2014; Bitler et al. 2009). They include O-glycan structures like the monosaccharide modification with N-acetylgalactoseamine-α1-*O*-Ser/Thr (Tn antigen) and disaccharide galactose-β1-3N-acetylgalactoseamine-α1-*O*-Ser/Thr (T antigen, also known as Thomsen-Friedenreich antigen or core 1; Chapter 1.2.2.4) as well as their sialylated versions in lower abundance (Nath & Mukherjee 2014). Since these structures are mainly absent on healthy tissue (Figure 6), cancer patients develop antibodies against Tn and T antigens, and the presence of these antibodies correlates with the prognosis for patients (Varki et al. 2009). Moreover, mucin glycoconjugates like CA125, CA19-9 or CA15-3 are serological tumor markers which are overexpressed in ovarian, pancreatic or breast cancer. Following the serum level of these glycoconjugates is used for diagnostic purposes, to measure tumor burden or tumor recurrence (Fuster & Esko 2005). The interaction of MUC1 with β-catenin is important for tumor development and invasion, including metastatic development (Schroeder et al. 2003).

While Her2 is only expressed on about 20% of breast cancer patients, MUC1 is expressed on 90% of breast cancers (Thie et al. 2011). In addition, in other indication it is found on a high

percentage of cancer cells which makes it an interesting target for cancer therapy (Mukherjee et al. 2001). Approaches to target TA-MUC1 on tumors include the development of PankoMab, a humanized IgG1 antibody targeting a glyco-peptide conformational mixed epitope within the extracellular tandem repeat domain. Binding is strictly dependent on the tumor-associated glycosylation within the epitope, which distinguishes hPM from other anti-MUC1 antibodies (Danielczyk et al. 2006). hPM IgG antibody is currently tested in a phase II efficacy study for the treatment of ovarian, fallopian tube or primary peritoneal cancer (clinicaltrials.gov identifier: NCT01899599). The tumor-specific glyco-peptide conformational epitope of TA-MUC1 represents an interesting novel target to increase diversity of the investigated targets.

1.2.2.4 Thomsen-Friedenreich antigen

The disaccharide galactose-β1-3N-acetylgalactoseamine-α1-*O*-Ser/Thr (T or TF antigen, also known as core 1 structure and CD176; Figure 6) is expressed on carcinoma-associated antigens of human tumor cells (Springer & Desai 1975; Springer 1984; Hang & Bertozzi 2005). In the first step of the biosynthetic pathway, N-acetylgalactoseamine (GalNAc) is linked to a hydroxyl group of a serine or threonine residue of a protein. The enzymes catalyzing this reaction are called polypeptide α-N-acetylgalactosaminyltransferases (ppGalNAcTs) and use uridine diphosphate (UDP)-GalNAc as a substrate, releasing UDP after transfer of the monosaccharide to the amino acid. For the synthesis of the TF antigen disaccharide, UDP-Gal:GalNAcα1-*O*-Ser/Thr glycopeptide β3-galactosyltransferase (T-synthase) transfers galactose (Gal) from the UDP-Gal substrate to the Tn antigen. While this is the main modification of the Tn antigen, in normal tissue two additional glycosyltransferases are well known and yield glycans like Sialyl-Tn antigen and core 3 (Ju et al. 2011). The oncofetal TF antigen is expressed on 90% of all carcinomas, qualifying it as a pan-carcinoma antigen. Proteins carrying TF antigen include CD44v6 and MUC1 which show increased expression during cancer invasion and metastasis (Yu 2007). The main carrier protein of TF antigen is MUC1 within its tandem repeat domain. TF expression on MUC1 correlates with poor prognosis for patients with gastric cancer and metastases in the lymph nodes (Baldus et al. 1998; Yu 2007). TF expression on colorectal carcinomas is a risk factor for the development of liver metastases and TF was also proposed to be a marker for cancer stem cells (Cao et al. 1995; Karsten & Goletz 2013). Antibodies specifically binding to TF were generated by several groups (Clausen et al. 1988; Karsten et al. 1995; Goletz et al.

2003). Recently, phage display technology was used to produce anti-TF antibody fragments for diagnostic or therapeutic application (Yuasa et al. 2013). KaroMab is a humanized IgG antibody which specifically binds the TF antigen (Goletz et al. 2003). In the presented study, it is the only antibody that recognizes an antigen consisting solely of carbohydrates. To assess the potential of other isotypes for cancer therapy this carbohydrate target was included.

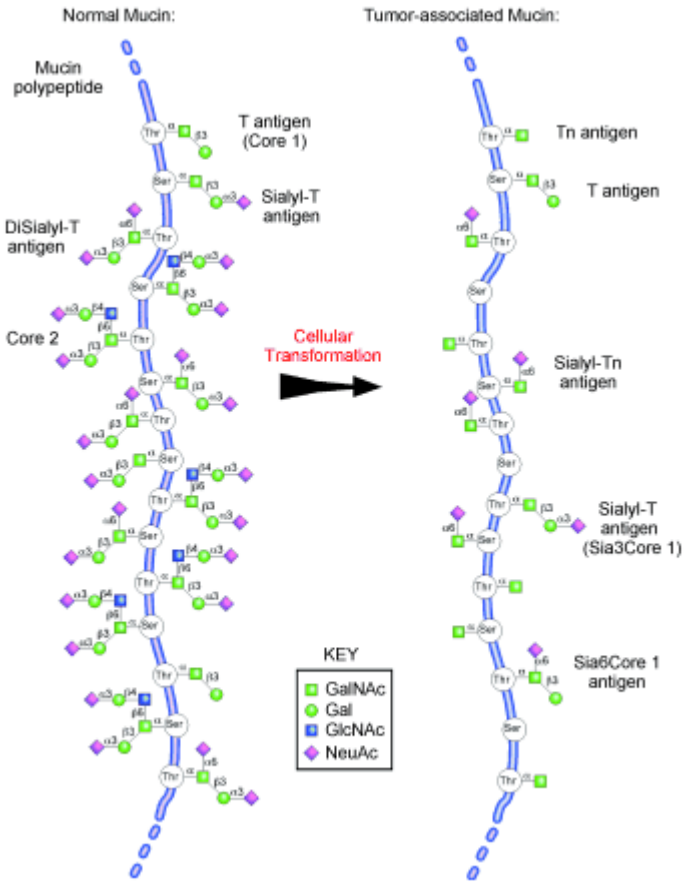

Figure 6 Cellular transformation of cancer cells results in aberrantly glycosylated tumor-associated mucin 1 (TA-MUC1) within the tandem repeat domain. Glycan modifications of serine and threonine residues within tandem repeats are shorter and the degree of glycosylation is lower for TA-MUC1. Both, Tn and Thomsen-Friedenreich (TF or T) antigen modifications are found on TA-MUC1 of cancer cells as compared to heathy tissue. In addition the apical orientation is lost and TA-MUC1 is overexpressed on cancer cells. Upon cellular transformation, glycans are less frequent sialylated with NeuAc. GalNAc: N-acetylgalactoseamine; Gal: galactose; GlcNAc: N-acetylglucoseamine; NeuAc: N-acetylneuraminic acid. Figure from Ju et al. (Ju et al. 2011).

1.2.2.5 B-lymphocyte antigen CD20

During B cell differentiation, CD20 expression starts in the late pro-B cell stadium and is lost during terminal plasma cell differentiation (Cragg et al. 2005; Boross & Leusen 2012). The exact biological role of CD20 is not known, but a role in calcium ion transport was proposed (Tedder & Engel 1994). The 33 to 35 kDa CD20 molecule spans the membrane four times

with cytoplasmatic C- and N-termini and one small and one large extracellular loop (Figure 7) (Cragg et al. 2005). The large extracellular loop contains the alanine-asparagine-proline (ANP)-binding motif of therapeutic mAbs like rituximab, tositumomab or obinutuzumab (Polyak & Deans 2002; Niederfellner et al. 2011). The approval of Mabthera (rituximab) by the Food and Drug Administration (FDA) dates back to 1998 and it is used for the treatment of non-Hodgkin lymphoma and chronic lymphocytic leukemia (Boross & Leusen 2012).

On the surface of a cell, CD20 localizes in homodimers and homotetramers (Figure 7) (Bubien et al. 1993). CD20-targeting antibodies are distinguished by their different effects on target cells. Type I anti-CD20 antibodies (e.g. rituximab, ofatumumab) redistribute CD20 into Triton X-100-insoluble lipid rafts and are potent in CDC (Bologna et al. 2012; Lim et al. 2010). In contrast, type II anti-CD20 antibodies (e.g. obinutuzumab, tositumomab) are more potent in ADCC, mediate homotypic target cell adhesion and lysosome-mediated cell death (Alduaij et al. 2011; Herter et al. 2013).

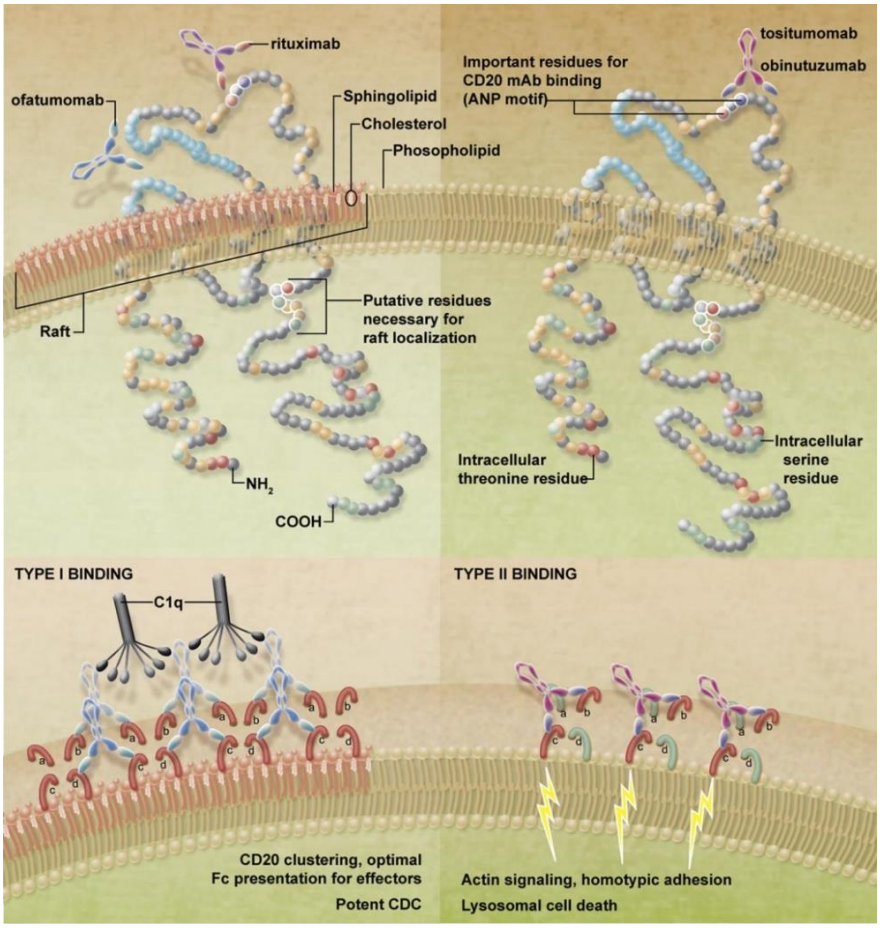

Figure 7 Different binding of type I and II anti-CD20 antibodies for cancer therapy. Both types of anti-CD20 antibodies bind within the same alanine-asparagine-proline (ANP)-binding motif of the large extracellular loop (top). Still, different orientations result in different effector functions on CD20-positive cancer cells. Moreover, only type I anti-CD20 antibodies mediate the formation of CD20-containing lipid rafts within the membrane (lower left). Figure form Cragg (Cragg 2011).

Due to different binding characteristics, type I anti-CD20 antibodies are able to bind twice as much molecules on CD20-positive target cells compared to type II anti-CD20 antibodies (Figure 7). While both types differ in CDC and ADCC potency, they are comparable effective in ADCP using monocyte-derived macrophages (MDM) as effector cells (Herter et al. 2013). In this study, humanized type II anti-CD20 antibody obinutuzumab was used as model antibody. It constitutes the only antibody that was developed for non-solid, hematological cancer indications and increased diversity of investigated targets.

1.2.3 Towards the development of human-like biotherapeutics

Today, different expression systems are used for the production of therapeutic antibodies. But, in most cases rodent cells are genetically modified in order to produce recombinant proteins. For example, Mabthera, Gazyvaro, Vectibix and Herceptin are produced in Chinese hamster ovary (CHO) cells and Erbitux is produced in murine Sp2/0 cells (Walsh 2014). One important posttranslational modification of antibodies is glycosylation which consist of multiple branched monosaccharide units. Within the endoplasmic reticulum and Golgi of eukaryotes, many enzymes are responsible for the composition of the glycans attached to proteins and both, enzymes and the resulting glycans differ between species (Varki et al. 2009). While rodent and human expression systems share common characteristics, some distinct features can affect safety and efficacy of therapeutic proteins. Structures which are absent in human glycans like α(1-3)-linked galactose or α(2-3)-linked N-glycolylneuraminic acid are potentially immunogenic for patients (Jefferis 2009). Moreover, CHO cells are not capable to link N-acetylneuraminic acid in α(2-6) configuration which is present in human glycans (Jefferis 2009). These limitations of commonly used non-human expression systems can be overcome by fully human systems like the myelogenous leukemia-derived GlycoExpress (GEX) cell lines. In addition to the fully human glycans, glycoengineering was used to generate cell lines which produce biologics with specific glycosylation patterns. H9D8 or Fuc^- GEX cell lines are used for the production of proteins with high sialylated glycans or high sialylated glycans with low fucose levels, respectively (personal communication with Dr. Antje Danielczyk). The reduction in core fucose of N-glycans within the Cγ2 domain of IgG antibodies results in increased FcγRIIIa affinity and Fc-mediated effector functionality (Ferrara et al. 2011; Gerdes et al. 2013).

1.3 Aim of the project – increasing the functional diversity of cancer immunotherapy

Today, all approved monoclonal antibodies for cancer therapy are IgG isotype antibodies (Scott, Wolchok, et al. 2012; Beck & Reichert 2014). Methods for IgG production and purification are well known and this isotype benefits from prolonged serum half-life through receptor-mediated recycling. However, several studies indicate better cytotoxic effects against cancer cells *in vitro* when engaging FcαRI on granulocytes. Using granulocytes as source of effector cells, FcαRI-engagement can induce potent antibody-dependent cellular cytotoxicity (ADCC) against tumor cells (Valerius et al. 1997; Huls et al. 1999; Dechant et al. 2002; van Egmond et al. 2001; Otten et al. 2005; Dechant et al. 2007; Beyer et al. 2009; Lohse et al. 2011). Of all leukocytes in human blood, granulocytes (also called polymorphonuclear leukocytes) are the most numerous cell population and therefore attractive components of the immune system to target cancer cells. They are relatively short lived, a few days, and their numbers increase during infection or inflammation. Among granulocytes, neutrophils are the most numerous and play a crucial role in innate immune responses. Eosinophils and basophils belong to granulocytes as well, and like neutrophils, they possess granules with toxic components which can be released upon activation (Murphy 2011). Hence, effectively recruiting these cells which are found in the tumor microenvironment could potentially improve current immunotherapeutic approaches (Dumitru et al. 2013). Recombinant IgA antibodies or bispecific antibodies simultaneously binding FcαRI and tumor antigen can recruit these immune effector cells to cancer cells. However, the production and purification of monoclonal IgA antibodies is not well established (Tanikawa et al. 2008; Beyer et al. 2009). IgA production rates and yields using conventional expression systems are often low and assembly is sometimes not complete. The presence of serum in growth medium hinders further development in order to produce potential biotherapeutics for human use (Chintalacharuvu et al. 2007; Dechant et al. 2007; Beyer et al. 2010; Reinhart et al. 2012). The high number of glycosylation sites potentially results in more heterogeneous recombinant products as compared to IgG antibodies. IgA antibody glycans are surface exposed and involved in pathological conditions which highlights the importance of human-like IgA production (Field et al. 1994; Kokubo et al. 1997; Mattu et al. 1998; Allen et al. 1999; Royle et al. 2003; Pouria et al. 2004; Woof & Russell 2011). Compared to IgG antibodies, processes for affinity purification of IgA are not well established. IgA antibodies were purified using the jackfruit lectin jacalin or Protein L. Both methods have their limitations since they only recognize IgA1 and certain kappa LC subgroups, respectively (Roque-Barreira & Campos-

Neto 1985; Kondoh et al. 1986; Nilson et al. 1992). Moreover, *in vivo* efficacy evaluation of therapeutic IgA antibodies is difficult due to the lack of an IgA receptor homologue in mice and the relatively short serum half-life (Murphy 2011; Boross et al. 2013).

In vitro anti-tumor cell activity of recombinant IgA antibodies targeting one specific antigen was evaluated before. The aim of this study was to generate a panel of recombinant IgA antibodies targeting heterogeneous tumor-associated antigens and to elucidate the potential of IgA isotype antibodies for cancer immunotherapy (Chapter 1.2.2). Therefore, the mechanisms of action of IgA antibodies as cancer immunotherapy agents could be investigated not only for one antibody that targets a particular antigen, but for a range of IgA antibodies against multiple targets. The antibodies were specific for epidermal growth factor receptors, glyco-peptide and glycan epitopes as well as a surface marker for B cells. Hence, using multiple heterogeneous targets enabled the evaluation of IgA isotype antibodies as cancer immunotherapeutics on a broader basis. Both, IgA Fab- and Fc-mediated effector functions were evaluated. To compare IgA1 and IgA2 antibodies, for one target (tumor-associated mucin 1) both subclasses were generated. IgA monomer and dimers in association with J chain were generated to compare their target binding avidity. Moreover, in a protein engineering approach, a mixed-isotype variant was investigated that consist of an IgG with IgA1 Cα3 domain and could combine benefits of two isotypes. In order to account for the importance of human-like glycosylation, the fully human GlycoExpress (GEX) expression system was used for antibody production.

2 Materials and methods

2.1 Materials

2.1.1 Antibodies, peptides and proteins

ELISA and Western blot antibodies (concentrations or dilutions are indicated)

Anti-alpha chain from IgA Quantitation Kit (1:100 for Western blots)	E80-102	Bethyl Laboratories (Montgomery, USA)
Anti-goat IgG (1:2,000)	705036	Jackson ImmunoResearch (West Grove, USA)
Anti-human IgA horseradish peroxidase (POD) (1:5,000)	309-035-011	Jackson ImmunoResearch
Anti-human IgG POD (1:10,000)	109-035-098	Jackson ImmunoResearch
Anti-J chain (5 µg/mL)	C58617	LifeSpan Biosciences (Seattle, USA)
Anti-kappa LC (1µg/mL)	ab1050	Abcam (Cambridge, UK)
Anti-mouse IgG POD (1:2,000)	P0447	Dako (Glostrup, Denmark)
Anti-Tetra His (1 µg/mL)	LS-C15474	LifeSpan Biosciences

Flow cytometry antibodies (dilutions are indicated or 5 µL per 100 µL cell suspension were used)

Anti-CD3 fluorescein isothiocyanate (FITC)	555332	BD Biosciences (San Jose, USA)
Anti-CD16 AlexaFluor 647	557710	BD Biosciences
Anti-CD19 allophycocyanin (APC)	555415	BD Biosciences
Anti-CD32 phycoerythrin (PE)	552884	BD Biosciences
Anti-CD64 FITC	555527	BD Biosciences
Anti-CD89 PE	555686	BD Biosciences
Anti-human IgA Cyanine (Cy) 3 (1:200)	109-166-011	Jackson ImmunoResearch

Anti-human IgG Cy3 (1:200)	109-165-098	Jackson ImmunoResearch
Mouse IgG1 AlexaFluor 647	557714	BD Biosciences
Mouse IgG1 FITC	555748	BD Biosciences
Mouse IgG1 PE	555749	BD Biosciences

Immunofluorescence antibodies (dilutions are indicated)

Anti-human IgA1 FITC (1:100)	ABIN376208	antibodies-online (Aachen, Germany)
Anti-human IgG Cy3 (1:100)	109-165-098	Jackson ImmunoResearch

Recombinant proteins and synthetic peptides, cytokines and reference antibody

EGFR (antigen ELISA)	E3641	Sigma-Aldrich (St. Louis, USA)
Her2 extracellular domain GST	internal by Lead Discovery Department Glycotope	
Asialoglycophorin A	A9791	Sigma-Aldrich
Custom synthetic MUC1 peptides	as described before (Danielczyk et al. 2006)	
CD89	YSP1147	Speed Biosystems (Gaithersburg, USA)
EGF-R/ErbB1 Fc Chimera (SPR)	344-ER	R&D Systems (Minneapolis, USA)
Interferon γ	130-093-882	Miltenyi Biotec
GM-CSF	300-03	Peprotech (Rocky Hill, USA)
M-CSF	300-25	Peprotech
MabThera, rituximab		Roche (Welwyn Garden City, UK)

DNA and protein ladders

GeneRuler 100bp Plus DNA Ladder	SM0324	Life Technologies (Carlsbad, USA)
GeneRuler 1kb DNA Ladder	SM0313	Life Technologies
HiMark Pre-Stained Protein Standard	LC5699	Life Technologies

2.1.2 Bacteria and medium composition

NEB 5-alpha Competent *Escherichia coli* (High Efficiency), C2987H, New England Biolabs

Bacteria were grown in Luria-Bertani (LB) broth (10 g/L tryptone, 5 g/L yeast extract, 10 mM sodium chloride) or LB agar plates, which were supplemented with 15 g/L agar (A5054, Sigma-Aldrich). Low salt LB broth for the adaption of cells, which were transformed by electroporation, was prepared with half of the sodium chloride concentration.

2.1.3 Chemicals

Unless otherwise noted, chemicals were purchased from Carl Roth (Karlsruhe, Germany), Merck KGaA (Darmstadt, Germany), or Sigma-Aldrich Chemie GmbH (Steinheim, Germany). Additional chemicals are specified in Annex 9.2.

2.1.4 Consumables

Consumables were purchased from the following companies: Cell culture dishes, centrifuge tubes, bottle-top filter (TPP), serological pipets (Greiner Bio One), pipette tips (Axygen Scientific and Gilson), white flat-bottom 96-well plates (Costar), electroporation cuvettes (Amaxa and Eppendorf), nitrocellulose membrane (GE Healthcare, Little Chalfont, UK), gels for SDS-PAGE (Bio-Rad), protein solution concentrators, sterile filter (Merck Millipore), syringes and needles (B. Braun, Melsungen, Germany).

2.1.5 Enzymes

Restriction enzymes

FastDigest HindIII	FD0504, Life Technologies
FastDigest BamHI	FD0054, Life Technologies
FastDigest XbaI	FD0684, Life Technologies
FastDigest PvuI	FD0624, Life Technologies
PvuI	ER0621, Life Technologies
T4 DNA ligase	15224, Life Technologies

Others

N-Glycosidase F	11365193001, Roche Diagnostics

2.1.6 Instruments

Agarose gel electrophoresis apparatus	Peqlab (Erlangen, Germany)
ÄKTA FPLC	GE Healthcare
ÄKTAPrime	GE Healthcare
AxioPlan 2 Microscope	Carl Zeiss (Oberkochen, Germany)
Balance, analytical AX205	Mettler-Toledo (Columbus, USA)
BBD 6220 CO_2 incubator	Thermo Fisher Scientific (Waltham, USA)
BD FACSCanto II	BD Biosciences
Biacore 2000	GE Healthcare
BIO-VISION documentation system 3000 superbright	Peqlab
ClonePix FL	Molecular Devices (Sunnyvale, USA)
Densitometer GS-800	Bio-Rad
Electronic Precision Balance DLT-2100	Sartorius (Göttingen, Germany)
Guava PCA-96 flow cytometer	Guava Technologies (Hayward, USA)
Heraeus Fresco 17 centrifuge	Thermo Fisher Scientific
Heraeus Megafuge 1.0R	Thermo Fisher Scientific
Heraeus Pico 17 centrifuge	Thermo Fisher Scientific
Herasafe KS Class II, Type A2 Biological Safety Cabinet	Thermo Fisher Scientific
Incubator, Innova 4000	Eppendorf
Infinite F200 microplate reader	Tecan (Männedorf, Switzerland)
Inverted contrasting microscope DM IL	Leica Microsystems (Wetzlar, Germany)
Liquid nitrogen container Arpege 140	Air Liquide Medicinal (Paris, France)
Mini-Protean Tetra system	Bio-Rad

Multifuge 3 S-R	Thermo Fisher Scientific
Nanodrop 2000c	Thermo Fisher Scientific
Nucleofector II	Amaxa (Cologne, Germany)
Pipetman pipettes	Gilson (Middleton, USA)
Research plus pipettes	Eppendorf (Hamburg, Germany)
Thermocycler TPersonal	Analytik Jena (Jena, Germany)
Thermomixer comfort	Eppendorf
Tras-Blot SD semi-dry system	Bio-Rad
UPLC 1290 Infinity	Agilent Technologies (Santa Clara, USA)

2.1.7 Eukaryotic cell lines

GlycoExpess H9D8 and Glycoexpress Fuc- were developed by Glycotope (Berlin, Germany) and used for antibody production.

The following target cells were used: A-431, BT-474, KG-1, Ls174, Panc-1, Raji, SK-BR-3, T47D and ZR-75-1. Media compositions, sources and media supplements are listed in Annex Annex 9.4.

2.1.8 Kits

Bethyl IgA Quantitation	E80-102, Bethyl
Cell Line Nucleofector Kit V	VACA-1003, Lonza
CellTiter-Glo Luminescent Cell Viability Assay	G7572, Promega
EndoFree Plasmid Maxi Kit	12362, Qiagen
GeneJET Plasmid Miniprep	K0503, Life Technologies
LudgerTag 2-AB (2-aminobenzamide) Glycan Labeling Kit	LT-KAB-A2, Ludger (Oxford, UK)
NucleoSpin Gel and PCR Clean-up	740609, Macherey-Nagel
Pan Monocyte Isolation Kit	130-096-537, Miltenyi Biotec

Phagoburst kit	Glycotope Biotechnology
PKH26 Red Fluorescent Cell Linker Kit	PKH26GL, Sigma-Aldrich
Quantum Simply Cellular anti-human IgG kit	816B, Bangs Laboratories (Fishers, USA)

2.1.9 Plasmids

Heavy chain expression plasmid pGT1 with puromycin resistance

Light chain expression plasmid pGT2 with methotrexate resistance

Joining chain expression plasmid pGT4 with neomycin resistance

2.1.10 Software

AxioVision version 4.8.2 (Zeiss; Oberkochen, Germany)

BD FACSDiva version 8.0 (BD Biosciences; San Jose, USA)

BIAevaluation version 4.1 (GE Healthcare; Little Chalfont, UK)

Compass DataAnalysis software 4.3 (Bruker; Billerica, USA)

Empower 3 software (Waters; Milford, USA)

Graphpad Prism software version 5.04 was used for graphical and statistical analyses (GraphPad Software; San Diego, USA)

ImageJ (Author Wayne Rasband, Research Services Branch, National Institute of Mental Health; Bethesda, USA)

Mendeley Desktop version 1.14 (Mendeley Ltd.; London, UK)

Microsoft Office version 2010 (Microsoft; Redmond, USA)

2.2 Molecular biology methods

2.2.1 DNA cloning of antibody-encoding sequences

DNA sequences encoding variable light or heavy chains were purchased from Geneart and supplied in a plasmid with ampicillin resistance. Variable heavy and light chain regions were

flanked by HindIII and BamHI restriction enzyme sites. Sequences encoding the constant light and heavy chain regions of IgG, IgA1 and IgA2 heavy chains were flanked by BamHI and XbaI restriction enzyme sites. DNA cloning was conducted according to standard protocols (Sambrook & Russell 2001). DNA concentrations were determined using a NanoDrop 2000c spectrophotometer (Thermo Fisher Scientific). Amino acid sequences used for the generated antibodies are listed in Annex 9.3.

2.2.2 Transformation and preparation of plasmid DNA

NEB 5-alpha competent *E. coli* (New England Biolabs) were used for transformation according to the manufacture's high efficiency protocol. Single colonies were used to inoculate 5 mL LB medium cultures, which were grown overnight shaking at 37 °C. Plasmid isolation was carried out using the GeneJET Plasmid Miniprep Kit (Thermo Fisher Scientific) according to the manufacturer's protocol. For large scale expression plasmid preparation, 100 mL LB medium cultures were inoculated with 100 µL of 5 mL overnight cultures and grown overnight shaking at 37 °C. The EndoFree Plasmid Maxi Kit (Qiagen) was used for plasmid isolation according to the manufacturer's protocol.

2.2.3 Agarose gel electrophoresis

Agarose gel electrophoresis was carried out according to standard protocols (Sambrook & Russell 2001) using a TAE buffer system (Bio-Rad) and HEEO ultra-quality agarose (Carl Roth). An appropriate volume of 6-times loading dye solution (Thermo Fisher Scientific) was added to each sample and GeneRuler 100bp Plus DNA Ladder or GeneRuler 1kb DNA Ladder (both Life Technologies) were used as standards. Prior to DNA visualization with a BIO-VISION documentation system 3000 superbright (Peqlab), gels were stained for 30 min using GelRed (Biotrend).

2.2.4 Enzymatic digestion of DNA

DNA was digested using restriction enzymes (Chapter 2.1.5) according to the manufacture's protocols.

2.2.5 Ligation of DNA fragments

For ligation of inserts into vectors, DNA fragments were isolated from agarose gels using the NucleoSpin Gel and PCR Clean-up (Macherey-Nagel) according to the manufacture's protocol. Ligation was performed using the T4 ligase (Life Technologies) according to the manufacture's protocol. Fifty ng of vector were used at a 1 to 5 molar ratio of vector to insert, reaction time was 16 hours at 16 °C. Subsequently, the reaction mixture was added to 25 µL NEB 5-alpha competent *E. coli* (New England Biolabs) and transformation was carried out according to the manufacture's high efficiency protocol.

2.2.6 Linearization of plasmid DNA for stable transfections

Prior to stable transfection, plasmids were linearized using a restriction enzyme with unique restriction site. Plasmid DNA was digested for 16 h at 37 °C with PvuI (Life Technologies) in Digestion Buffer R (Life Technologies), 5 µL enzyme were used for 100 µg DNA in a final volume of 200 µL. For plasmid DNA extraction, one sample volume of phenol/chloroform/isoamyl alcohol (25:24:1 volume ratio, Carl Roth) was added and mixed by vortexing. After centrifugation at 3,500x g for 10 min, the upper phase was transferred into a new 1.5 mL centrifuge tube. After repeating the first steps of extraction, one sample volume of trichloromethane (Carl Roth) was added and mixed by vortexing. After centrifugation at 16,200x g for 1 min, the upper phase was transferred into a new 1.5 mL centrifuge tube. After a second addition of trichlormethane and centrifugation in a peqGold PhaseTrap A tube (Peqlab), the upper phase was transferred into a new centrifuge tube. One tenth 3 M sodium acetate and 2.5-times ethanol of the sample volume was added and mixed by vortexing for DNA precipitation. After centrifugation at 16,200x g for 10 min, the supernatant was discarded and the pellet was washed with 100 µL 70% (v/v) ethanol in deionized water. Following centrifugation at 16,200x g for 10 min, the supernatant was discarded and the pellet was air dried. Washing and drying of the DNA pellet as well as subsequent handling of the DNA was carried out under a laminar flow cabinet. The dried DNA pellet was resuspended in 100 µL UltraPure water (Life Technologies).

2.3 Cell culture methods – clone development and antibody production

2.3.1 Transient transfection with antibody-encoding plasmids

The day prior to transient expression, cells were seeded at $2x10^5$ cells/mL. The day of transfection, cells were counted to confirm logarithmic growth and vitality higher than 90%. Transient expression was carried out in 6-well plates, $2x10^5$ cells/mL were seeded in 2 mL and grown for 3 to 4 h. Expression plasmids encoding the HC and LC (1.88 µg and 0.63 µg, respectively) and PLUS reagent (Thermo Fisher Scientific) were added to 500 µL OptiMEM (Thermo Fisher Scientific) and mixed by vortexing. Following 15 min incubation at room temperature, 6.3 µL Lipofectamine LTX (Thermo Fisher Scientific) was added and mixed by vortexing. Following 30 min incubation at room temperature, the mixture was slowly added to the cell suspension during gentle mixing. Supernatant containing the secreted protein was harvested after 3 or 4 days incubation at 37 °C, 5% CO_2 in a humidified incubator. Cells and cell debris were removed by centrifugation, 3,345x g for 15 min.

2.3.2 Stable transfection with antibody-encoding plasmids

Nucleofector kit V (Lonza) was used for stable transfections. The day prior to stable transfection, $2x10^5$ cells/mL were seeded. For transfection, cells were counted to confirm logarithmic growth and more than 90%vitality. For electroporation, $2x10^6$ cells were centrifuged at ~300x g for 5 minutes and resuspended in 100 µL Nucleofector solution containing expression plasmids and transferred into a cuvette. Nucleofector program T-003 was used for electroporation using a Nucleofector II instrument (Amaxa). Next, the cell suspension was gently pipetted into pre-warmed culture medium using a plastic Pasteur pipette. Cell concentration and vitality were checked after 24 h and selection pressure media was added after 48 h.

2.3.3 Clone development and cell culture maintenance for the production of monoclonal antibodies

If not otherwise noted, all eukaryotic cells were grown at 37 °C, 5% CO_2 and 90% relative humidity. Cell concentration was either estimated microscopically or cells were counted using Guava ViaCount (Merck Millipore, 4000) with the Guava PCA-96 flow cytometer (Guava

Technologies, Hayward USA). Dilution with fresh medium was conducted every 2 to 3 days and cells were seeded at about $2x10^5$ cells/mL. Centrifugation of cell suspensions was carried out at ~300x g for 5 minutes and cells were cultured in T25 culture flasks at a volume of 5 mL.

For clone development, selection pressure was increased stepwise once the cells were adapted to the present selection pressure. At a selection pressure of 100 nM methotrexate and 0.4 µg/mL puromycin, clones with high antibody production were selected. Therefore, 500 cells/mL were seeded in 2 mL semi-solid media in 6-well plates. Semi-solid medium for 8 6-well plates contained 40 mL CloneMatrix concentrate (Molecular Devices), 40 mL two-times concentrated Glycotpe medium and 1 mL fluorescein-labeled anti-IgG (H+L) CloneDetect (Molecular Devices). Detection of IgA antibodies, which possess the same kappa LC like IgG, by anti-IgG (H+L) was confirmed by fluorescence dot blot. For each antibody, 2 to 4 6-well plates with cell pools were seeded for cloning. Fluorescently labeled detection antibody allowed estimation of relative antibody production for each formed colony within the semi-solid medium. Each colony represented one clone and high producing clones were selected based on total exterior fluorescence using a ClonePix instrument (Molecular Devices). Selected clones (80 to 95 per antibody) were picked by the ClonePix robot and seeded in 150 µL fresh media without selection pressure in 96-well plates. Once clones reached sufficient cell densities, selection assays were performed. Clones were selected based on antibody production relative to cell count or production solely based on antibody titers. The best 10 to 30 clones were transferred into 24-well plates in 0.5 mL medium with selection pressure and further propagated. Subsequent selections were based on maximal titers within 3 to 4 days of culture or specific production rate determination (Chapter 2.3.4). Usually 3 to 5 clones per antibody were kept for antibody production and preserved by cryogenic conservation.

2.3.4 Determination of the specific production rate

Clones were screened for antibody production per cell per day. Prior to cell counting, cells were washed in fresh medium to remove antibody already secreted into the culture medium. Next, $4x10^4$ cells/mL were seeded in 0.5 mL medium without selection pressure in 24-well plates. After 3 or 4 days incubation, the volume of the cell suspension was measured, cells were counted and supernatant samples were taken for titer ELISA (Chapter 2.4.7). The specific production rate was calculated under the assumption of exponential growth during the

3 or 4 day incubation time using the following formula: specific production rate [pg/cell/day] = $titer_{antibody}$ [pg/mL]/integral cell area, where integral cell area [cell x d/mL] = (final cell count [cells/mL] – $4x10^4$ cells/mL)/log_e(final cell count [cells/mL]/$4x10^4$ cells/mL) x time of culture [d].

2.3.5 Preparation of cryogenic cell culture stocks in liquid nitrogen and re-cultivation

For long term conservation of antibody producing cell pools or clones, cryogenic stocks were prepared. The day before conservation, cells were counted and seeded with maximal $2x10^5$ cells/mL in medium without selection pressure. For conservation, cells were counted and vitality of more than 90% was confirmed. For each cryogenic conservation vial to be prepared, $1x10^6$ to $2x10^6$ cells were centrifuged and resuspended in 1 mL freezing medium containing 90% Glycotope medium and 10% dimethyl sulfoxide (DMSO). Vials containing cell suspension were transferred into a 4 °C pre-cooled cryo freezing container (Nalgene). The container was stored at -80 °C for 1 to 4 weeks and subsequently vials were transferred into liquid nitrogen tanks.

For re-cultivation of frozen cells, the vial was removed from the liquid nitrogen tank and placed on ice. For each vial one well in a 6-well plate was prepared with pre-warmed medium without selection pressure. Prior to seeding in the plates, frozen cells were washed with fresh 10 mL medium to remove DMSO. After washing, cells were plated in the prepared 6-well plate. Once vitality reached 90%, cells were cultivated with selection pressure.

2.3.6 Antibody production in spinner cultures

Antibodies were produced in 250 mL to 1 L spinner culture flasks on a mixing platform at 60 rpm. Cells were cultivated in the absence of selection pressure for about one week. Supernatants were harvested by centrifugation at 3,345x g for 30 min at 4 °C once vitality dropped below 75%. Prior to storage at -20 C, supernatants were filtered using a 1 µm glass fiber filter membrane (Pall).

2.3.7 Perfusion process in 2 L stirred tank bioreactor

For inoculation to a final cell concentration of $2x10^5$ viable cells/mL, cells were grown in spinner culture as described before. The working volume was 1 L using a 2 L stirred tank

bioreactor (BBI Biotech Quad System 4 x 2l) and the following process parameters: 37 °C, 40% dissolved oxygen, pH 7.0, 300 to 400 rpm stirrer speed depending on dissolved oxygen. During the process medium was continuously fed while harvesting supernatant discontinuously using a Centritech Lab II (Berry Wehrmiller, Pneumatic scale) in intermittent mode. The wait time between cycles was adjusted to control the perfusion rate and thereby keeping a constant working volume of 1 L.

When glucose dropped below 2.5 g/L (usually by day 4 or 5), continuous operation was started by feeding Glycotope medium at a perfusion rate of 0.25 V/d. Perfusion was stepwise increased to 0.50 V/d, 1.00 V/d, 1.50 V/d and 2 V/d when glucose concentration dropped below 2.5 g/L or every other day. Maximum perfusion rate was two reactor volumes per day. When maximum perfusion rate was reached, feed media was gradually replaced by enriched two-times concentrated Glycotope medium.

2.4 Biochemical and immunological methods

2.4.1 Antibody purification by affinity chromatography

Culture supernatants or bioreactor harvests (Chapters 2.3.6 and 2.3.7) were thawed overnight at room temperature and filtered using 0.22 µm bottle top filters (TPP).

For IgA purification, 1 mL KappaSelect columns (GE Healthcare) were used with an ÄKTAPrime (GE Healthcare) or FPLC system. All solutions used for antibody purification were 0.22 µm filtered using a bottle top filter (TPP). Columns were stored at 4 °C in 20% ethanol in deionized water. Prior to use, columns were washed with at least 5 column volumes (CV) deionized water and equilibrated with at least 5 CV PBS. As for washing and equilibration, the flow rate for sample loading was set to 1 mL/min. Purifications were carried out at room temperature and the supernatants were kept on ice during sample loading. After sample loading, the column was washed with at least 30 CV PBS. Antibodies were eluted with 10 CV 0.1 M glycine pH 2.5 and 1 mL fractions were collected in 1.5 mL centrifuge tubes containing 200 µL 2.45 M potassium phosphate buffer pH 7.2 for neutralization. Fractions containing protein according to UV absorbance at 280 nm were pooled. Buffer exchange of the solution into PBS was carried out by concentrating and diluting using 50,000 molecular weight cut off Amicon tubes (Millipore). The protein solution was diluted with PBS followed by concentration to 10% to 20% of the starting volume at 3,345x g at 10 °C.

For adequate buffer exchange, this step was repeated at least 7 times, followed by 0.22 µm filtration using a syringe filter. Antibodies were stored at 4 C.

IgG and IgG-Ca3 antibodies were purified as described for IgA antibodies using MabSelect SuRe comuns (GE Healthcare) and 0.1 M citrate, 0.15 M sodium chloride pH 3.6 buffer for elution.

2.4.2 Determination of protein concentration

Protein concentration of purified antibodies was measured using a NanoDrop 2000c (Thermo Fisher Scientific) spectrophotometer. Extinction coefficients were calculated based on the amino acid sequences using ProtParam (http://web.expasy.org/protparam/) and antibody concentrations were calculated based on the absorbance at 280 nm with the Lambert-Beer law (Gasteiger et al. 2005).

2.4.3 Sodium dodecyl sulfate polyacrylamide gel electrophoresis (SDS-PAGE) and Western blots

SDS-PAGE and Western blots were performed according to standard protocols (Sambrook & Russell 2001). For SDS-PAGE gels, 3 µg of each sample was loaded per lane. A Tris glycine buffer system was used with Mini-Protean TGX gels (Bio-Rad) and a Mini-Protean Tetra system (Bio-Rad). Proteins were visualized with colloidal Coomassie. For Western blots, 0.5 µg of each sample were loaded per lane. Proteins were transferred on nitrocellulose membranes (GE) using a Tras-Blot SD semi-dry system (Bio-Rad).

2.4.4 Size exclusion chromatography

If not otherwise noted, size exclusion chromatography (SEC) was carried out on an ÄKTAPrime system (GE Healthcare) using a Superdex200 10/300 GL column (GE Healthcare) with PBS as running buffer. All solutions used for SEC were 0.22 µm filtered using a bottle top filter (TPP). The column was stored at room temperature in 20% ethanol in deionized water. Prior to use, the column was washed with 1 CV deionized water and then equilibrated with at least 1 CV PBS. As for washing and equilibration, the flow rate for analytical SEC was set to 0.5 mL/min. For preparative SEC the flow rate was set to

0.3 mL/min and 0.5 mL fractions were collected. Fractions corresponding to peaks in the UV absorbance signal at 280 nm were pooled. SECs were carried out at room temperature.

For analytical SEC of small sample volumes (Chapter 3.2.4), SEC was carried out on a 1200 Series HPLC system (Agilent) using an Aquity UPLC Protein BEH450 4.6 mm x 150 mm column (Waters). The flow rate was set to 0.3 mL/min and running buffer was 100 mM sodium phosphate pH 6.8. Five µg of samples were injected and column temperature was set to 40 °C. In order to account for different systems used for SEC, elution volumes were adjusted based on monomer elution volumes. An IgG antibody served as positive control for monomers.

2.4.5 Enzymatic deglycosylation of N-glycans

N-glycans of antibodies were enzymatically cleaved using N-Glycosidase F (Roche Diagnostics). For deglycosylation, 50 µg antibody in 50 µL PBS were denatured and reduced by addition of 2.5 µL 2% (w/v) SDS, 1 M 2-mercaptoethanol (Sigma-Aldrich) and incubation for 5 min at 100 °C. When samples were cooled down to approximately 37 °C, 2.5 µL 15% (w/v) Nonidet P 40 (Sigma-Aldrich) and 3 units N-Glycosidase F were added. After incubation for 24 h, approximately 3 µg were used for SDS-PAGE analysis (Chapter 2.4.3) in reducing conditions.

2.4.6 N-glycan profiling

N-glycan profiling was performed by the Glycosylation Analytics group of Dr. Sven Bahrke at Glycotope, Berlin.

N-glycans were enzymatically liberated from antibodies and fluorescently labeled with 2-aminobenzamide (2-AB) for fluorescence detection during hydrophilic interaction liquid chromatography (HILIC) coupled to electrospray ionization-quadrupole time-of-flight mass spectrometry (ESI-qTOF) with collision-induced dissociation (CID) for structure identification. A detailed description of the method for N-glycan profiling is given in Annex 9.5.

2.4.7 Enzyme-linked immunosorbent assays (ELISAs)

Antibodies specific for antibody isotypes, antigens or antibodies specific for a tagged receptor (Chapter 2.1.1) were coated overnight on Maxisorp 96-well plates (Nunc) at a concentration of 0.5 µg/mL to 1 µg/mL. Serial dilutions of antibody samples were prepared and isotype specific HRP-conjugated antibodies were used for detection. ELISAs were conducted according to standard protocols (Sambrook & Russell 2001).

IgA antibody concentrations in supernatants were determined using the human IgA ELISA Quantitation Set (Bethyl) according to the manufacturer's protocol.

In case of hPM, a synthetic TA-MUC1 glycosylated peptide was used as antigen. To confirm the mixed glycan-peptide epitope, a non-glycosylated peptide served as negative control. The assay was described previously by Danielczyk et al. (Danielczyk et al. 2006).

For FcαRI ELISA, after blocking the plate, each well was incubated with a constant concentration of His-tagged recombinant CD89 prior to sample incubation.

ELISAs were developed using TMB microwell substrate solution (Tebu-bio) and sulfuric acid was used to stop the reaction. For detection at 450 nm and 620 nm an Infinite F200 microplate reader (Tecan) was used.

2.4.8 Surface plasmon resonance

A Biacore 2000 (GE Healthcare) instrument was used for surface plasmon resonance experiments. In all experiments antigens were immobilized on CM5 chips (GE Healthcare) and antibody was passed through the flow cell. The amine coupling kit (GE Heathcare) was used to immobilize antigens according to the manufacture's protocols. If not otherwise noted, HBS-EP (GE Healthcare) buffer was used as running buffer and buffer exchange into running buffer was conducted for antibody samples (as described in Chapter 2.4.1). Starting concentrations were between 1,500 nM and 2,400 nM for IgA2 monomers and IgG antibodies. The starting concentration for IgA2 dimers was 760 nM. Seven fourfold serial dilutions and a running buffer blank were injected for each run. In kinetic experiments a flow rate of 50 µL/min was used and samples were injected for 5 minutes association time, followed by 17 minutes dissociation time. Equilibrium dissociation constants were determined using BIAevaluation software version 4.1 (GE Healthcare). Maximal responses were fitted locally and curves were fitted using bivalent and tetravalent binding models for

monomeric and dimeric antibodies, respectively. Equilibrium dissociation constants were calculated based in first association and dissociation rates.

2.4.9 Immunofluorescence

Cells were diluted to a concentration of $2x10^5$ cells/mL in order to obtain scattered single cells on glass slides with ten wells. Twenty-five µL drops were left for 30 minutes on the slides to allow sedimentation. Subsequently, the medium was gently removed from the slides. Once dyed in a laminar flow cabinet, the slides were stored at -80 °C. Prior to staining, cells were fixed by addition 50 µL 5% (v/v) formaldehyde in PBS for 5 minutes and then washed three times using PBS. To avoid unspecific binding, the wells were blocked using 50 µL cell culture medium for 30 minutes. Next, 50 µL of primary antibody dilutions in cell culture medium were added and incubated for 1 h at room temperature. After three wash steps, secondary fluorophore-labeled antibody (Chapter 2.1.1) was added and incubated for 0.5 to 1 h at room temperature. After three wash steps, for nucleic counterstaining 50 µL of 0.5 µg/mL 2-(4-Amidinophenyl)-6-indolecarbamidine dihydrochloride in PBS was used and incubated for 5 minutes. After three wash steps, cell were mounted with 25 µL Aqua-Poly/Mount (Polysciences, Warrington, USA) per well and slides were covered with a glass coverslip.

2.4.10 Flow cytometry

If not otherwise noted, $1x10^5$ to $2x10^5$ cells were used for flow cytometry analyses using a BD FACSCanto II (BD Biosciences) in 96-well plate format. Staining with primary labeled antibodies, non-labeled antibodies or labeled secondary antibodies (Chapter 2.1.1) were conducted in 50 µL PBS containing 5% heat-inactivated fetal bovine serum (Biochrom) for 20 to 30 min at 4 °C. Subsequently, cells were washed twice with PBS and resuspended in 100 µL for flow cytometry analyses. For data evaluation, BD FACSDiva software version 8.0 (BD Biosciences) was used.

2.4.11 Determination of antigen binding sites on the surface of target cells

Quantum Simply Cellular anti-human IgG kit (Bangs Laboratories) was used according to the manufacturer's protocol. IgG isotype antibodies were used to determine binding sites and

classify target cells regarding to antigen binding sites: + ($1x10^4$-$1x10^5$), ++ ($1x10^5$-$5x10^5$) or +++ (>$5x10^5$).

2.5 Methods for biofunctional evaluation

Unless otherwise noted, cells were centrifuged at ~300x g for 5 minutes.

2.5.1 Proliferation inhibition

For proliferation inhibition of target cells, 5,000 cells in 75 µL medium were transferred in 96-well flat bottom plates. Subsequently, 75 µL two-fold concentrated antibody diluted in medium were added to the cells. After 3 to 4 days incubation at 37 °C, 5% CO_2 in humidified incubator, metabolic active cells were measured using the CellTiter-Glo Luminescent Cell Viability Assay (Promega) kit according to the manufacturer's protocol. Proliferation was expressed relative to a control grown in the absence of antibody. Ten µM aphidicolin served as positive control for proliferation inhibition. In some cases pictures were taken after incubation using a light microscope connected with a digital ocular camera.

2.5.2 Isolation of granulocytes from whole blood

Peripheral blood was drawn from healthy donors using heparin coated Vacutainer (BD Biosciences). Usually 45 mL blood were used for granulocyte isolation. Nine mL blood were layered on top of 20 mL 1.079 g/mL Easycoll solution (Biochrom) diluted in PBS using 50 mL conical centrifuge tubes. After a centrifugation at 400x g for 30 min with minimal acceleration and break settings, granulocytes were present on top of the blood pellet. The upper phase, the upper interphase and the upper Easycoll phase were discarded. The blood pellet and about 2 mL of the Easycoll phase made up about 7 mL in volume. The tubes were filled up to about 47 mL with Pharm Lyse (BD Biosciences), mixed thoroughly and incubated for 15 minutes at room temperature. After centrifugation at 600x g for 5 min, the supernatant was discarded and the granulocyte pellets were pooled in one 50 mL conical centrifugal tube. Subsequently, two wash steps with PBS were conducted and granulocytes were seeded in RPMI 1640 medium (Biochrom) containing 2 mM L-glutamine (Biochrom), 10% heat-inactivated fetal bovine serum (Biochrom) and 100 U/mL Interferon γ (Miltenyi Biotec) at

$1x10^6$ cells/mL. Granulocytes were used in ADCC assays after overnight incubation at 37 °C, 5% CO_2 in a humidified incubator.

2.5.3 Respiratory burst assay

The Phagoburst kit (Glycotope Biotechnology, Heidelberg, Germany) was used for the respiratory bust assay. The manufacturer's protocol was adapted to investigate the dependency on target cells for activation of granulocytes and monocytes. Heparin anticoagulated peripheral blood was drawn from healthy donors and 100 µL were used for each sample. The final volume was 140 µL for each duplicate, 20 µL antibody, controls or PBS and 20 µL target cell suspension or PBS were added. After 30 min incubation at 37 °C, 20 µL stimulation solution (reagent D) were added. The following steps were according to the manufacturer's protocol for flow cytometry analysis using a BD FACSCanto II (BD Biosciences).

2.5.4 Antibody-dependent cellular cytotoxicity assay

ADCC assays were based on antibody concentration-dependent europium release of target cells in the presence of granulocytes as effector cells.

Prior to europium loading, target cells were washed with PBS and $3x10^6$ target cells were resuspended in 100 µL cold europium buffer containing 50 mM Hepes (Carl Roth), 93 mM sodium chloride (Roth), 5 mM potassium chloride (Roth), 2 mM magnesium chloride (Merck Millipore), 10 mM diethylenetriaminepentaacetic acid (Sigma-Aldrich), 2 mM europium-III acetate (Sigma-Aldrich) pH 7.4. After 10 minutes incubation on ice, target cells were electroporated using a Nucleofector II (Amaxa), followed by another 10 minutes incubation on ice. Then, target cells were gently pipetted into 13 mL RPMI containing 5% (v/v) heat-inactivated fetal bovine serum (Biochrom) and centrifuged. This wash step was repeated six times before pipetting target cells in the assay plate.

ADCC assays were conducted in round bottom 96-well plates. Twenty µL of tenfold concentrated antibody dilutions in RPMI containing 5% (v/v) heat-inactivated fetal bovine serum (Biochrom) or controls were transferred into plates. Next, 100 µL of $5x10^4$ europium-loaded washed target cells per milliliter were added. Then, 80 µL of $5x10^6$ effector cells per milliliter were added and plates were incubated for 3 to 5 h at 37 °C, 5% CO_2 in a humidified incubator. After incubation, plates were centrifuged and 20 µL supernatant were transferred

into white 96-well plates containing 200 µL enhancement solution (PerkinElmer). After 10 min incubation in the dark, fluorescence was measured using a microplate reader (Tecan). Samples and controls were analyzed in triplicates and sextuplicates, respectively. Specific lysis was calculated relative to the maximal europium release using 1% (v/v) Triton X-100 (Sigma-Aldrich) in the absence of effector cells and antibody: specific lysis [%] = ($signal_{sample}$ – mean $signal_{spontaneous\ release}$)/(mean $signal_{maximal\ release}$ – mean $signal_{spontaneous\ release}$) x 100%. Target cells in the absence of effector cells and antibody served as spontaneous release controls.

For statistical analysis, significant differences of maximal lysis were calculated by repeated measures one-way ANOVA with Bonferroni multiple comparison post-test using GraphPad Prism. P values blow 0.05 were considered significant.

2.5.5 Antibody-dependent cellular phagocytosis assay

Buffy coats served as source for monocytes which were subsequently differentiated into macrophages. Monocytes were isolated by magnetic sorting using the Pan Monocyte Isolation Kit and LS columns (both Miltenyi Biotec) according to the manufacturer's protocol.

For macrophage differentiation, $6x10^5$ monocytes per mL were cultured over six to seven days in AIM-V medium (Thermo Fisher Scientific) containing 2 mM L-glutamine (Biochrom), 25 mM HEPES (Carl Roth), 50 µM 2-mercaptoethanol (Sigma-Aldrich), 2% (v/v) heat inactivated human AB serum (Sigma-Aldrich), 10 mM 1,25-dihydroxyvitamin D3 (Sigma-Aldrich) at 37 °C, 5% CO_2 in a humidified incubator. After the first day, cultivation was continued in the presence of 500 U/mL GM-CSF or 50 ng/mL M-CSF (both Peprotech) to promote differentiation to M1- or M2-like macrophages, respectively. During the cultivation, fresh medium was supplied every two to three days.

The day before the phagocytosis assays, target cells were labeled with the fluorescent dye PKH26 (Sigma-Aldrich) according to the manufacturer's instructions.

The day of phagocytosis assays, MDM were harvested with trypsin and adjusted to $1x10^6$ cells/mL in medium. Using low binding 96-well round bottom plates (Nunc), 100 µL MDM were used and 50 µL of harvested target cells at a concentration of $4x10^5$ cells/mL were added. Subsequently 40 µL of samples or controls were added. For inhibition of phagocytosis, 10 µL cytochalasin D (Enzo) to yield a final concentration of 2.5 µg/mL were added. Otherwise 10 µL PBS was used in samples for phagocytosis. After incubation for 3 h

to 4 h at 37 °C, 5% CO_2 in a humidified incubator, cells were centrifuged at ~490x g for 5 min and washed with PBS. Next, cells were stained for 15 min at 4 °C with a mixture of APC-labeled anti-CD45 antibody and 7-aminoactinomycin D (7-AAD) to exclude dead cells using 3 µL per well and a final concentration of 20 µg/mL, respectively. After a wash step with PBS, cells were resuspended in 100 µL and 60 µL were analyzed by flow cytometry. The following compensations were used to account for overlapping fluorescence signals: 7-AAD to PE 18.78, PE to 7-AAD 9.57, APC to 7-AAD 20.93 and 7-AAD to APC 0.28. Percent phagocytosis was calculated based on CD45/PKH26 double-positive cells relative to CD45-positive cells.

2.5.6 B cell depletion in whole blood

B cell depletion in whole blood was adapted from Moessner et al. (Mossner et al. 2010). Whole blood from healthy donors withdrawn in heparin coated Vacutainer (BD Biosciences) was used in B cell depletion assays. Twenty µL tenfold concentrated antibody was added to 180 µL whole blood in 96-well round bottom plates. After incubation, 40 µL whole blood were added to a mixture of 5 µL FITC-labeled anti-CD3 and 5 µL APC-labeled anti-CD19 antibodies in 96-well round bottom plates. After incubation for 20 min at 4 °C, 200 µL Pharm Lyse buffer (BD Biosciences) were added for erythrocyte lysis. After 20 min incubation at room temperature, the plates were centrifuged and the supernatant was discarded. The lysis was repeated and after centrifugation the cell pellet was resuspended in 100 µL PBS for flow cytometry analysis. CD3 and CD19 served as marker for T and B cells, respectively. B cell counts relative to control T cell counts were evaluated and B cell depletion was calculated relative to a control without antibody according to following formula: B cell depletion [%] = 100% – $(\text{B cell count/T cell count})_{\text{sample}}$/mean $(\text{B cell count/T cell count})_{\text{medium controls}}$ x 100%.

3 Results

The aim of this study was to generate a panel of IgA antibodies against five different tumor-associated antigens in order to elucidate the potential of IgA isotype antibodies as cancer immunotherapeutics. The following chapter is divided into three parts. First, the production of monoclonal recombinant IgA antibodies is described. Second, biochemical integrity and target binding is shown. In the third part, different mechanisms of action of IgA antibodies against cancer cell lines are presented.

For IgA antibodies used in this study isotypes are indicated as IgA1 or IgA2. All IgA2 antibodies were of IgA2m(1) allotype. IgA antibodies derived from cells co-expressing the J chain polypeptide are indicted by IgA1J or IgA2J. Using separation techniques, IgA monomers, dimers and higher order multimers were generated which is indicated for those preparations in following chapters. All IgG antibodies were monomeric and of IgG1 isotype, which is not indicated in the following chapters.

3.1 Clone development for the production of monoclonal IgA antibodies

Feasibility of IgA antibody production in GlycoExpress (GEX) cell lines was confirmed by small-scale expression using transient transfections and subsequent IgA-specific titer enzyme-linked immunosorbent assays (ELISA) of supernatant samples. Next, to produce as homogeneous antibodies as possible in high yields, clone development was conducted after stable transfection with antibody-encoding plasmids. All antibodies were successfully expressed in GEX-H9D8 and in case of hPM IgA antibodies additionally in GEX-Fuc$^-$ (Table 2). Besides IgA antibodies, in a protein engineering approach an IgG-IgA mixed-isotype construct (anti-Her2) and an IgG antibody (anti-CD20) were generated. Except anti-CD20 hOM IgG, all antibodies were already available as IgG isotype for comparison with IgA antibodies.

Table 2 Overview of generated antibodies.

IgG Name (abbreviation for other isotypes)	Target	Originator antibody, species	Isotypes/subclasses/ constructs generated	Expression cell lines
PankoMab (hPM)	TA-MUC1	None, humanized	IgA1, IgA1J, IgA2, IgA2J	GEX-H9D8 and GEX-Fuc$^-$
TrasGEX (hTM)	Her2	trastuzumab, humanized	IgA2, IgA2J, IgG-Cα3	GEX-H9D8
CetuGEX (CM)	EGFR	cetuximab, chimer	IgA2, IgA2J	GEX-H9D8
KaroMab (hKM)	TF antigen	None, humanized	IgA2	GEX-H9D8
ObiGEX (hOM)	CD20	obinutuzumab, humanized	IgA2, IgA2J IgG	GEX-H9D8

Antibodies were produced in GlycoExpress (GEX) cell lines; co-expression of the J chain is indicated by IgA1J or IgA2J; TF antigen: Thomsen-Friedenreich antigen

3.1.1 Clone development and spinner cultures

Prior to cloning of single cell-derived clones, antibody production was confirmed by titer ELISA for stably transfected cell pools. Cell pools were kept viable and antibody production was enhanced by gradually increasing selection pressure for heavy chain (HC)- and light chain (LC)-encoding plasmids. After single cell cloning, specific production rate screenings served as selection criterion between different clones. The time frame between stable transfection and clone selection based on specific production rates was about four to six months.

For one antibody, clones showed comparable productivity and titers. In contrast, differences in antibody production were observed between antibodies targeting different antigens. For example, expression levels in spinner culture of hTM IgA2 were noticeably higher than for CM IgA2, 49.77 mg/L to 59.7 mg/L and 5.87 mg/L to 7.2 mg/L, respectively. In case of hPM, IgA1 expression levels were higher than IgA2, 42 mg/L and 4 mg/L, respectively (Table 3).

Two methods were used for J chain co-expression which associates with multimeric IgA (Figure 1). In case of hPM IgA2J, the J chain was encoded on the same plasmid as the HC, while a separate J chain-encoding plasmid was used for hPM IgA1J, hTM IgA2J and CM IgA2J antibodies. In both cases, J chain co-expression did not result in pronounced changes of IgA expression levels (Table 3). For hPM IgA1, hTM IgA2 and CM IgA2, high producing

clones were used for subsequent transfection with a J chain-encoding plasmid. After transfection, hTM and CM IgA2 clones were screened for J chain expression by anti-J chain Western blots. The expression level of J chain differed between clones and affected IgA multimerization (Chapter 3.2.3).

To combine functionalities against cancer cells of two isotypes by protein engineering, an IgG-IgA mixed-isotype antibody was generated. Mixed-isotype hTM IgG-Cα3 construct consists of hTM IgG1 with IgA1 Cα3 domain fused to the C terminus of Cγ3 domain. The majority of residues responsible for FcαRI binding are located in the Cα3 domain of IgA antibodies (Chapter 1.1.4). Hence, both IgG and IgA specific receptors on the surface of effector cells could be activated by the mixed-isotype construct.

Table 3 IgA, IgG and mixed-isotype construct mean antibody production in selected GEX-H9D8 clones.

Antibody	q(mAb) [pg/cell/day]	Titer [mg/L]
hTM IgA2	53.3 ±12.4	55.8*
hTM IgA2J	19.5 ±5.4	41.5 ±1.7
hPM IgA1	10.9 ±1.3	41.8 ±11.9
hPM IgA1J	10.8 ±1.5	32.8*
hKM IgA2	11.9 ±4.5	24.7*
hOM IgA2	n.d.	15.3*
CM IgA2J	3.6 ±0.6	9.8 ±2.7
hPM IgA2J	5.2 ±0.7	9.7*
CM IgA2	2.4 ±0.5	6.5*
hPM IgA2	4.6 ±2.3	4.0 (one clone)
hOM IgG1	54.7 ±6.4	172.0 ±32.0*
hTM IgG-Cα3	n.d.	3.8 ±1.5

q(mAb): specific production rate; titer in supernatants of spinner cultures upon harvest; q(mAb) and titer for 4 to 5 selected clones; mean ± standard deviation; *: mean titer of two clones; n.d.: not determined

In summary, a panel of IgA antibodies against five different tumor antigens was successfully expressed. Additionally, an IgG-IgA mixed-isotype version of hTM was generated. The production of hTM IgA2 antibodies was much higher than the production of the other

generated IgA antibodies. In all cases, production yields using serum-free media were sufficient for subsequent purification, biochemical assessment and biofunctional evaluation of IgA antibodies' mechanisms of action against cancer cell lines. Moreover, to evaluate feasibility to produce large amounts of monoclonal IgA antibodies, hTM IgA2 was cultivated in a bioreactor under serum-free conditions.

3.1.2 High-yield production of hTM IgA2 by cultivation in a bioreactor

One major challenge of therapeutic IgA antibodies is the production of sufficient amounts of recombinant protein (Beyer et al. 2009). To investigate feasibility of high-yield production under conditions compatible with large-scale good manufacturing practice (GMP) production, hTM IgA2 producing cells were cultivated in a 2 L bioreactor. In the controlled environment using a continuous perfusion process with serum-free medium, high cell densities were reached. Maximal cell concentrations were $5x10^7$ viable cells/mL which is about ten-times higher than maximal cell density in spinner cultures. More importantly, once the culture had reached the maximal perfusion rate, IgA titers reached up to 282 µg/mL and the mean titer for the duration of the perfusion process was 200 µg/mL. Therefore, at a perfusion rate of 2 L/d, the process yielded on average 400 mg IgA per day. Viability of cells was stable above 90% for the duration of the cultivation. As indicated by the arrow, cells were removed from the bioreactor by bleeding about 25% of the reactor volume to avoid cell concentrations exceeding $5x10^7$ viable cells/mL and ensure sufficient nutrient supply for the culture (Figure 8).

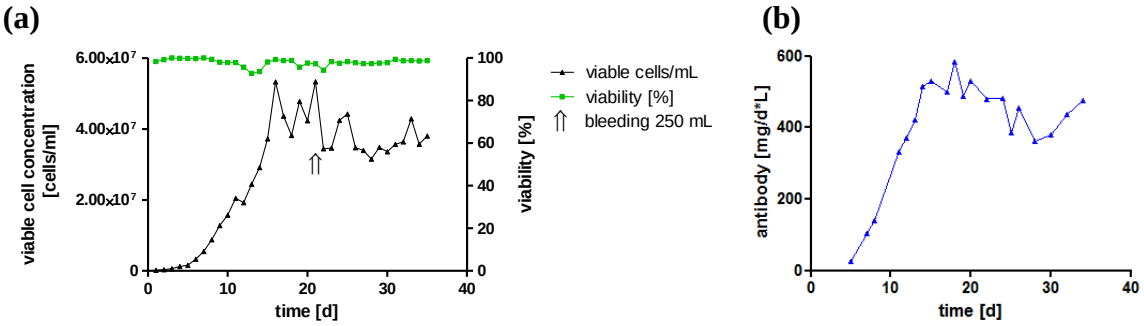

Figure 8 hTM IgA2 was produced in high yield by a perfusion process in a bioreactor. The working volume was 1 L using a 2 L stirred tank bioreactor. A Centritech was used for supernatant harvest and cell retention. **(a)** Viable cell concentration (black) and viability (green) during the 35 day process is shown. To maintain cell concentrations blow $5x10^7$ viable cells/mL, 250 mL were removed from the bioreactor (indicated by arrow). **(b)** Productivity (blue) was calculated based on titer ELISA values multiplied by the perfusion rate and the working volume.

This represents the first report of continuous cultivation of an IgA-producing culture in a bioreactor. Feasibility of high yield production of recombinant monoclonal IgA antibodies was shown. The total IgA antibody yield was 11 g within 35 days cultivation. While this represents an exemplary IgA antibody production in a bioreactor, for standard IgA antibody production 1 L spinner cultures yielded sufficient material to confirm biochemical integrity and elucidate biofunctionality against cancer cell lines (Table 3).

3.2 Biochemical integrity of novel recombinant monoclonal IgA antibodies

Biochemical integrity of the novel IgA antibodies for cancer immunotherapy targeting five different antigens was shown.

Subsequent to purification by affinity chromatography (Chapter 3.2.1), size exclusion chromatography (SEC) served as analytical and preparative method under native conditions. SEC was used to analyze contents of and to prepare IgA monomers, dimers and higher order multimers (Chapters 3.2.2, 3.2.3 and 3.2.4). Sodium dodecyl sulfate polyacrylamide gel electrophoresis (SDS-PAGE) and Western blots were used to assess purity and identity of purified IgA preparations under denaturing conditions (Chapter 3.2.5). Moreover, relative levels of J chain expression were assessed by anti-J chain Western blots (Chapter 3.2.3).

Prior to biofunctional assessment (Chapter 3.3), specific target binding and FcαRI binding were confirmed by antigen enzyme-linked immunosorbent assay (ELISA) or surface plasmon resonance (Chapters 3.2.8 and 3.2.9) and FcαRI ELISA (Chapter 3.2.10), respectively. Target cell binding was confirmed by immunofluorescence and flow cytometry (Chapter 3.2.8).

3.2.1 IgA antibodies can be purified using light chain-specific affinity chromatography

IgA antibody purification is not well established, however, Beyer et al. (Beyer et al. 2009) reported affinity chromatography methods for the purification of IgA1 and IgA2 antibodies. While buffer exchange in PBS was required by the method described before (Beyer et al. 2009), here, supernatants were directly loaded on chromatography columns. IgA antibodies were eluted with 0.1 M glycine buffer at pH 2.5. As shown for hPM IgA1, only a minor antibody fraction was eluted using less acidic buffers and no additional antibody was eluted using more acidic buffers (Figure 9).

hOM IgG and hTM IgG-Cα3 were successfully purified using MabSelect SuRe columns as per standard conditions used for IgG antibody purification (Chapter 2.4.1).

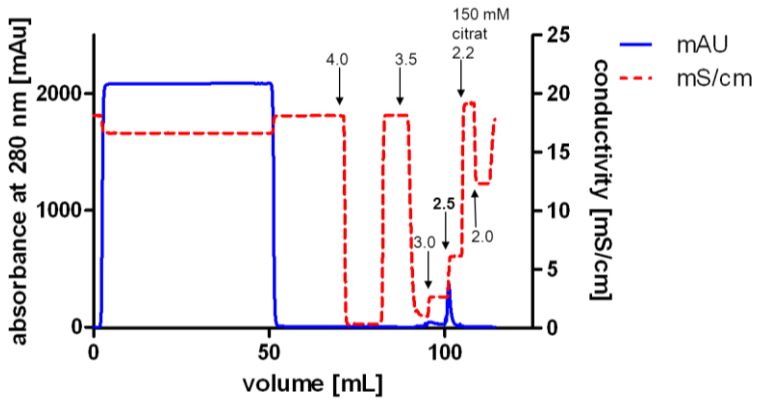

Figure 9 Screening of conditions for elution of IgA antibodies from affinity chromatography columns. Different buffers with decreasing pH values (indicated by number) were screened for elution of hPM IgA1 from KappaSelect columns. Glycine buffer with pH 2.5 was used for subsequent purifications including IgA2 antibody purifications.

Single-step affinity chromatography specific for kappa LC allowed for purification of all IgA antibodies from culture supernatants. Purity and identity were confirmed by SDS-PAGE and Western blots (Chapter 3.2.5), respectively.

3.2.2 IgA antibodies form monomers and multimers

The produced IgA antibodies formed mainly monomers consisting of two heavy chains (HCs) and two light chains (LC). Nevertheless, in the absence of J chain co-expression, IgA antibodies associated to dimers and higher order structures as shown by SEC under native conditions (Figure 10). Among all IgA antibodies without J chain, similar SEC profiles were obtained with a major peak at about 15 mL elution volume representing IgA monomers. Between 13 mL and 10 mL elution volume, dimers and higher order multimers were eluted. Absolute elution volumes depend on the fast protein liquid chromatography (FPLC) system used, qualitatively no differences were observed. While dimers were separated from monomers, dimers and higher order structures were not well separated (Figure 10). Compared to monomers and dimers, relative differences in molecular weight for dimers and trimers are smaller and probably resulted in incomplete separation of these multimers. Therefore, in preparative SEC, monomers could be separated from dimers, higher order structures and fragments while separation of dimers and higher order structures was difficult to accomplish. For hTM and hKM IgA2, fragments at higher elution volumes were present in SEC profiles

(shown for hTM IgA2, Figure 10b). The area of the IgA monomer peaks at 280 nm was 60 to 85% of the total area of the UV signal. hPM IgA1 monomers eluted slightly earlier than hPM IgA2 monomers (Figure 10a), which differ in size due to the extended hinge region for IgA1 antibodies (Figure 1). In case of CM IgA2 monomers, the smaller elution volume as compared to hTM IgA2 monomers might be caused by the variable domains which differ in size and sequences and could result in more or less compact assembly (Figure 10b).

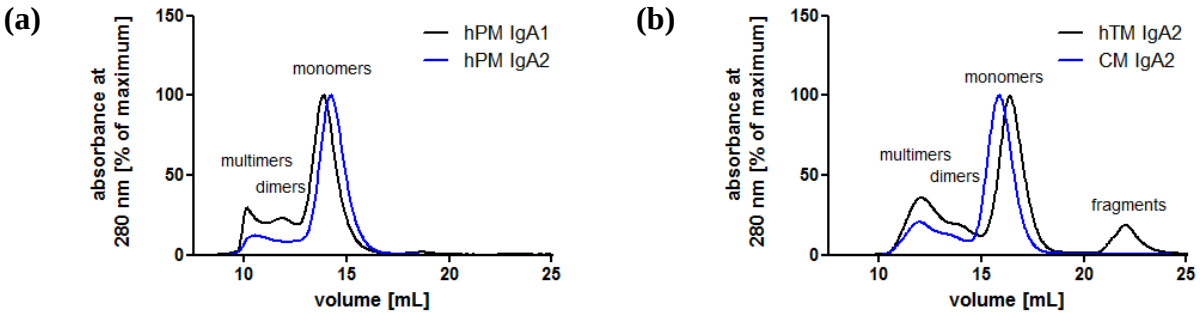

Figure 10 Exemplary size exclusion chromatograms of IgA1 and IgA2 antibodies lacking J chain co-expression. (a) IgA antibodies lacking J chain co-expression showed a major peak for monomeric molecules consisting of two heavy chains (HC) and two light chains (LC). At lower elution volumes, dimers and higher order multimers were eluted. The monomer peak of hPM IgA1 eluted earlier than for hPM IgA2 because of the larger size due to the extended hinge region. **(b)** As shown for hTM and CM IgA2 antibodies, chromatograms of IgA2 antibodies with different targets were comparable. However, hTM IgA2 antibody showed a peak at high elution volume, indicating the presence of fragments.

3.2.3 J chain co-expression promotes association of IgA multimers

Following evaluation of IgA antibodies without J chain by SEC under native conditions, IgAJ antibodies which were generated by co-expression of the J chain polypeptide were investigated. The J chain polypeptide associates with IgA dimers or multimers (Figure 1). As shown for hTM and CM IgA2 antibodies by SEC, co-expression with the J chain resulted in a reduction of monomers and an increase of dimers and higher order multimers. Monomer contents of IgA antibodies without J chain were 55% and 70% for hTM and CM IgA2, respectively (Figure 11). By J chain co-expression, the amount of monomers decreased to 27% and 20% for hTM and CM IgA2J, respectively. As discussed below, relative contents of dimers to higher order multimers differed between antibodies as well as clones producing a particular antibody (Figure 13).

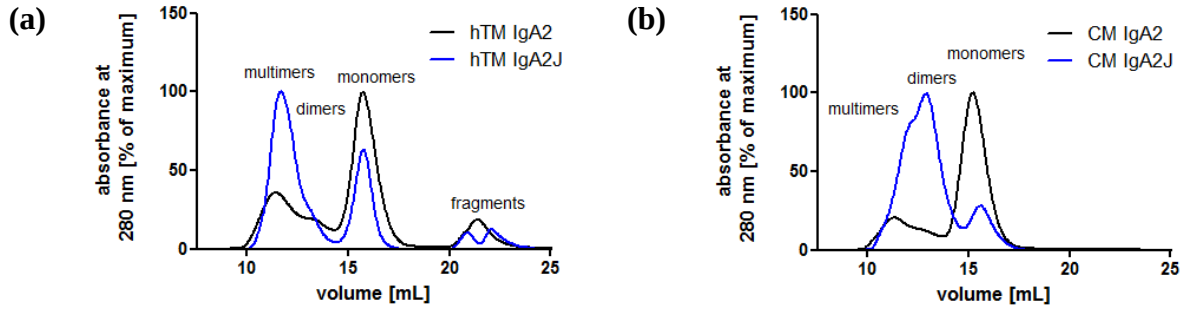

Figure 11 J chain co-expression promotes dimer and multimer formation of IgA antibodies. Comparison of hTM **(a)** and CM IgA2 **(b)** with and without J chain co-expression by size exclusion chromatography (SEC). Co-expression of the J chain resulted in a decrease of monomers and increase in dimers and multimers. Monomer contents were 56% and 75% for hTM and CM IgA2 antibodies, respectively. Monomer contents were 27% and 16% for hTM and CM IgA2J, respectively.

For preparative SEC-separated hPM IgA2J, Western blots revealed that the J chain was present in the dimer/multimer fraction only (Figure 12a). Moreover, H9D8- or Fuc$^-$-derived hPM IgA2J antibodies were analyzed by Western blots for J chain expression (Figure 12b). The difference in J chain expression for hPM IgA2J produced in H9D8 or Fuc$^-$ corresponded to monomer contents as analyzed by SEC. Compared to hPM IgA2 produced in H9D8, hPM IgA2 produced in Fuc$^-$ showed higher J chain expression and more dimers and multimers (Figure 12b and c).

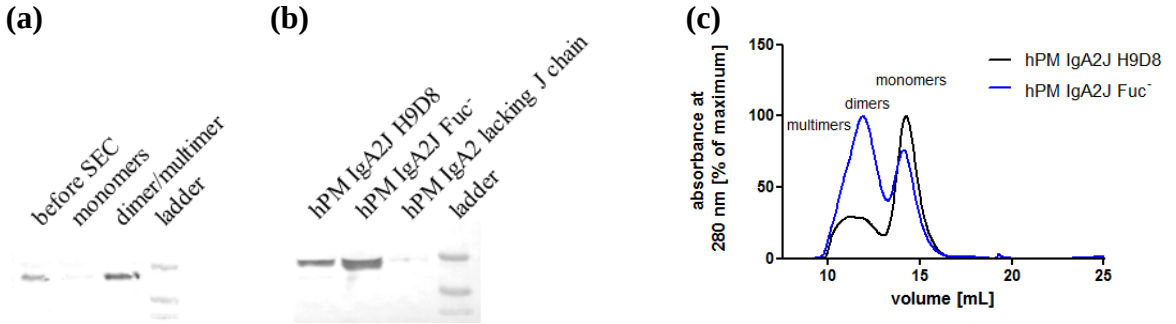

Figure 12 J chain expression and multimer formation for hPM IgA2J antibodies produced in different cell lines. (a) J chain was only present in the multimer fraction as shown for size exclusion chromatography (SEC)-separated hPM IgA2J by Western blot (lane 1: before separation, lane 2: monomers, lane 3: multimers; H9D8-derived). **(b)** J chain expression differed between hPM IgA2J antibodies produced in GEX-H9D8 (lane 1) and GEX-Fuc$^-$ (lane 2). **(c)** Increased J chain expression of hPM IgA2J Fuc$^-$-derived (blue) translated into reduced monomer contents compared to hPM IgA2J H9D8-derived (black) as shown by SEC.

In further clone developments for hTM IgA2J and CM IgA2J, clone screening for high J chain expression was conducted using anti-J chain Western blots (data not shown). Therefore, J chain expression was confirmed and relative expression levels could be compared for the tested clones. Clones with the highest intensities in anti-J chain Western blots were selected for cryogenic conservation, antibody production and purification.

For hTM and CM IgA2J, antibodies produced by different clones were purified to investigate the effect of different J chain expression levels on multimer formation. While J chain expression and SEC profiles were comparable for two hTM IgA2J clones, CM IgA2J clone 2 showed increased J chain expression in Western blots as well as fewer monomers in SEC profiles. Moreover within the multimer fraction, CM IgA2J clone 2 showed a shift towards more dimers as compared to CM IgA2J clone 1 (Figure 13a and b). Therefore, CM IgA2J produced from clone 2 was used for the preparation of dimers in subsequent preparative SECs. The preparation of clean dimers was difficult to accomplish because of the small relative difference in size of dimers and trimers as compared to dimers and monomers, factor 1.5 compared to factor 2, respectively. However, this procedure allowed for production of clean CM IgA2J dimers, only a minor shoulder of higher order structures was present as confirmed by analytical SEC (Figure 13c). The yield for the dimer preparation was about 9% of total protein load because only fractions eluting after the dimer peak maximum towards smaller molecule size were pooled prior to the second preparative SEC. The amount was sufficient for comparison of IgA2 monomers and IgA2J dimers in surface plasmon resonance kinetic analysis of antigen binding (Chapter 3.2.9) as well as proliferation inhibition assays (Chapter 3.3.1).

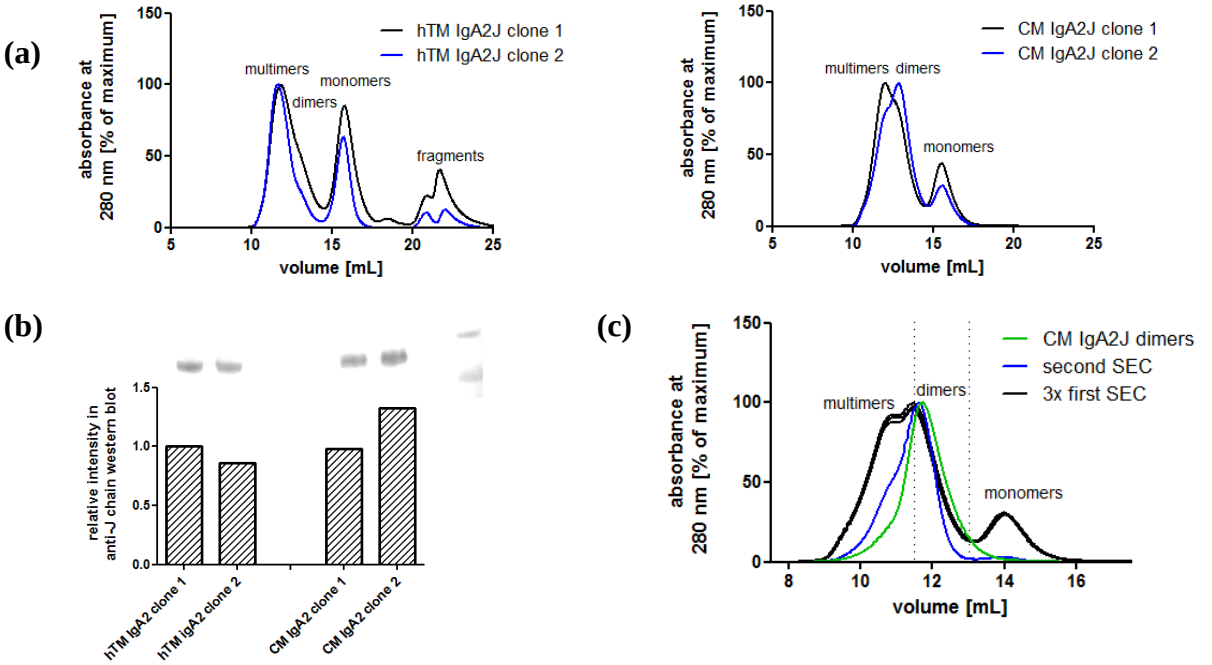

Figure 13 IgA multimerization and J chain expression of two hTM and two CM IgA2J antibody producing clones. (a) Analytical size exclusion chromatography (SEC) of two hTM IgA2J (left) and two CM IgA2J clones (right). Multimer and monomer contents were comparable for both hTM IgA2J clones while clone 2 of CM IgA2J showed an increased dimer content as compared to clone 1. **(b)** Relative J chain expression levels by Western blot (top). Intensities were assessed using imageJ software and calculated relative to hTM IgA2 clone 1 (column graph, bottom). For hTM IgA2J both clones showed comparable SEC profiles and similar J chain expression levels. In contrast, CM IgA2J clone 2 showed more dimers than clone 1 as well as a decrease in monomer contents and higher J chain expression. **(c)** CM IgA2J dimers were generated from clone 2 in two subsequent SECs by fractionating the right side of the dimer peak (vertical dotted lines). The first SEC was conducted three times to obtain sufficient material for the second SEC. Clean CM IgA2J dimers were generated as analyzed by additional analytical SEC (green).

As shown for hPM IgA2J, hTM IgA2J and CM IgA2J, clones with high J chain expression showed reduced monomer content in SEC profiles as compared to clones with lower J chain expression. CM IgA2J clones showed different dimer contents which was not observed for hTM IgA2J. The high dimer content of CM IgA2J clone 2 allowed for preparation of clean IgA2J dimers. For the antibodies generated, J chain expression levels differed between antibodies and clones for one antibody. In summary, J chain co-expression promotes the formation of dimers and higher order multimers of IgA antibodies.

3.2.4 Purified IgA antibodies are stable during long-time storage

Stability of IgA antibodies is especially a concern for IgA2m(1) allotype due to the lack of disulfide bonds between LC and HC (Lohse et al. 2012) (Figure 1). Using SEC, stability of IgA antibodies was investigated after long-time storage for up to 2 years. As shown for hPM

IgA2 after 1 year storage at 4 °C in PBS, monomer preparations were not prone to aggregation or fragmentation, monomer content exceeded 95%. Affinity-purified hPM IgA1 and hTM IgA2 showed comparable SEC profiles after 2 and 1.5 years storage, respectively (Figure 14b and Figure 14c).

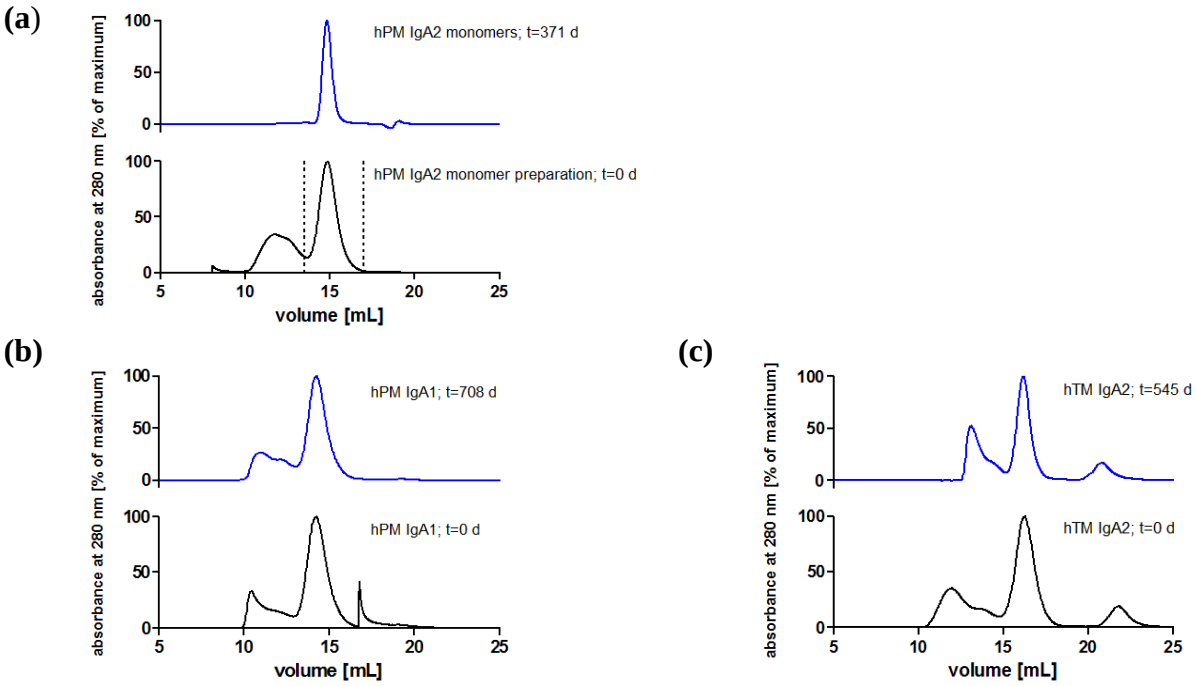

Figure 14 IgA antibodies are stable during long-time storage. Long-time stability (blue) of monomers and non-separated IgA was investigated by size exclusion chromatography (SEC). **(a)** hPM IgA2 monomers were generated and after 1 year storage no aggregation or fragmentation was observed. Fractions pooled for monomer generation are indicated (vertical dotted line). After 2 and 1.5 years storage, comparable SEC profiles were obtained for hPM IgA1 **(b)** and hTM IgA2 **(c)**, respectively. Before and after storage hPM IgA1 had 74% and 70% monomer contents, respectively. In case of hTM IgA2, monomer contents were 56% before and after storage. Different chromatography systems used for analysis resulted in slightly different elution volumes (Chapter 2.4.4). For hPM IgA1 t=0 days, the program was paused at about 16.5 mL resulting in the artificial spike in the chromatogram.

The generated IgA monomers and non-separated IgA antibodies were stable during long-time storage at 4 °C in PBS.

3.2.5 Heavy chain-light chain association differs between IgA1 and IgA2 isotype antibodies

Evaluation of IgA antibodies in non-reducing sodium dodecyl sulfate polyacrylamide gel electrophoresis (SDS-PAGE) is more complex than for IgG antibodies. IgA1 and IgA2 antibodies differ in inter-chain disulfide bonds (Chapter 1.1.2, Figure 1). In reducing SDS-

PAGE, IgA and IgG antibodies showed comparable band patterns with two bands corresponding to the size of HC and LC (compare Figure 15a and Figure 17c).

IgA1 and IgA2 antibodies showed comparable SEC profiles (Figure 10), whereas distinct band patterns were observed between the two subclasses in SDS-PAGE analysis (Figure 15). The main difference in non-reducing gels was the presence of major bands corresponding to the size of free HC and LC dimers (HC2 and LC2, respectively) for IgA2 antibodies which were absent or less pronounced for IgA1 antibodies. IgA2 antibodies generated for this study were of IgA2m(1) allotype, which does not possess disulfide bonds between LC and HC but instead between the two LCs of an IgA2 monomer unit (Chapter 1.1.2, Figure 1). This resulted in the formation of HC homodimers (HC2) and molecules containing two HC and one LC in denaturing conditions used for SDS-PAGE (Figure 15). This dissociation was also observed for IgA2 antibodies without fragments in SEC profiles. Hence, dissociation was a result of SDS-PAGE conditions and not present under native conditions as used for SEC. For both, IgA1 and IgA2 antibodies, free LC monomers were observed as well while no fragments were observed in SEC profiles. This indicates that some LCs were not covalently linked to IgA1 HCs and some IgA2 LC did not form LC homodimers. Both isotypes showed weak bands corresponding to the size of multimers which were detected in SEC as well and were formed to some degree in the absence of J chain (Chapter 3.2.2). After reduction, IgA1 and IgA2 had comparable band patterns with two bands corresponding to the size of HC and LC. Identity of bands was confirmed by anti-human kappa LC or anti-human alpha HC Western blots (Figure 15). The more diffuse bands of HCs for IgA2 antibodies could be caused by the presence of multiple N-glycosylation sites. Due to an additional glycosylation site within the variable domain, hPM IgA2 and IgA1 possess five and three N-glycosylation sites per HC, respectively (Figure 1) and N-glycans can differ in both size and charge (Chapter 3.2.7).

Purity of purified IgA antibodies was confirmed by SDS-PAGE in reducing and non-reducing conditions (Figure 15). As estimated visually in colloidal Coomassie-stained gels, purity exceeded 95% after single-step affinity chromatography. No additional bands were present in reducing conditions and bands in non-reducing conditions corresponded to characteristic LC and HC associations.

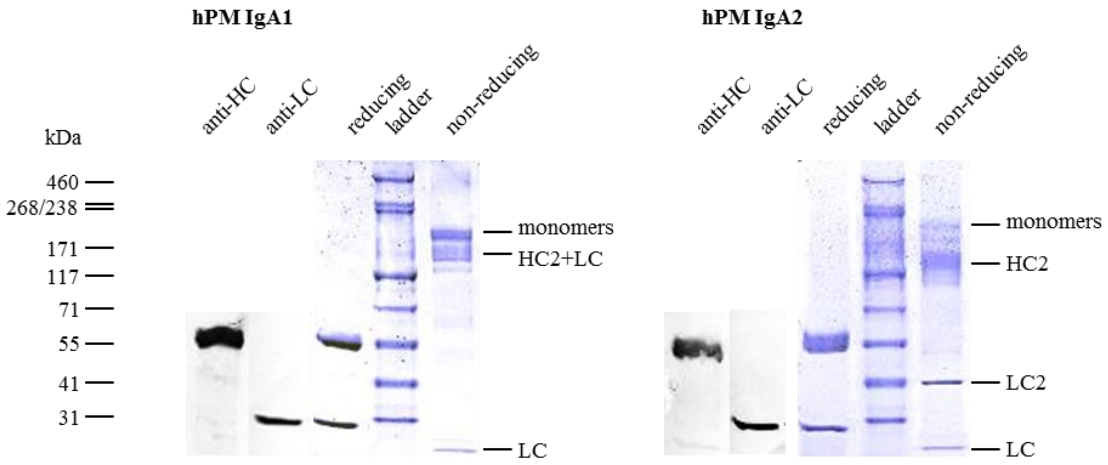

Figure 15 Purity assessment and comparison of IgA1 and IgA2 by sodium dodecyl sulfate polyacrylamide gel electrophoresis (SDS-PAGE) and Western blots. As shown for hPM IgA1 and IgA2 antibodies by SDS-PAGE using 4-15% gradient gels, affinity purified antibodies exclusively showed bands as expected for IgA antibodies. In reducing conditions only bands corresponding to the size of heavy chain (HC) and light chain (LC) were detected. Identities of bands in reducing conditions were confirmed by anti-HC and anti-LC Western blots (2 left lanes). In non-reducing conditions, IgA1 antibodies showed a major band corresponding to monomers (HC2+LC2) and minor bands for free LC and monomers lacking one LC (HC2+LC). In contrast, IgA2 antibodies dissociated mainly in HC and LC dimers (HC2 and LC2, respectively) and LC. This is characteristic for IgA2 antibodies due to the lack of disulfide bonds between LCs and HCs (Chapter 1.1.2). Bands with less intensity were detected which corresponded to the size of IgA2 monomers or IgA2 monomers lacking one LC.

Enzymatic deglycosylation of hPM IgA1J using PNGase F confirmed N-glycosylation and resulted in increased migration speed for the HC when compared to an untreated sample (Figure 16). In contrast, the migration of non-glycosylated LC was not effected by glycosidase treatment. Moreover, a shift in migration speed for the faint band underneath the LC was observed. This band corresponded to the size of the J chain which possesses one N-glycosylation site.

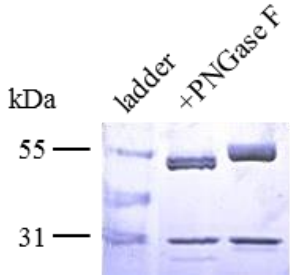

Figure 16 hPM IgA1J N-glycosylation was confirmed by enzymatic deglycosylation followed by sodium dodecyl sulfate polyacrylamide gel electrophoresis (SDS-PAGE). After treatment of hPM IgA1J with PNGase F, the migration speed for the heavy chain was increased (middle lane) while no shift in migration speed was observed for the light chain or the control without PNGase F (right lane) in reducing SDS-PAGE using a 4-15% gradient gel. The faint band underneath the light chain shifted in migration speed too, which corresponds to the size of the J chain possessing one N-glycosylation site.

Subsequent to analysis of monomer contents by SEC and confirmation of purity and identity of IgA antibodies by SDS-PAGE and Western blots, target binding was assessed by ELISA, surface plasmon resonance and flow cytometry (Chapters 3.2.8 and 3.2.9).

3.2.6 IgA Cα3 domain causes IgA-like multimerization when fused to an IgG antibody

Mixed-isotype hTM IgG-Cα3 construct was compared with hOM IgG antibody by SEC and SDS-PAGE. The construct was generated by fusing IgA1 Cα3 domain to the C terminus of full-length hTM IgG heavy chain (Figure 17a). In SEC profiles of hTM IgG-Cα3 construct, a major peak for monomers and peaks for dimers and higher order multimers were detected (Figure 17b). This was in contrast to SEC profiles of IgG antibodies which possessed more than 95% monomers. SEC analysis of three hOM IgG purifications revealed a mean monomer content of 98%. Hence, fusion of the Cα3 to IgG resulted in increased IgA-like dimerization and multimerization (compare Figure 17b to Figure 10).

Purity of hTM IgG-Cα3 construct and hOM IgG was confirmed by SDS-PAGE (Figure 17c). In reducing gels, for mixed-isotype hTM IgG-Cα3 construct bands corresponding to the size of LC and modified HC were detected. The latter consisting of IgA1 Cα3 domain including the tailpiece fused to the C terminus of IgG HC. Compared to reduced hOM IgG control, the HC but not the LC of hTM IgG-Cα3 constructs showed bands corresponding to higher molecular weight. In non-reducing gels, hTM IgG-Cα3 monomers showed an increase in size when compared to IgG due to the additional IgA-derived domain. Moreover, bands corresponding to the size of hTM IgG-Cα3 dimers and higher order multimers were present. SDS-PAGE band patterns in non-reducing conditions corresponded well with SEC profiles.

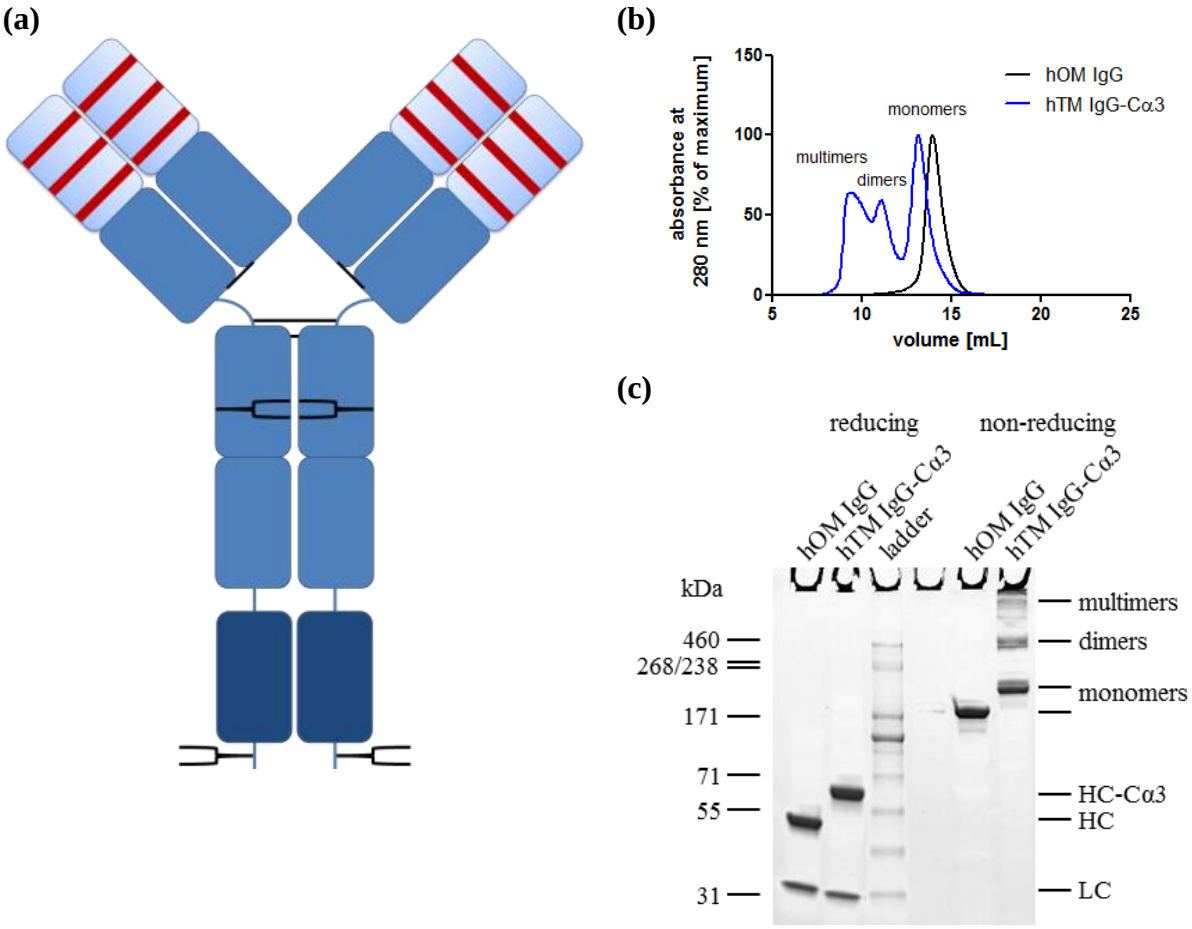

Figure 17 hTM IgG-Cα3 construct showed IgA antibody-like association into dimers and multimers, a comparison to hOM IgG antibody. (a) Schematic illustration of mixed-isotype hTM IgG-Cα3 construct including 2 N-glycosylation sites (*Y*) per heavy chain. Variable domains including complementary-determining regions (light blue with red bars), IgG Cγ, common Cκ (both blue) and Cα3 domains (dark blue) are indicated. **(b)** While hOM IgG antibody (black) showed one monomer peak in size exclusion chromatography, hTM IgG-Cα3 construct (blue) showed a major monomer peak as well as dimers and higher order multimers. Due to the larger size, hTM IgG-Cα3 monomers eluted at smaller elution volumes compared to hOM IgG monomers. **(c)** Clean hTM IgG-Cα3 construct and hOM IgG were prepared by affinity chromatography as shown by sodium dodecyl sulfate polyacrylamide gel electrophoresis using a 4-15% gradient gel. In reducing conditions, bands corresponding to the size of light and heavy chains or light and modified heavy chains were detected for hOM IgG or hTM IgG-Cα3, respectively. No additional bands were detected. For hTM IgG-Cα3 construct in non-reducing conditions, a major band corresponding to the size of hTM IgG-Cα3 monomers, and bands corresponding to the size of dimers and higher order multimers were present. The size of hTM IgG-Cα3 construct monomers in non-reducing conditions and heavy chain in reducing conditions was increased as compared to hOM IgG antibody and heavy chain, respectively.

In conclusion, IgG-IgA mixed-isotype hTM IgG-Cα3 construct and hOM IgG antibody were successfully generated. Monomer and multimer contents of the mixed-isotype construct were comparable to IgA antibodies. Purity of both, the mixed-isotype construct and hOM IgG antibody, was confirmed. Mixed-isotype construct binding to FcαRI was investigated (Chapter 3.2.10) because most of the amino acid residues involved in binding this Fc receptor

lye within the Cα3 domain (Chapter 1.1.4). Target cell binding and biofunctionality of anti-CD20 hOM IgG and IgA2 antibodies were evaluated (Chapter 3.3.6).

3.2.7 Human N-glycosylation profiles of IgA antibodies

Glycosylation impacts stability, biological function and clearance of antibodies (Arnold 2007). IgA antibodies possess a more complex N-glycosylation than IgG antibodies and IgA N-glycans point towards to outside of the molecule (Mattu et al. 1998). IgA1 antibodies have 2 N-glycosylation sites and IgA2m(1) antibodies have 4 N-glycosylation sites per heavy chain as compared to 1 N-glycosylation site for IgG antibodies (Figure 1). Depending on the amino acid sequence, antibodies might have additional N-glycosylation sites within the variable domains as in case of hPM and CM antibodies.

Here the N-glycan profiles for hTM IgA2 and hOM IgA2 were analyzed to evaluate predominant glycan structures and the degree of sialylation for recombinant IgA antibodies produced by the human GEX expression system.

For the two IgA antibodies analyzed, complex N-glycosylation profiles were obtained by hydrophilic-interaction liquid chromatography (HILIC) with subsequent electrospray ionization-quadrupole time-of-flight mass spectrometry (ESI-qTOF) mass spectrometry of liberated and labeled N-glycans. All three N-glycan types which can be attached to proteins were identified: complex, oligomannose and hybrid type (Varki et al. 2009) (Figure 18).

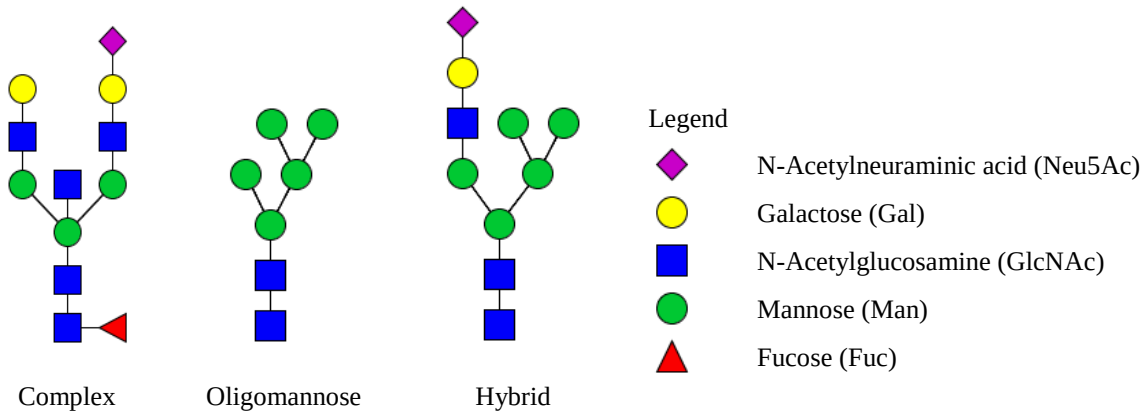

Figure 18 Different types of N-glycans which can be attached to asparagine residues of proteins. Three different types of N-glycans can be attached to the asparagine-x-serine/threonine sequon of a protein: oligomannose, complex and hybrid type. During translation, within the endoplasmic reticulum (ER) an oligomannose glycan with three terminal glucose residues is attached to the protein. This glycan is further enzymatically processed in the ER and during vesicular transport though the Golgi compartments to yield one of the three different types of N-glycans shown here. Adopted from Varki et al. (Varki et al. 2009).

Non-complex type N-glycans included 25% oligomannose plus 8% hybrid type and 19% oligomannose and 9% hybrid type for hTM IgA2 and hOM IgA2, respectively (Table 4).

Table 4 Three types of N-glycans were detected on IgA antibodies.

	Relative molar amount of glycan types [%]		
Antibody	**Complex type**	**Oligomannose**	**Hybrid type**
hTM IgA2	64	25	8
hOM IgA2	66	19	9

About 4% and 5% of N-glycans could not be annotated for hTM and hOM IgA2, respectively.

For both hTM IgA2 and hOM IgA2, the most prominent complex type glycan structure was sialylated, digalactosylated, biantennary and fucosylated. More than 60% of complex type N-glycans of both antibodies were sialylated (Table 5).

Table 5 Relative abundance of glycan parameters for complex type N-glycans.

	Relative molar amount of glycan parameters [%]					
Antibody	**F1**	**B1**	**S0**	**S>0**	**G0**	**G>0**
hTM IgA2	64	15	32	62	3	91
hOM IgA2	79	9	29	64	11	81

F: glycans with fucose, B: glycans with bisecting N-acetylglucosamine, S: glycans with sialic acid, G: glycans with galactose, numbers indicate monomer units per N-glycan

In summary, human N-glycosylation was confirmed for both, hTM IgA2 and hOM IgA2 antibodies. Recombinant IgA antibodies showed complex, oligomannose and hybrid type N-glycans. As expected for a human expression system, non-human glycan structures like α(1-3)-linked galactose or N-glycolylneuraminic acid were not detected. This is in contrast to other expression systems used for the production of therapeutic antibodies (Jeffries 2009).

3.2.8 IgA antibodies bind their corresponding antigens and target cell lines

Target binding of IgA antibodies was investigated by ELISA, immunofluorescence, flow cytometry and surface plasmon resonance (Chapter 3.2.9). Antigen and target cell binding was a prerequisite for subsequent evaluation of IgA antibodies in biofunctional assays (Chapter 3.3). Different cancer cell lines were used depending on the antigens present on the surface of a target cell and the antibody to be tested (Table 6).

Table 6 Overview of cancer cell lines used in different assays.

Cell line	Origin	Antibodies binding cell line (antigen binding sites)	Assays using cell line
A-431	Epidermoid carcinoma	CM (++)	Proliferation inhibition
BT-474	Breast cancer	hTM (+++)	Proliferation inhibition, ADCP
KG1	Acute myelogenous leukemia	Negative control for hPM	IF
Ls174T	Colon cancer	hTM (+), CM (+)	ADCC
Panc-1	Pancreas cancer	hTM (+), CM (++), hKM (+), hPM (++)	ADCC
Raji	Burkitt's lymphoma	hKM (+), hOM (n.d.)	Flow cytometry
SK-BR-3	Breast cancer	hTM (+++), CM (+)	ADCC
T47D	Breast cancer	hPM (+++)	ADCP
ZR-75-1	Breast cancer	hPM (+++)	Flow cytometry, IF, ADCC, ADCP

IF: immunofluorescence; ADCC: antibody-dependent cellular cytotoxicity; ADCP: antibody-dependent cellular cytotoxicity; antigen binding sites were determinded using IgG antibodies; antigen binding sites, +: $1x10^4$-$1x10^5$; ++ $1x10^5$-$5x10^5$; +++ >$5x10^5$; n.d.: not determined

hPM IgA antibody binding to a mixed glycan-peptide epitope characteristic for TA-MUC1 was shown by ELISA. To confirm dependency on the tumor-associated glycan of the epitope, a non-glycosylated peptide served as negative control. As shown for hPM IgA1, minor binding was shown for the peptide lacking glycosylation. The signal for the non-glycosylated peptide was less than 10% of the signal for the glycan-peptide for the highest concentration tested (Figure 19a). Like hPM IgG (data not shown), hPM IgA1 antibodies are specific for the glycan-peptide epitope of TA-MUC1 as shown by concentration-dependent binding signals (Figure 19a).

For hPM IgA2J, binding to ZR-75-1 target cells was shown by flow cytometry. Concentration-dependent binding in percent positive cells and median fluorescent intensity (MFI) was observed (Figure 19b).

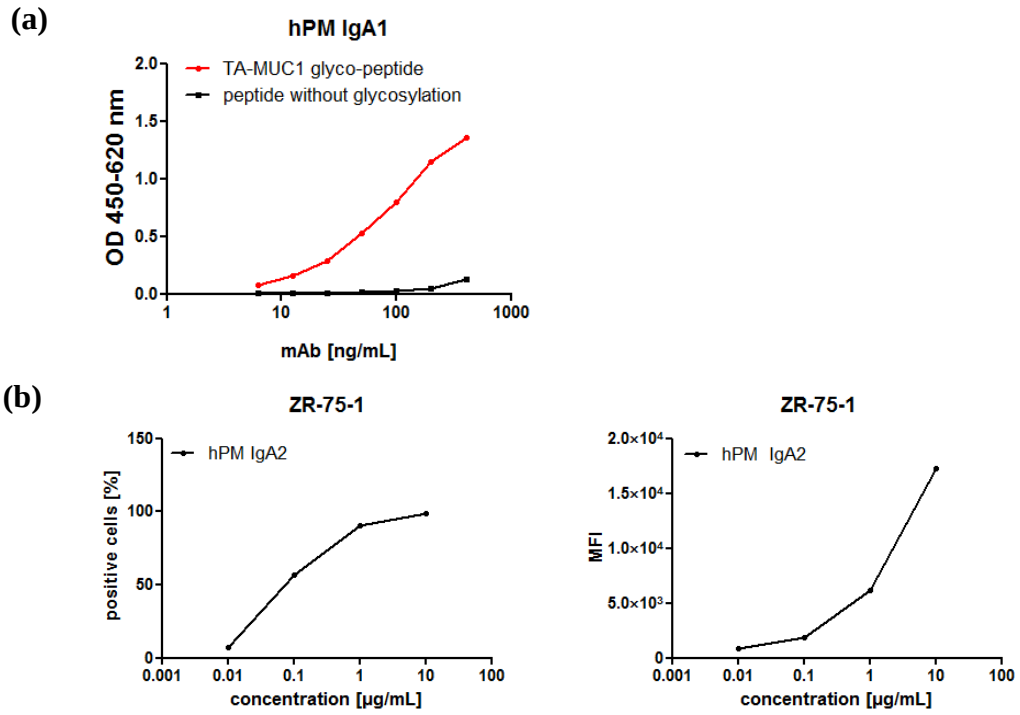

Figure 19 Specific antigen binding and ZR-75-1 target cell binding of hPM IgA antibodies were confirmed by enzyme-linked immunosorbent assay (ELISA) and flow cytometry. (a) Antigen ELISA using TA-MUC1 peptide (red) and non-glycosylated MUC1 peptide as negative control (black). hPM IgA1 specifically binds to the glycosylated TA-MUC1 peptide, less than 10% binding signal for the non-glycosylated peptide at the highest concentration tested. **(b)** Concentration-dependent binding of hPM IgA2 to ZR-75-1 target cells was shown as percent positive cells (left) and median fluorescence intensity (MFI, right). Mean values of duplicates are shown. One out of at least two independent experiments is shown.

Specific binding to target cells was shown by immunofluorescence microscopy. hPM IgA1 showed binding to TA-MUC1-positve ZR-75-1 but no binding to the antigen-negative KG1 cell line was detected. hPM IgG positive control showed comparable specificity for ZR-75-1. Controls with secondary antibodies specific for IgG or IgA only were negative (Figure 20).

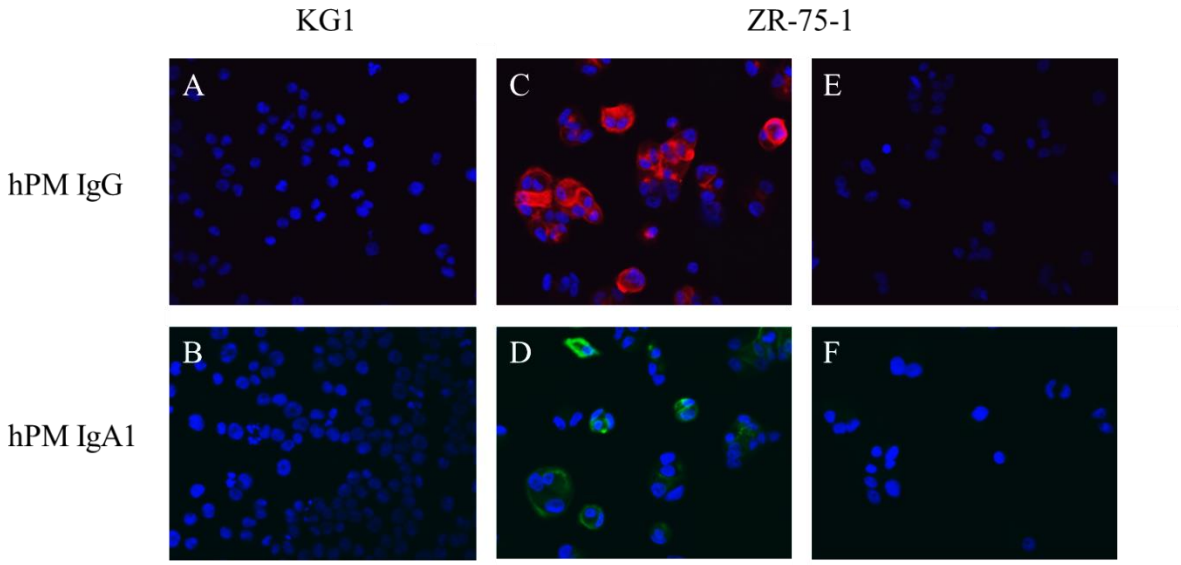

TA-MUC1 expression	-	+	+
antibody added	+	+	-

Figure 20 Immunofluorescence microscopy confirmed specific binding of hPM IgA1 to target cells. hPM IgG positive control antibody (upper panel, red staining) and hPM IgA1 (lower panel, green) using DAPI (blue) for nuclei counter staining. TA-MUC1-negative cell line KG1 served as negative control using 10 µg/mL hPM IgG or IgA1 (A and B). Binding to ZR-75-1 target cells was shown for hPM IgG and IgA1 using 1 µg/mL (C and D). Secondary detection antibodies for IgG and IgA alone did not result in unspecific staining of ZR-75-1 target cells (E and F).

ELISA was used to confirm antigen binding for hTM and CM IgA2 antibodies which target EGF receptors. For hTM and CM IgA2 antibodies antigen binding was confirmed using Her2 and EGFR ELISA, respectively. hPM IgA2 and hTM IgA2 served as matched isotype negative control in Her2 and EGFR ELISA, respectively. hTM and CM IgA2 antibodies showed concentration-dependent binding, while negative controls did not bind (Figure 21). Antigen binding of hTM IgG-Cα3 construct was confirmed by IgG-specific Her2 ELISA (data not shown).

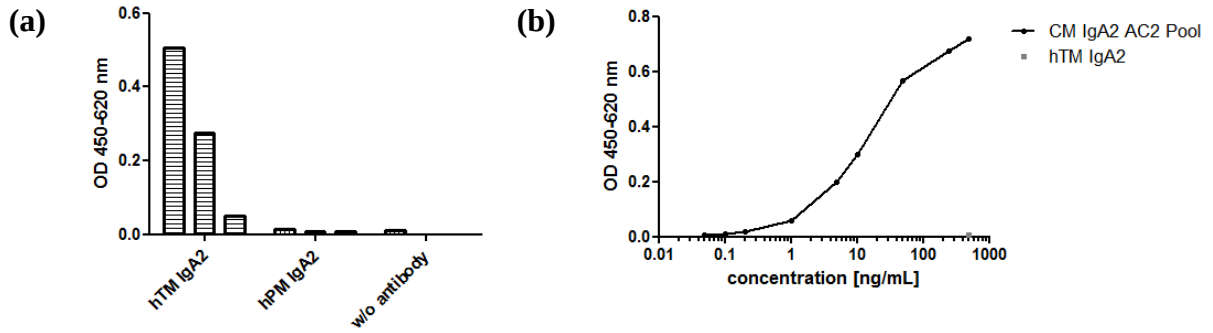

Figure 21 Antigen binding of hTM IgA2 and CM IgA2 was shown by enzyme-linked immunosorbent assay (ELISA). Her2 and EGFR were coated on ELISA plates to investigate hTM IgA2 and CM IgA2 binding, respectively. **(a)** Transiently expressed hTM IgA2 was tested for antigen binding to Her2. Three dilutions (undiluted, 1:10 and 1:100 dilution from left to right) of non-purified supernatant samples from cells expressing hTM IgA2 and hPM IgA2 were used. Concentration-dependent binding of hTM IgA2 to Her2 was confirmed. Irrelevant matched isotype hPM IgA2 and undiluted supernatant without antibody negative controls did not bind. **(b)** For CM IgA2, antigen binding was confirmed for purified antibody. Irrelevant matched isotype hTM IgA2 served as negative control. Mean values of duplicates are shown.

For hKM IgA2 antibody, target cell binding was confirmed in early stage of clone development. Therefore, non-purified culture supernatants of cell pools were used in flow cytometry binding experiments to Raji target cells. No saturation was reached, however, hKM IgA2 antibodies bound Raji target cells concentration-dependent (Figure 22a). Binding of hKM IgA2 antibody to TF antigen was shown by surface plasmon resonance using immobilized asialoglycophorin (AGP). AGP carries multiple O-glycosylation sites which, due to the lack of sialic acid residues, include the TF antigen (Piscano et al. 1993). Concentration-dependent binding of hKM IgA2 monomers to AGP immobilized on a CM5 chip was shown. For antigen binding analysis, the difference in response units (RU) before and after injections was considered. Relative changes of RU were proportional to hKM IgA2 concentrations injected (Figure 22b).

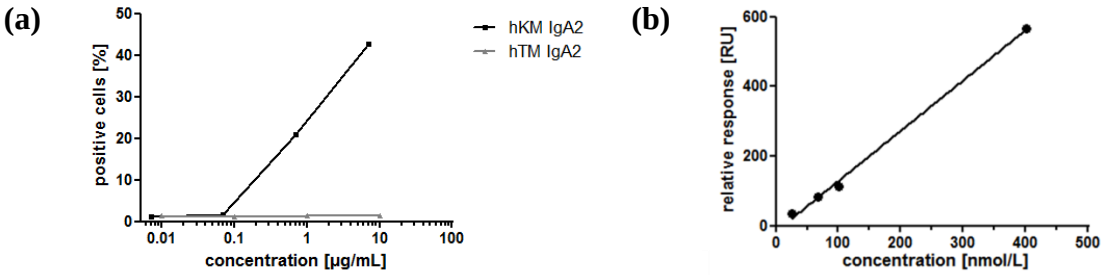

Figure 22 Binding of hKM IgA2 to Raji target cells and immobilized asialoglycophorin (AGP) by flow cytometry and surface plasmon resonance, respectively. (a) Unpurified supernatant of hKM IgA2 antibody producing cell culture was used in flow cytometry experiments. IgA antibody concentrations were determined by titer enzyme-linked immunosorbent assay and purified hTM IgA2 antibody served as negative control. Mean values of duplicates are shown. **(b)** AGP carrying the TF antigen was immobilized on one flow cell of a CM5 chip and a second flow cell served as reference. Varying concentrations of purified hKM IgA2 monomers were injected at a flow rate of 10 µL/min for 2 min association time and followed by 5 min dissociation time. Concentration-dependent biding was illustrated by relative maximal response units as a function of hKM IgA2 antibody concentration. One out of two independent SPR experiments.

hOM IgA2 and IgG antibody binding to target cells was shown by flow cytometry and confirmed in biofunctional B cell depletion assays (Chapter 3.3.6).

In summary, all antibodies retained antigen binding when switching to IgA isotype or changing the format as for mixed-isotype hTM IgG-Cα3 construct. Moreover, specific binding of hPM IgA1 to antigen-positive cells was confirmed by immunofluorescence microscopy. For hPM, hKM and hOM IgA antibodies, binding to target cell was shown by flow cytometry. For hTM and CM IgA2 antigen binding kinetic was investigated by surface plasmon resonance (Chapter 3.2.9) and target cell binding was indirectly shown in biofunctional assays (e.g. inhibition of target cell proliferation, Chapter 3.3.1).

3.2.9 IgA dimers show increased antigen binding avidity compared to IgG antibodies

Surface plasmon resonance was used to compare antigen binding kinetics of IgG and IgA antibodies. Her2 or EGFR were immobilized on CM5 chips to evaluate binding of hTM or CM antibodies, respectively. The EGFR chip was also used to compare binding kinetics of CM IgA2 monomers and IgA2J dimers.

Binding kinetics of hTM IgA2 monomers to Her2 immobilized on a CM5 chip was investigated. Injections of multiple antibody concentrations revealed comparable binding kinetics for hTM IgA2 monomers and IgG antibodies. Both isotypes showed rapid association within 5 minutes, followed by slow dissociation rates within 15 minutes. Equilibrium dissociation constants for IgA and IgG were 0.67 nM and 0.16 nM, respectively (Figure 23).

Both, hTM IgA2 and IgG showed high avidity sub-nanomolar equilibrium dissociation constants in a comparable range.

(a) hTM IgA2 monomers **(b)** hTM IgG

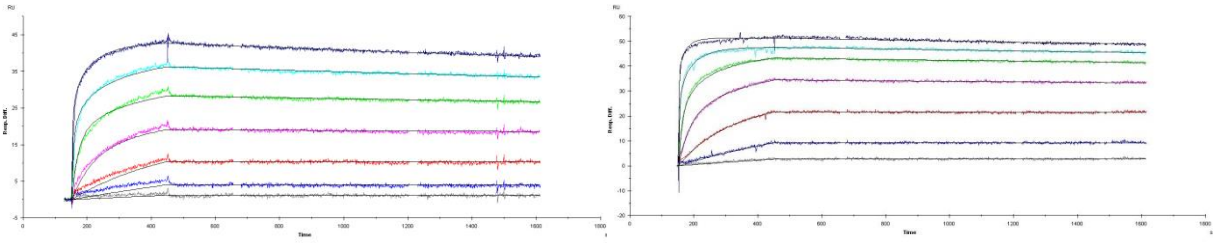

Figure 23 Kinetic analysis of hTM IgA2 monomers and hTM IgG binding to recombinant Her2. Her2 was immobilized on one flow cell of a CM5 chip and a second flow cell served as reference. Varying concentrations of hTM IgA2 monomers **(a)** or hTM IgG **(b)** were injected at a flow rate of 50 µL/min for 5 min association time and followed by 17 min dissociation time. After dissociation the chip was regenerated by subsequent 1 min injections of 10 mM glycine pH 1.5 and 10 mM NaOH. The difference between the flow cell with immobilized Her2 and reference flow cell was plotted. For each antibody, one out of two independent experiments is shown.

As for hTM, CM IgA2 monomers bound their antigen in a similar concentration range as CM IgG. Injections of multiple antibody concentrations revealed comparable binding kinetics for CM IgA2 monomers and IgG antibodies. Equilibrium dissociation constants for IgA2 and IgG were 47 nM and 20 nM, respectively, indicating high avidity binding in low nanomolar ranges (Figure 24). For both isotypes, sensorgrams had similar shapes, rapid association within 5 minutes, followed by faster dissociation rates within 15 minutes as compared to hTM IgA2 and IgG antibodies binding to Her2 (Figure 23). CM IgA2J dimers had an about 17-fold lower equilibrium dissociation constants compared to CM IgA2 monomers, 2.8 nM compared to 47 nM, respectively. Association of CM IgA2J dimers was slower compared to CM IgA2 monomers and IgG while CM IgA2J dimers showed decreased dissociation rates compared to CM IgA2 monomers and IgG antibodies (Figure 24). It was shown that binding of monomeric antibodies, either IgA2 or IgG, results in higher dissociation constants compared to dimeric IgA2 antibodies. This indicates an increase in avidity which could be attributed to higher valence of dimeric antibodies.

(a) CM IgA2 monomers

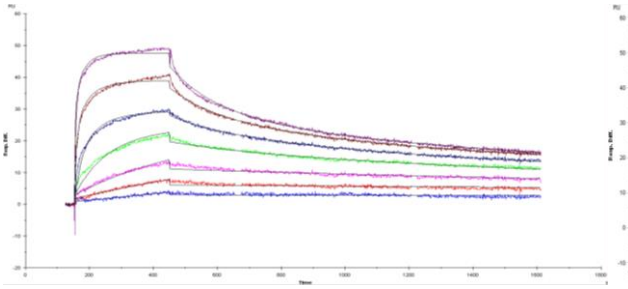

(b) CM IgA2 dimers

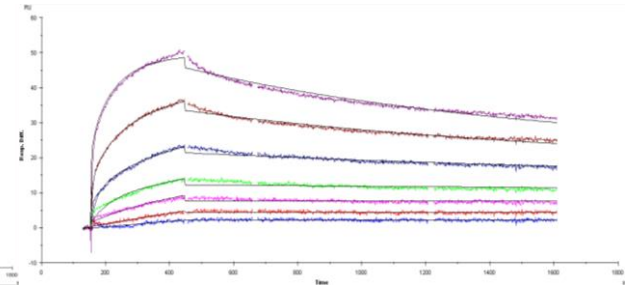

(c) CM IgG

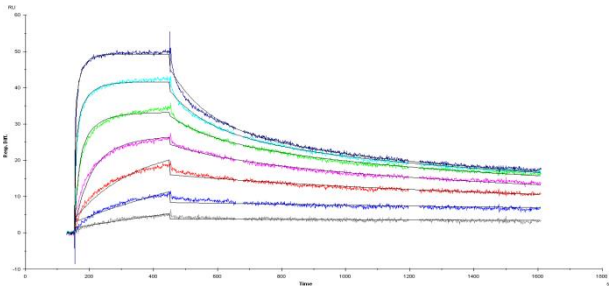

Figure 24 Kinetic analysis of CM IgA2 monomers, CM IgA2J dimers and CM IgG binding to recombinant EGFR. EGFR was immobilized on one flow cell of a CM5 chip and a second flow cell served as reference. Varying concentrations of CM IgA2 monomers **(a)**, CM IgA2J dimers **(b)** or CM IgG **(c)** were injected at a flow rate of 50 µL/min for 5 min association time and followed by 17 min dissociation time. After dissociation the chip was regenerated by a 24 s injection of 10 mM NaOH. The difference between the flow cell with immobilized EGFR and reference flow cell was plotted. One out of two (IgA2 monomers and IgG) and one (IgA2J dimers) independent experiments is shown.

In kinetic analysis, CM IgA2J dimers showed higher binding avidity compared to IgA2 monomers or IgG antibodies. In contrast, hTM and CM IgA2 monomers showed comparable binding kinetics like the corresponding IgG isotype antibodies. Therefore, it could be shown that tetravalence of dimeric IgA results in stronger antigen binding as compared to bivalent monomeric antibody formats regardless of the isotype.

3.2.10 Recombinant IgA antibodies bind Fc alpha receptor I

The main Fc receptor for IgA antibodies is Fc alpha receptor I (FcαRI; also called CD89) which is expressed on the surface of immune effector cells. Upon crosslinking of FcαRI cellular activation takes place that could result in effector functions against cancer cells (Chapter 1.1.4, Figure 2). Binding to FcαRI is a prerequisite for Fc-mediated effector functions of IgA antibodies. Hence, binding of IgA antibodies to commercially available, recombinant FcαRI was investigated by ELISA. Compared to ELISA formats relying on antibody-antigen binding, higher concentrations were needed to investigate the less affine antibody-Fc receptor interaction which is in the micromolar range (Wines et al. 1999).

Concentration-dependent binding was shown for both, monomers and multimer-containing IgA preparations. Higher signals were obtained for IgA multimers than for monomers using same mass concentrations and controls lacking FcαRI or IgA antibody were negative (data not shown). Higher signals for multimers could be caused by increased Fc avidity or more binding sites for secondary detection antibody on multimeric IgA antibodies. Binding of CM IgA2 monomers to FcαRI was shown (Figure 25a).

Mixed-isotype hTM IgG-Cα3 construct binding to FcαRI was investigated because most of the residues responsible for FcαRI binding are within IgA Cα3 domain (Chapter 1.1.4, Figure 2). Compared to hTM IgG control, hTM IgG-Cα3 bound to FcαRI (Figure 25b). Specificity of receptor binding was shown by inhibition with hTM IgA2. In the presence of 50 µg/mL hTM IgA2, signals of hTM IgG-Cα3 were reduced to the level of hTM IgG. Therefore, hTM IgG-Cα3 could interact with both IgA and IgG specific receptors on the surface of immune effector cells. However, binding signals were low as compared to IgA antibodies binding to FcαRI.

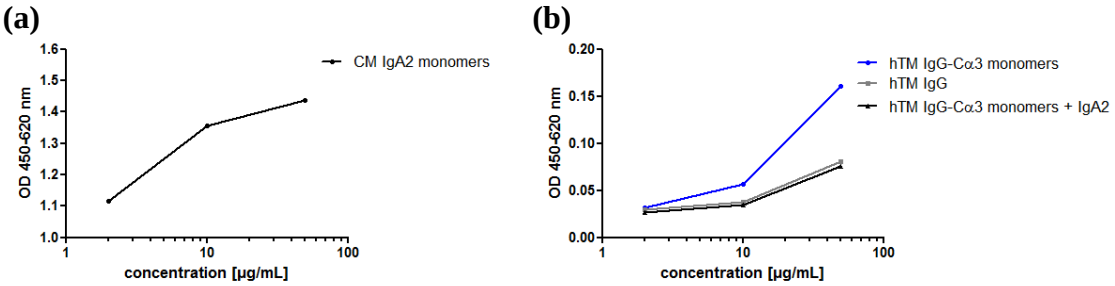

Figure 25 Specific binding of IgA antibody and mixed-isotype construct to FcαRI extracellular domain. Mean values of duplicates are shown. One out of at least two independent experiments is shown. **(a)** CM IgA2 monomers binding to recombinant FcαRI was shown by enzyme-linked immunosorbent assay (ELISA). **(b)** Mixed-isotype hTM IgG-Cα3 construct (blue) binding to FcαRI was shown by ELISA. Specificity was shown by inhibition with 50 µg/mL hTM IgA2 (black). Controls with hTM IgG isotype antibodies (grey) resulted in marginal background signals.

Antibody concentration-dependent binding to the main IgA Fc receptor was confirmed for the recombinant monoclonal IgA antibodies. Moreover, Cα3 domain fused to IgG enabled IgG-IgA mixed-isotype antibody to bind the IgA receptor. While binding was much weaker for IgG-IgA mixed-isotype construct, specificity was shown by inhibition of the interaction with IgA antibodies. Subsequently, IgA antibodies were investigated in biofunctional assays to elucidate mechanisms of action against cancer cell lines.

Together, biochemical integrity was confirmed subsequent to purification and IgA antibodies associated into characteristic monomers, dimers and multimers. Co-expression of the J chain polypeptide was shown by Western blots and resulted in increased association to dimers and higher order multimers. In kinetic experiments by surface plasmon resonance, comparable antigen binding of both, IgA and IgG isotype monomers, was shown. In contrast, IgA2 dimers bound with increased avidity to their target as compared to monomeric antibodies. Next, biofunctional assessment of IgA antibodies by Fab- and Fc-mediated modes of action against cancer cell lines was conducted to elucidate the potential of IgA antibodies for cancer immunotherapy.

3.3 Novel IgA antibodies for cancer immunotherapy – mechanisms of action

To evaluate the potential of tumor antigen-specific IgA antibodies for cancer immunotherapy, different effector functions were assessed. Subsequent to confirmation of biochemical integrity for the novel recombinant monoclonal IgA antibodies (Chapter 3.2), biofunctionality against cancer cell lines (Table 6) was evaluated. Both, Fab-mediated and Fc-mediated mechanisms of action were investigated.

For Fab-mediated effector functions, the potential of IgA antibodies to inhibit proliferation of target cells was investigated. Fc-mediated mechanisms of action included antibody-dependent cellular cytotoxicity (ADCC) and antibody-dependent cellular phagocytosis (ADCP). Proliferation inhibition is mediated by antigen binding through the Fab domain of an antibody. In contrast, ADCC and ADCP rely on simultaneous antigen and Fc receptor binding on the surface of immune effector cells (Chapter 1.2) (Weiner et al. 2010). Two subsets of immune effector cells, granulocytes and macrophages, were used for ADCC and ADCP, respectively.

In case of anti-CD20 antibodies, characteristics to distinguish type I from type II anti-CD20 IgG antibodies were investigated. Both types differ in relative number of antigen binding sites on target cells and the potential of B cell depletion in whole blood. For hOM IgA2 antibody, target cell binding and B cell depletion assays were used to confirm biofunctionality (Chapter 3.3.6).

3.3.1 IgA antibodies inhibit cancer cell line proliferation

One important Fab-mediated effector function of antibodies targeting epidermal growth factor receptors like EGFR or Her2 is the prevention of uncontrolled cancer cell proliferation (Krawczyk & Kowalski 2014; Baselga & Swain 2009). By EGFR binding, antibodies like cetuximab prevent binding of activating ligands and thereby inhibit proliferation. Trastuzumab prevents proliferative signaling which is initiated by homo- and heterodimerization of its target Her2. Upon binding to Her2, trastuzumab inhibits phosphorylation of cytoplasmic kinases and thereby proliferative signaling of this receptor (Chapters 1.2.1) (Weiner et al. 2010). Inhibition of cancer target cell line (Table 6) proliferation in the presence of hTM and CM IgA or IgG antibodies targeting Her2 and EGFR, respectively, was investigated.

hTM IgA2 and hTM IgG showed comparable proliferation inhibition of SK-BR-3 target cells within 5 d relative to a control grown in medium without antibody. hTM IgA2 and IgG resulted in minimal proliferation of 59% and 51%, respectively (Figure 26a). As indicated by one experiment using SK-BR-3 target cells, hTM IgG-Cα3 construct (illustrated in Figure 17a) and hTM IgG were comparable in proliferation inhibition. hTM IgG-Cα3 and IgG resulted in minimal proliferation of 61% and 68%, respectively (Figure 26b). The antimitotic agent aphidicolin which inhibits DNA synthesis served as positive control for proliferation inhibition (Pedrali-Noy et al. 1982). In the presence of 10 µM aphidicolin, 10-13% target cell proliferation was observed. Irrelevant hOM IgA2 and IgG matched isotype negative control antibodies did not affect proliferation of SK-BR-3 target cells. Inhibition of proliferation was also shown microscopically. In the presence of hTM IgA2 viewer cells were visible as compared to the control with hOM IgA2 (Figure 26c).

CM IgA2 and IgG antibodies were comparable in proliferation inhibition of A-431 target cells within 4 d relative to a control grown in medium without antibody. Minimal proliferation was about 56% for CM IgA2, CM IgA2J dimers, CM IgA2J multimers or CM IgG antibodies. There was no difference in proliferation inhibition between CM IgA2 monomers and IgA2J dimers using same mass concentrations. Irrelevant hOM IgA2 and IgG matched isotype negative control antibodies did not affect proliferation of A-431 target cells. In the presence of 10 µM aphidicolin, 5% proliferation of target cells was observed (Figure 26d).

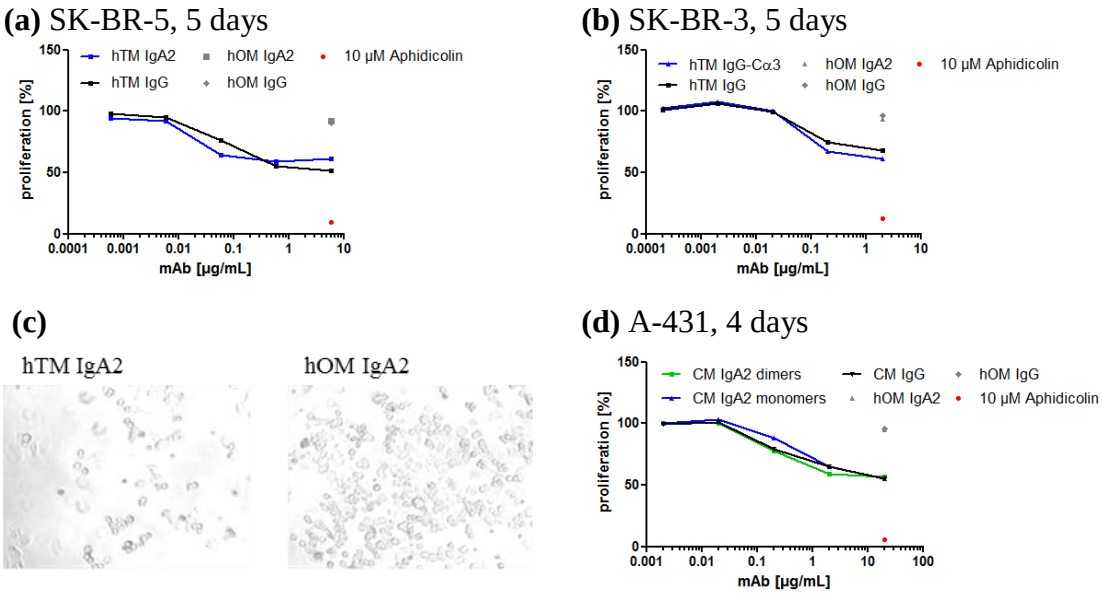

Figure 26 Inhibition of cancer cell line proliferation by hTM and CM IgA2 and IgG antibodies. Proliferation within 4 to 5 days relative to a control grown in medium without antibody was calculated. Mean values of duplicates are shown. **(a)** hTM IgA2 and IgG antibodies were comparable potent in proliferation inhibition of SK-BR-3 target cells. One out of three independent experiments is shown. **(b)** hTM IgG-Cα3 and IgG antibodies were comparable potent in proliferation inhibition of SK-BR-3 target cells. One exemplary experiment is shown. **(c)** Inhibition of proliferation was also shown microscopically. Cultivation of SK-BR-3 target cells in the presence of hTM IgA2 (left) resulted in viewer visible cells as compared to the control grown in the presence of hOM IgA2 irrelevant matched isotype negative control (right). One out of three independent experiments is shown. **(d)** CM IgA2 monomers, IgA2 dimers and IgG antibodies were comparable in proliferation inhibition of A-431 target cells. For SK-BR-3 and A-431, hOM IgA2 and IgG antibodies served as irrelevant matched isotype negative controls. One out of three independent experiments is shown.

In summary, as shown for both isotypes, IgA2 and IgG, targeting Her2 and EGFR inhibited proliferation of corresponding target cells. IgG, IgA2 and mixed-isotype construct were comparable effective in this Fab-mediated mechanism of action against cancer cell lines. As shown for CM IgA2 antibodies, proliferation inhibition was not dependent on monomer, multimer or dimer contents.

Next, Fc-mediated biofunctionality of IgA antibodies targeting tumor-associated antigens was investigated. Therefore, the potential of IgA antibodies to activate different effector cell populations in human blood was investigated.

3.3.2 IgA antibody-mediated activation of effector cells in human blood depends on target cells

Neutrophils, basophils and eosinophils constitute different cell populations in circulation belonging to the group of granulocytes. Upon activation granulocytes release cytotoxic

granules which include reactive oxygen species (ROS) (Murphy 2011). Like granulocytes, monocytes express the IgA Fc-binding receptor FcαRI which, upon activation, mediates cellular cytotoxicity (Chapter 1.1.4) (van Egmond et al. 2001). The potential of IgA antibodies to activate granulocytes and monocytes as effector cells in whole blood was investigated by measuring ROS using flow cytometry.

In the presence of ZR-75-1 target cells (Table 6), hPM IgA1 induced reactive oxygen production in granulocytes and monocytes. For $5x10^6$ target cells per milliliter, 100 µg/mL hPM IgA1 resulted in activation of up to 17% and 21% for granulocytes and monocytes, respectively. In the absence of antibody or when using target cell concentrations of $5x10^4$ or below, activation was <4% and <8% for granulocytes and monocytes, respectively. Phorbol 12-myristate 13-acetate (PMA) was used as positive control for induction of ROS. PMA activates protein kinase C resulting in oxidative activity within granulocytes (Majumdar et al. 1991; Sijtsema et al. 2000). Treatment of effector cells with PMA resulted in activation of 100% granulocytes and monocytes. Results for granulocyte and monocyte activation were qualitatively comparable (Figure 27).

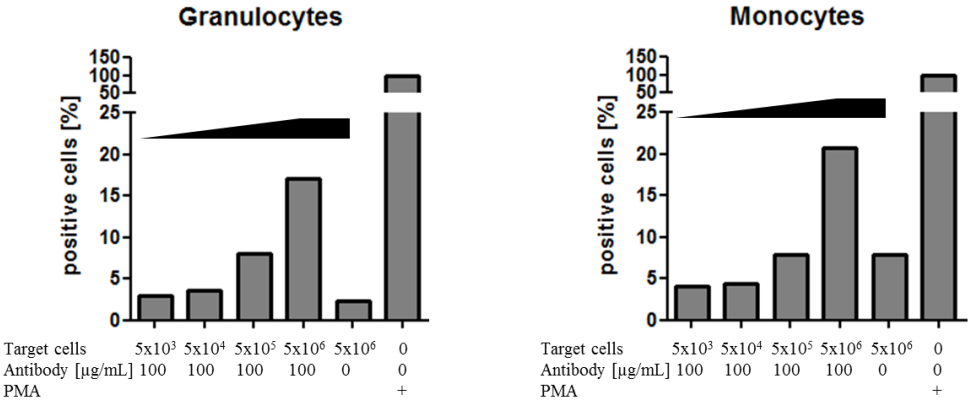

Figure 27 IgA antibody-mediated activation of granulocytes and monocytes in the presence of target cells. Mean values of duplicates are shown. One out of two independent experiments is shown. Antibodies and target cells were added to whole blood to investigate the potential of IgA antibodies to mediate effector cell activation. Activation was investigated by measuring the induction of reactive oxygen species (ROS) by flow cytometry. Addition of hPM IgA1 antibody and ZR-75-1 target cells in whole blood resulted in activation of granulocytes and monocytes. With increasing target cell concentrations (indicated by black bar) more granulocytes and monocytes were activated. In the absence of antibody, granulocyte and monocyte activation was low. Granulocytes and monocytes were distinguished by flow cytometry with corresponding gates in forward versus sideward scatter plots. Phorbol 12-myristate 13-acetate (PMA) served as positive control for granulocyte and monocyte activation (+).

As shown for hPM IgA1 in whole blood, IgA antibodies mediated the activation of granulocytes and monocytes in the presence of target cells. In the absence of antibody or when using low target cell concentrations, no granulocyte or monocyte activation was

observed. Hence, these two immune effector cell populations were used in subsequent cellular cytotoxicity assays to evaluate IgA antibodies' Fc-mediated mechanisms of action (Chapters 3.3.3, 3.3.4 and 3.3.5).

3.3.3 IgA2 antibodies are more potent than IgA1 antibodies in antibody-dependent cellular cytotoxicity

While proliferation inhibition is mediated by the interaction of the Fab domain of an antibody with its target on the surface of target cell, antibody-dependent cellular cytotoxicity (ADCC) is mediated by the Fc part of an antibody while the antibody is bound to a target cell. ADCC is an important effector function of therapeutic antibodies for cancer therapy (Chapter 1.2) (Weiner et al. 2010). Immune effector cells are recruited by antibodies to elicit cytotoxic effect on cancer cells. The antibody Fab domain specifically binds to its target on a cancer cell and thereby marks it for immune effector cells. Immune effector cells bind the Fc part of the antibody with Fc receptors. The presence of multiple targets and antibodies on the surface of a target cell results in crosslinking of Fc receptors which in turn initiates intracellular activation of immune effector cells (Chapter 1.2.1).

Usually NK cells which are present in isolated peripheral blood mononuclear cells (PBMCs) serve as effector cells for *in vitro* evaluation of IgG antibodies (Weiner et al. 2010). In contrast to granulocytes, NK cells do not express FcαRI which is required for IgA-dependent cellular cytotoxicity. Importantly, granulocytes constitute the most numerous leucocyte population in human blood (Murphy 2011; Valerius et al. 1997; Huls et al. 1999). Therefore, recruitment of granulocytes against cancer cells represents a promising strategy for cancer immunotherapy. The potential of IgA antibodies to activate granulocytes was shown (Chapter 3.3.2) and others used granulocytes as effector cell to evaluate IgA antibodies' biofunctionality (Dechant et al. 2007; Beyer et al. 2009; Lohse et al. 2012). Hence, granulocytes were used as effector cells for IgA-mediated cellular cytotoxicity against cancer cell lines (Table 6).

Granulocytes were isolated form heparinized whole blood from heathy donors (Chapter 2.5.2). Purity was assessed by flow cytometry and exceeded 95%. Prior to using granulocytes in ADCC assays, Ig receptor expression was determined. FcγRs and FcαRI expression was detected on purified granulocytes. FcαRI was abundantly expressed on purified granulocytes, 98% of granulocytes were positive. Out of the three main IgG Fc receptors, CD32 and CD16 were the most prominent receptors on granulocytes, 99% and 82% positive cells, respectively.

CD64 was found on 50% of granulocytes. No distinction between activating or inhibitory IgG receptor isoforms was possible with the anti-Fc receptor antibodies used for flow cytometry. However, expression of the relevant Fc receptors was confirmed in order to use granulocytes in subsequent biofunctional assessment of IgA and IgG antibodies. Purified granulocytes were used as effector cells in ADCC experiments to elucidate the potential of IgA antibodies to mediate lysis of cancer cell lines. Firstly, TA-MUC1 targeting hPM IgA1 and IgA2 antibodies were compared in granulocyte ADCC assays (this Chapter). Secondly, biofunctionality of three additional IgA2 antibodies targeting Her2, EGFR and TF was shown (Chapter 3.3.4). To account for background cytotoxicity in ADCC assays, specific lysis of the medium control lacking antibody was subtracted from reported maximal lysis values.

hPM IgA antibody-mediated cytotoxicity against ZR-75-1 target cells was investigated in granulocyte ADCC experiments. IgA antibody concentration-dependent specific lysis of target cells was shown. For IgA antibodies without J chain, hPM IgA2 resulted in higher maximal lysis than hPM IgA1 (Figure 28a and d). However, the difference was not as pronounced as for hPM IgA2J and hPM IgA1J which were generated by co-expression of the J chain. hPM IgA2J resulted in more than twice as high maximal lysis as compared to hPM IgA1J, 30% and 11%, respectively (Figure 28b and d). As shown for hPM IgA2 antibodies, the production cell line did not affect ADCC potency. Maximal lysis was comparable for H9D8-derived or Fuc^--derived hPM IgA2 (Figure 28c and d). Irrelevant serum IgA antibody negative control did not mediate lysis of ZR-75-1 target cells (Figure 28a).

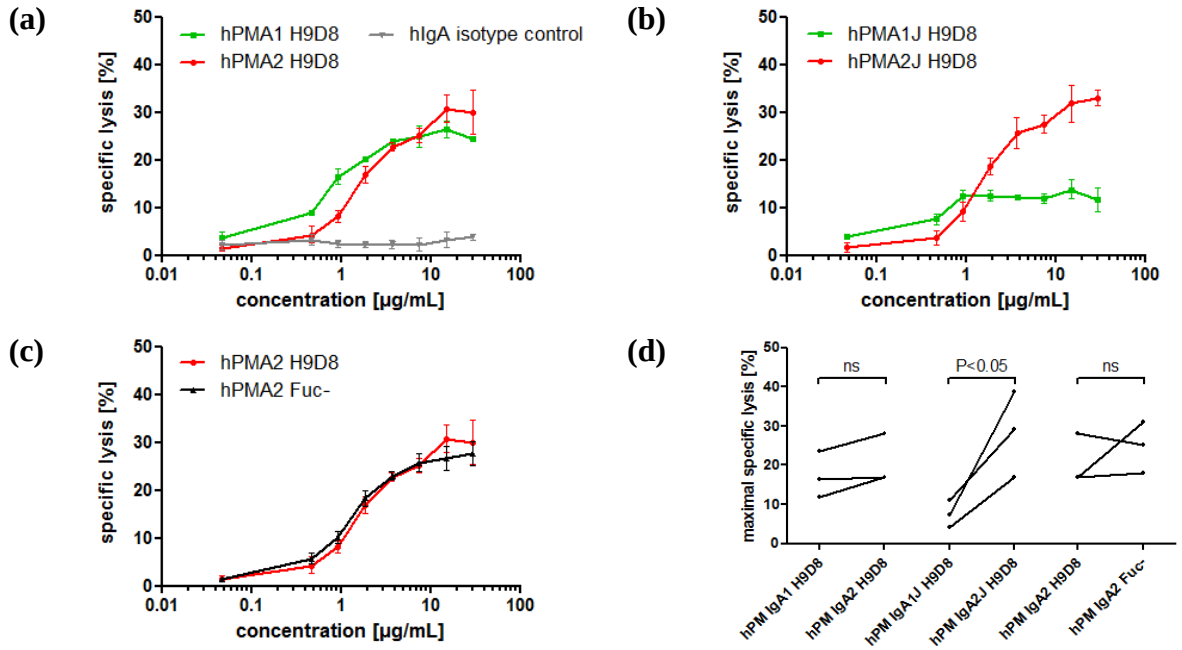

Figure 28 Antibody-dependent cellular cytotoxicity mediated by hPM IgA antibodies against cancer cell lines. Granulocytes isolated from peripheral blood were used as effector cells. IgA antibody concentration-dependent specific lysis of ZR-75-1 target cells was observed. Mean values of triplicates are shown, error bars indicate standard deviation. One out of three independent experiments is shown. **(a)** Compared to hPM IgA1, hPM IgA2 resulted in higher maximal lysis. The difference was more pronounced for IgA antibodies co-expressed with the J chain. **(b)** hPM IgA2J resulted in more than two-times higher maximal lysis compared to hPM IgA1J. **(c)** Maximal lysis for hPM IgA2 antibodies derived from H9D8 or Fuc$^-$ expression systems was comparable. **(d)** Three independent experiments confirmed higher maximal lysis for hPM IgA2 than IgA1 and that hPM IgA2J resulted in significant higher maximal lysis than hPM IgA1J. No significant difference between H9D8- and Fuc$^-$-derived hPM IgA2 was observed. ns: no significant difference with $P \geq 0.05$.

hPM IgA antibody-mediated cytotoxicity against target cells was shown using granulocytes as effector cells. Maximal lysis was higher for IgA2 compared to IgA1 and for IgA2J compared to IgA1J antibodies. No difference between H9D8- and Fuc$^-$-derived hPM IgA2 was observed. Subsequently, IgA2 and IgG antibodies with other specificities were compared in granulocyte ADCC experiments (Chapter 3.3.4).

3.3.4 IgA2 antibodies mediate antibody-dependent cellular cytotoxicity against cancer cell lines

Apart from hPM IgA antibodies targeting TA-MUC1, three additional IgA antibodies targeting different tumor-associated antigens were tested in ADCC assays using granulocytes as effector cells. Biofunctionality of hTM, CM and hKM IgA2 antibodies was investigated using corresponding target cell lines (Table 6).

For hTM and CM IgA2 antibodies, ADCC activity was tested using different cell lines. hTM IgA2 was effective in mediating cytotoxicity against SK-BR-3 target cells. Higher concentrations of hTM IgA2 were needed to reach comparable specific lysis as for hTM IgG. However, maximal specific lysis was higher for hTM IgA2 than for hTM IgG. Maximal lysis of both hTM IgA2 and IgG differed depending on the donor used for effector cell isolation. Donor 1 resulted in higher maximal lysis than donor 2, about 89% and 34% for hTM IgA2, respectively. Nevertheless, qualitatively results were comparable (Figure 29a).

While hTM IgA2 was more potent in mediating maximal lysis than hTM IgG against SK-BR-3 target cells, this was not the case for two additional target cells tested. For Panc-1 target cells, hTM IgA2 resulted in 15% maximal lysis as compared to hTM IgG mediated lysis of 60% of target cells. Similarly for Ls174T, hTM IgA2 did not reach as high maximal lysis as hTM IgG, 16% and 26%, respectively. As for SK-BR-3, higher concentrations of IgA as compared to IgG antibodies were needed to mediate lysis of Panc-1 and Ls174T target cells (Figure 29b).

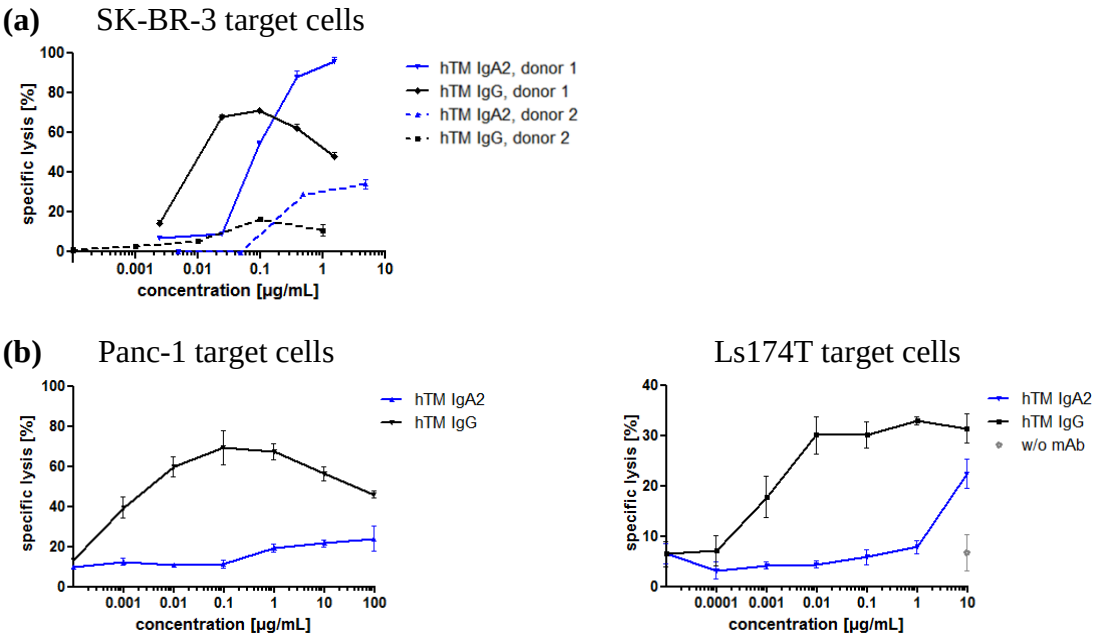

Figure 29 Antibody-dependent cellular cytotoxicity mediated by hTM IgA2 and IgG antibodies against different cancer cell lines. Granulocytes isolated from peripheral blood were used as effector cells. Mean values of triplicates are shown, error bars indicate standard deviation. **(a)** hTM IgA2 and IgG antibodies mediated specific lysis of SK-BR-3 target cells. Maximal lysis was higher for hTM IgA2 than for hTM IgG antibody. Maximal lysis reached by IgA2 and IgG antibodies differed between donors. In two separate experiments, higher maximal lysis was reached for hTM IgA2 and IgG using donor 1 (solid line) compared to donor 2 (dotted line). Two out of four independent experiments are shown. **(b)** Granulocyte ADCC using Panc-1 (left) and Ls147T (right) as target cells. For both target cell lines, hTM IgG was more potent than hTM IgA2.

Mixed-isotype hTM IgG-Cα3 construct was comparable to hTM IgG in granulocyte ADCC using SK-BR-3 target cells (Figure 30).

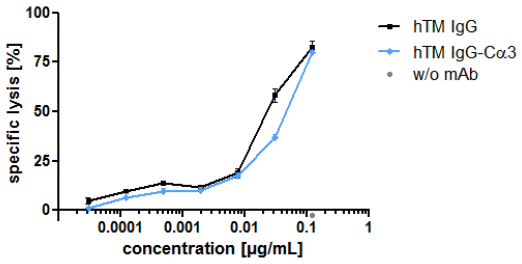

Figure 30 Antibody-dependent cellular cytotoxicity mediated by hTM IgG and IgG-Cα3 antibodies against SK-BR-3 target cells. Granulocytes isolated from peripheral blood were used as effector cells. Comparable ADCC activity was observed for hTM IgG and IgG-Cα3 antibodies. Mean values of triplicates are shown, error bars indicate standard deviation. One out of two independent experiments is shown.

Like hTM IgA2, CM IgA2 was tested in granulocyte ADCC using SK-BR-3, Panc-1 and Ls174T as target cells. CM IgA2 mediated lysis of SK-BR-3 target cells at concentrations exceeding 10 µg/mL while CM IgG did not mediate lysis of SK-BR-3 target cells (Figure 31a). This was in contrast to hTM IgA2 and IgG antibodies, both isotypes mediated lysis of SK-BR-3 target cells. When comparing the two IgA antibodies against EGFR or Her2, CM IgA2 resulted in lower maximal lysis of SK-BR-3 target cells as compared to hTM IgA2, 31% and 89%, respectively (Figure 29 and Figure 31). This could be caused by higher Her2 antigen density as compared to EGFR antigen density on the surface of SK-BR-3 target cells (Table 6).

As for hTM IgA2 and IgG antibodies, CM IgA2 was less effective against Panc-1 and Ls174T target cells than CM IgG antibody. For Panc-1 target cells, CM IgA2 concentration-dependent target cell lysis was low and resulted in maximal lysis of 17%. In contrast, CM IgG mediated lysis of up to 82% of Panc-1 target cells. In case of Ls174T target cells, CM IgA2 resulted in maximal lysis of 9% while CM IgG maximal lysis was 37%. CM IgG required lower antibody concentrations than CM IgA2 to mediate lysis of Panc-1 and Ls174T target cells (Figure 31b).

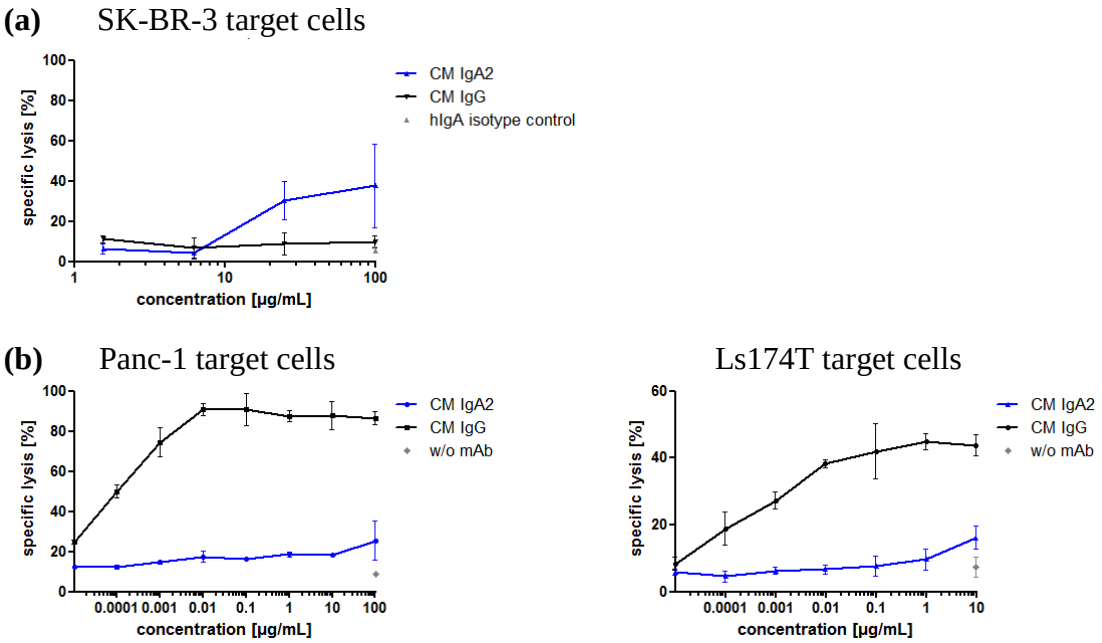

Figure 31 Antibody-dependent cellular cytotoxicity mediated by CM IgA2 and IgG antibodies against different cancer cell lines. Granulocytes isolated from peripheral blood were used as effector cells. Mean values of triplicates are shown, error bars indicate standard deviation. **(a)** CM IgA2 mediated lysis of SK-BR-3 target cells while CM IgG did not mediate lysis of SK-BR-3 target cells. **(b)** Granulocyte ADCC using Panc-1 (left) and Ls147T (right) as target cells. For both target cell lines, CM IgG was more potent than CM IgA2. One out of two independent experiments is shown.

ADCC activity of hKM IgA2 antibody was shown for one cancer cell line. hKM IgA2 effectively mediated lysis of Panc-1 target cells at antibody concentrations exceeding 1 µg/mL and hKM IgG mediated marginal target cell lysis, 22% and 5%, respectively (Figure 32). Similarly, hPM IgA2 mediated lysis of Panc-1 target cells while no lysis was observed for hPM IgG (data not shown).

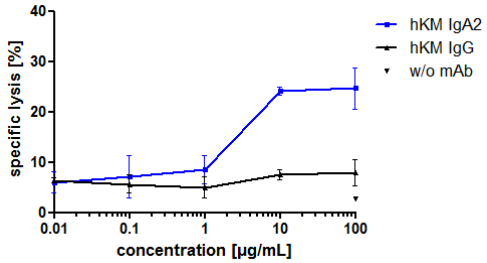

Figure 32 Antibody-dependent cellular cytotoxicity mediated by hKM IgA2 and IgG antibodies against Panc-1 target cells. Granulocytes isolated from peripheral blood were used as effector cells. hKM IgA2 mediated lysis of Panc-1 target cells while hKM IgG did not mediate lysis of Panc-1 target cells. Mean values of triplicates are shown, error bars indicate standard deviation.

The potential of one IgA1 antibody (Chapter 3.3.3) and four IgA2 antibodies to mediate cellular cytotoxicity against different target cells was shown. hPM IgA1, hPM IgA2, hTM

IgA2, CM IgA2 and hKM IgA2 antibodies mediated specific target cell lysis when using granulocytes as effector cells. ADCC activity varied between the different cancer cell lines and between the antigens targeted with different antibodies. hTM IgA2 was more potent than CM IgA2 against SK-BR-3 target cells which express about ten times more binding sites for hTM than for CM (Table 6). Both, hTM and CM IgA2 antibodies were more potent than their corresponding IgG isotype antibodies against SK-BR-3 target cells. However, for Panc-1 and Ls174T, hTM and CM IgG antibodies mediated higher maximal lysis than the corresponding IgA2 antibodies. hKM and hPM IgA2 mediated lysis of Panc-1 target cells while hKM and hPM IgG antibodies mediated cytotoxicity was negligible. For hTM and CM IgG antibodies, maximal lysis was higher for Panc-1 than for Ls174T target cells. In case of CM, higher maximal lysis corresponds with higher antigen density. Conversely, hTM resulted in higher maximal lysis for Panc-1 target cells as compared to Ls174T while the number of antigen binding sites is comparable (Table 6).

Recombinant monoclonal IgA antibodies recruited granulocytes to elicit cytotoxic effects against cancer cell lines. Due to the high abundance of granulocytes in circulation, this represents a promising mode of action for cancer immunotherapy. Next, as a second Fc-mediated effector function using macrophages as effector cells, the potential of IgA antibodies to mediate cellular phagocytosis of cancer cell lines was investigated.

3.3.5 IgA2 antibodies mediate antibody-dependent cellular phagocytosis of cancer cell lines

Antibodies targeting tumor antigens mediate phagocytosis of cancer cell lines by different effector cells including granulocytes, dendritic cells and macrophages (Akewanlop et al. 2001; Dhodapkar et al. 2002; Golay et al. 2013). In addition to granulocytes, macrophages represent an interesting effector cell population which is found in large numbers within the tumor microenvironment (Lewis et al. 1995). Therefore, as a second Fc-mediated effector function for IgA antibodies, antibody-dependent cellular phagocytosis (ADCP) of cancer cell lines was investigated using monocyte-derived macrophages (MDM) as effector cells. Primary monocytes can be differentiated to macrophages by cultivation in medium promoting macrophage differentiation (Chapter 2.5.5) (Keler et al. 2000). In addition, activated macrophages can be categorized as M1 and M2 phonotype macrophages. While M1 phenotype macrophages mediate anti-tumor effects, M2 phenotype macrophages are known for their immune suppressive functions (Schmid & Varner 2010). However, antibody-

mediated anti-tumor effects of M2 phenotype macrophages were described (Herter et al. 2013).

For ADCP assays, CD45 was used as marker for MDM detection and target cells were stained with PKH26. Using flow cytometry, phagocytosis was calculated based on CD45/PKH26 double-positive cells relative to total CD45-positive cells. Unspecific phagocytosis for controls with irrelevant matched isotype control antibody or without antibody in the range of 5% to 20% was observed in ADCP assays. Therefore, phagocytosis relative to controls without antibody or irrelevant matched isotype control antibodies was evaluated. Unless otherwise noted, M1-like macrophages were used for ADCP assays. ADCP was shown for hPM IgA2, hTM IgA2 and mixed-isotype hTM IgG-Cα3 construct using corresponding target cells (Table 6) and MDM as effector cells.

hPM IgA2 mediated phagocytosis of ZT-75-1 and T47D target cells. For hPM IgA2 or IgG antibodies, phagocytosis was observed at concentrations exceeding 25 µg/mL and 6 µg/mL for ZR-75-1 and T47D, respectively. Maximal phagocytosis of ZR-75-1 target cells by hPM IgA2 and IgG were 10% and 17%, respectively. Maximal phagocytosis of T47D target cell by hPM IgA2 and IgG were 29% and 44%, respectively. Hence, for both target cells hPM IgG was more potent in mediating phagocytosis (Figure 33a).

hTM IgA2 and IgG mediated phagocytosis of BT-474 target cells. Compared to hTM IgA2, lower concentrations of hTM IgG were needed for phagocytic activity. Moreover, hTM IgG mediated phagocytosis up to 75%, while maximal phagocytosis for hTM IgA2 was 39%. Mixed-isotype construct hTM IgG-Cα3 reached comparable maximal phagocytosis like hTM IgG antibody (Figure 33b).

A minor fraction of MDM was cultivated in different medium which promotes differentiation in M2-like macrophages. Four antibody concentrations were tested for hTM IgA2 monomers and hTM IgG. For hTM IgA2 monomers higher maximal phagocytosis was reached using M2-like MDM as compared to M1-like MDM. In contrast to M2-like MDM, for M1-like MDM no further increase of phagocytosis was observed at concentrations exceeding 2 µg/mL hTM IgA2. hTM IgG-mediated phagocytosis was not further increased by using M2- compared to M1-like MDM (Figure 33c).

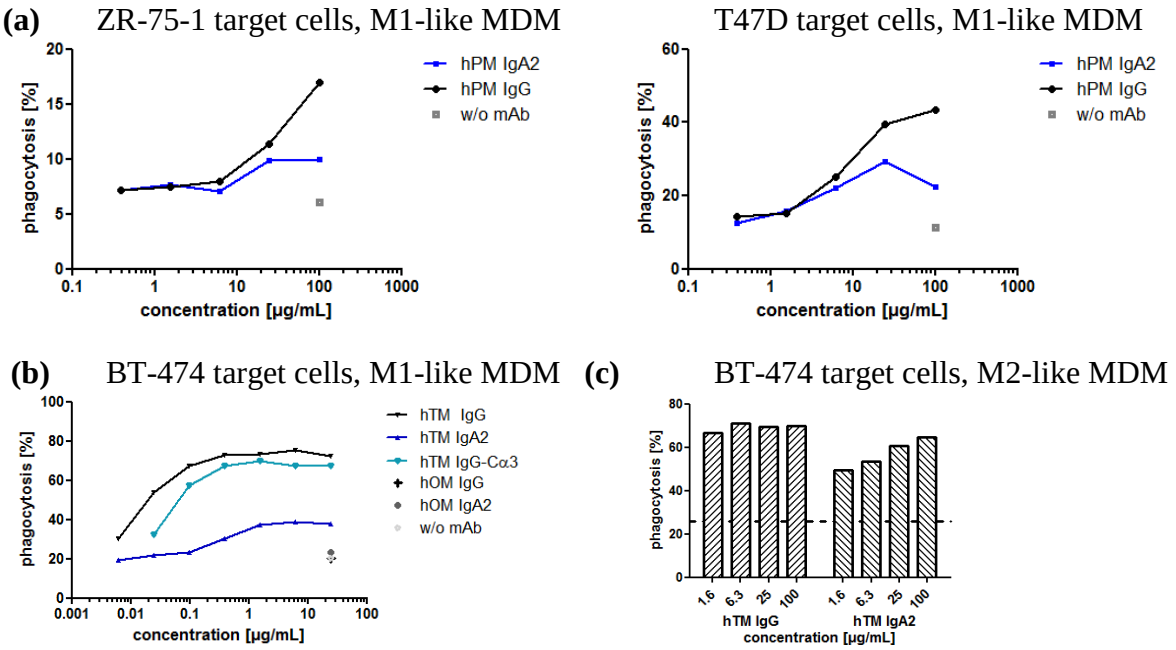

Figure 33 Antibody-dependent cellular phagocytosis (ADCP) mediated by hPM and hTM IgA2 antibodies against cancer cell lines. Monocyte-derived macrophages (MDM) were used as effector cells for ADCP assays. Mean values of duplicates are shown. **(a)** hPM IgA2 and IgG mediated phagocytosis of ZR-75-1 (left) and T47D (right) target cell lines. Maximal phagocytosis was higher for hPM IgG compared to hPM IgA2. **(b)** hTM IgA2 and IgG mediated phagocytosis of BT-474 target cell line. Maximal phagocytosis was higher for hTM IgG compared to hTM IgA2. Mixed-isotype hTM IgG-Cα3 construct and hTM IgG were comparable in mediating phagocytosis. Irrelevant matched isotype control antibodies did not result in phagocytosis of target cells. **(c)** A subset of MDM was cultivated under conditions promoting M2 phenotype differentiation. hTM IgA2 monomers reached comparable maximal lysis like hTM IgG antibody. At the concentrations tested, no concentration-dependent phagocytosis was observed for hTM IgG antibody. Background phagocytosis of a control using medium without antibody is indicated by the dotted line and was 26%.

hPM and hTM IgA2 antibodies mediated phagocytosis of corresponding target cells. For both antibodies, IgG isotype was more effective than IgA using monocyte-derived macrophages as effector cells. However, IgA-mediated phagocytosis could be further increased by using M2-like MDM as effector cells. Apart from proliferation inhibition and ADCC, phagocytosis was shown as additional mechanism of action of tumor antigen-targeting IgA antibodies.

3.3.6 Biofunctionality of anti-CD20 IgA2 and IgG antibodies and comparison of type I and II anti-CD20 IgG antibodies

While the antibodies investigated before for biofunctionality against cancer cell lines target antigens expressed on solid cancers, obinutuzumab (hOM) binds CD20 which is a target for hematological cancer indications. Anti-CD20 IgG antibodies can be classified as type I or type II (Chapter 1.2.2.5, Figure 7). To confirm type II characteristics for hOM IgG, target cell binding and B cell depletion in whole blood were assessed and compared to type I anti-CD20

Mabthera (rituximab). Whether depletion of B cells in whole blood was caused by Fab- or Fc-mediated effector functions could not be distinguished in this assay. However, this *in vitro* setup resembles the human situation because it includes all immunological components present in circulation (Herter et al. 2013). Biofunctionality of hOM IgA2 was shown by flow cytometry and B cell depletion assays.

Purified hOM IgG, hOM IgA2 and commercially available anti-CD20 IgG Mabthera were compared in binding to the CD20-positive Raji cancer cell line by flow cytometry. Regarding percent positive cells, binding curves of both anti-CD20 IgG antibodies, hOM and Mabthera, were overlapping. In contrast, Mabthera reached twice as high median fluorescence intensity (MFI) signals as hOM IgG (Figure 34a). This indicated that more binding sites were present on the surface of Raji cells for Mabthera compared to hOM IgG. For hOM IgA2, concentration-dependent binding curves for percent positive cells and MFI were observed (Figure 34b). No comparison between IgG and IgA2 antibodies in flow cytometry was possible because of different secondary antibodies used for detection.

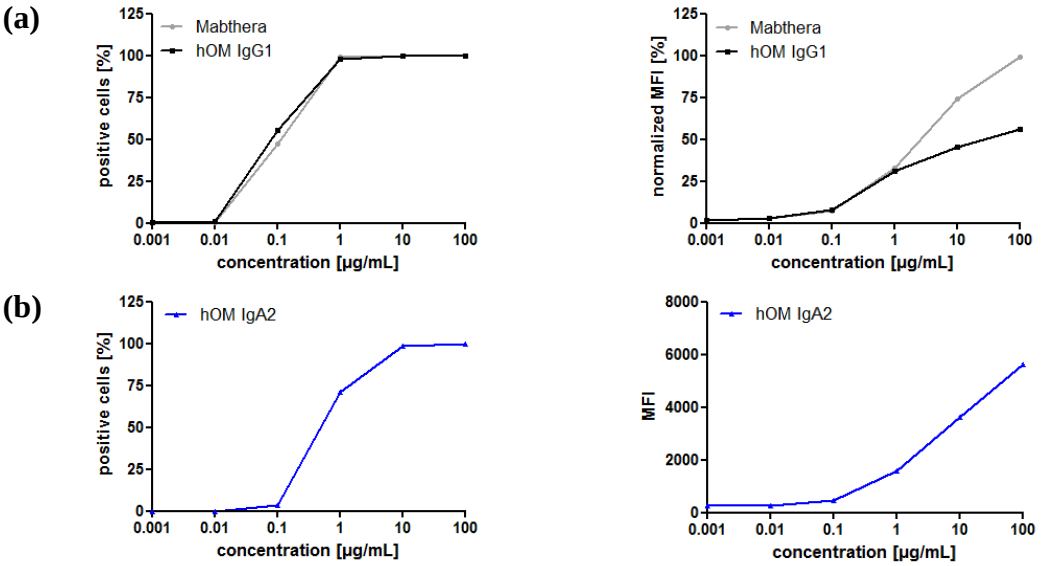

Figure 34 Raji target cell binding of novel anti-CD20 IgG and IgA2 antibodies by flow cytometry. Mean values of duplicates are shown. **(a)** Type I (hOM IgG) and type II (Mabthera) anti-CD20 antibodies showed overlapping curves with respect to positive cells (left). In contrast, median fluorescence intensity (MFI) was twice as high for type I as compared to type II anti-CD20 IgG antibody (right). MFI was normalized to 100% representing the maximal MFI for Mabthera. **(b)** Concentration-dependent binding of hOM IgA2 to Raji target cells was shown as percent positive cells (left) and MFI (right).

Using whole blood as source for target B cells and effector cells, functionality of hOM IgG, hOM IgA2 and Mabthera anti-CD20 antibodies was investigated. For hOM IgG and Mabthera, antibody concentration-dependent B cell depletion was shown. hOM IgG resulted

in higher maximal depletion and was more effective in B cell depletion at lower antibody concentrations than Mabthera. hOM IgA2 showed maximal B cell depletion at about 100 ng/mL, while less B cell depletion was observed at 1,000 ng/mL. In a concentration range up to 1,000 ng/mL, maximal B cell depletion was achieved with hOM IgG followed by hOM IgA2 followed by Mabthera (Figure 35).

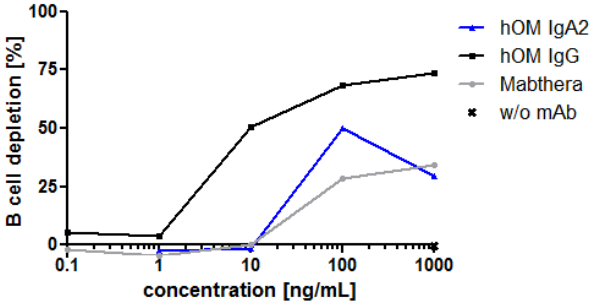

Figure 35 Anti-CD20 IgG and IgA antibodies mediate B cell depletion. Whole blood was used as source for target and effector cells. Mean values of duplicates are shown. One out of two independent experiments is shown. Antibodies were added to heparinized whole blood from healthy volunteers. After 24 h incubation time, B cell counts relative to T cell counts were assessed. B cell depletion was calculated relative to a buffer control without antibody. Both, hOM IgA2 and IgG showed increased B cell depletion as compared to Mabthera. For hOM IgG lower antibody concentrations were sufficient for effective B cell depletion and higher maximal B cell depletion was reached.

hOM IgG, IgA2 and Mabthera bound their target cells and were functional in whole blood B cell depletion assays. Type I (Mabthera) and type II (hOM) IgG antibodies showed distinct binding in flow cytometry experiments and activity in B cell depletion assays. There were more binding sites for type I than for type II anti-CD20 IgG antibodies on the surface of target cells and type II anti-CD20 hOM IgG antibody was more effective in depleting B cells in whole blood than type I anti-CD20 IgG antibody. Both, hOM IgA2 and IgG were functional in B cell depletion assays. In conclusion, biofunctionality of the generated anti-CD20 hOM IgG and IgA antibodies binding a target for hematological cancer indications was shown.

In summary, biofunctional IgA antibodies against five different tumor antigens were successfully generated. High yields of recombinant monoclonal IgA antibodies were produced in a human expression system. IgA production could be largely increased by cultivation in a bioreactor using a perfusion process. Specific antigen and Fc receptor binding was confirmed in biochemical assays. High avidity IgA dimers were generated by co-expression of the J chain polypeptide. IgA antibodies were functional against cancer cell lines by inhibiting

proliferation through Fab-mediated interaction with their targets. Moreover, as Fc-mediated mechanisms of action, granulocytes and monocytes were recruited by IgA antibodies resulting in cellular cytotoxicity against and phagocytosis of cancer cell lines. Apart from the four targets for solid cancer indications, an IgA antibody targeting CD20 which is a target for hematological cancer indications was biofunctional in whole blood. Together, IgA antibodies targeting five different targets were functional against cancer cell lines or target cells in whole blood.

4 Discussion

While monoclonal antibodies are established pharmaceuticals for cancer therapy, not all patients benefit from treatments (Weiner et al. 2010; Scott, Wolchok, et al. 2012). In order to improve cancer therapy by increasing the functional diversity of antibodies, the aim of this study was to elucidate the potential of IgA isotype antibodies as cancer therapeutics. For example, the interaction with other Fc receptors which are expressed differently on the surface of immune effector cells may improve efficacy. Many studies investigated anti-EGFR IgA antibodies (Beyer et al. 2009; Lohse et al. 2011; Lohse et al. 2012; Boross et al. 2013; Brunke et al. 2013), yet, studies of IgA antibodies with other tumor-targeting specificities remain scarce and no comparisons of a panel of IgA antibodies with multiple targets is available. IgA antibodies targeting Ep-CAM, human leukocyte antigen class II and CD20 were generated and functional against their target cells (Huls et al. 1999; Dechant et al. 2002; Pascal et al. 2012). Bispecific formats against a tumor antigen and FcαRI were used to simulate IgA-mediated Fc-dependent effector functions against target cells (Valerius et al. 1997; Deo et al. 1998; Stockmeyer et al. 2000; Bakema et al. 2011). Here, a panel of monoclonal IgA antibodies targeting five different antigens was successfully generated to elucidate the potential of this isotype on broad basis. Moreover, a mixed-isotype antibody was generated to combine advantages of two isotypes. Biochemical integrity was confirmed and biofunctionalities against cancer cell lines were shown.

4.1 Novel tumor-specific monoclonal IgA antibodies with human glycosylation

Several expression systems have been used for the production of recombinant IgA antibodies: myeloma cells (Atkin et al. 1996; Yoo et al. 2010), monkey-derived COS cells (Morton et al. 1993), insect cells (Carayannopoulos et al. 1994), baby hamster kidney cells (Dechant et al. 2002) and plants (Juarez et al. 2013; Larrick et al. 2001). However, most of the recombinantly produced IgA antibodies were expressed in Chinese hamster ovary (CHO) cells (Morton et al. 1993; Mattu et al. 1998; Pleass et al. 2003; Chintalacharuvu et al. 2007; Dechant et al. 2007; Beyer et al. 2009; Beyer et al. 2010; Yoo et al. 2010; Bakema et al. 2011; Lohse et al. 2012; Pascal et al. 2012; Reinhart et al. 2012; Brunke et al. 2013; Moldt et al. 2014). The glycosylation of biotherapeutic biologicals is important for function, bioavailability and tolerance in human circulation. Non-human glycan structures attached to a therapeutic

molecule can result in immunological reactions (Arnold et al. 2007). The functional role of IgA antibody N-glycans for Fc-mediated effector functions is controversial and discussed below (Chapter 4.3). But, the use of a human expression system is especially desired for molecules which are highly glycosylated. IgA antibodies possess up to ten N-glycosylation sites and in case of IgA1 multiple O-glycosylation sites within their constant regions (Figure 1). In contrast, IgG antibodies currently approved for cancer immunotherapy as well as other indications possess two N-glycosylation and no O-glycosylation sites. Moreover, glycan structures present in the Fc part of IgG antibodies are orientated towards the inter-HC space within the molecule while it has been shown that IgA antibody glycans are orientated away from the molecule and surface accessible (Mattu et al. 1998) (Figure 1). Immunological reactions towards non-human structures on therapeutics could result in neutralization, increased clearance or severe reactions upon exposures. Potential immunogenic carbohydrate structures on molecules produced in non-human expression systems include α(1-3)-linked galactose and N-glycolylneuraminic acid. In humans, glycans do not contain these structures or linkage-structure combinations (Jefferis 2009). In case of mouse myeloma-derived monoclonal antibody Erbitux (cetuximab, Merck), in certain populations the preexistence of IgE antibodies against the galactose-α(1-3)-galactose epitope present on the carbohydrate of Erbitux caused hypersensitivity reactions (Chung et al. 2008). Hence, using a human expression system like GEX-H9D8 or GEX-Fuc$^-$ for the production of IgA antibodies is even more important than for IgG antibodies because the number of glycosylation sites is not only much higher for IgA antibodies, but they are also orientated towards the outside of the molecule. Therefore, more potential immunogenic sites could be present as well as accessible on therapeutic IgA antibodies depending on the expression system they are produced in. Here, fully human glycosylated recombinant monoclonal IgA antibodies were successfully generated.

Non-human glycan structures which could potentially be immunogenic were not present on recombinant IgA antibodies produced for this study in GEX expression systems (Chapter 3.2.7). Moreover, sialylation is important to prolong IgA antibody serum half-life (Rifai et al. 2000; Boross et al. 2013; Brunke et al. 2013). As compared to other reported N-glycosylation profiles, the generated IgA antibodies possessed much higher sialylation degrees. Boross et al. reported maximal sialylation degrees of 20% for the IgA antibodies expressed in CHO cells (Boross et al. 2013). Brunke et al. reported 23% and no sialylated glycans for CHO-derived wild-type and stability-promoting mutated IgA2 antibodies, respectively (Brunke et al. 2013). N-glycosylation profiles of the IgA antibodies generated here revealed higher total sialylation

degrees. Sixty-two and 64% of complex type N-glycans were sialylated for hTM and hOM IgA2 antibodies, respectively (Chapter 3.2.7). Increasing sialylation results in decreased clearance by the asialoglycoprotein receptor (ASGP-R) in the liver (Boross et al. 2013). For human serum IgA1, 98% of N-glycans were reported to be sialylated (Mattu et al. 1998). However, due to clearance of less sialylated endogenous IgA antibodies, highly sialylated molecules could be enriched within circulation. The N-acetylneuraminic acid of sialylated IgA antibody N-glycans is mainly in α(2-6) configuration (Mattu et al. 1998). While CHO expression systems do not have the glycosyltransferase responsible for α(2-6)-linked N-acetylneuraminic acid (Jefferis 2009), both α(2-3)- and α(2-6)-linked sialylated glycans can be found in GEX-derived products.

Both, IgA1 and IgA2 with or without J chain were successfully produced using the human good manufacturing practice (GMP)-validated expression system in serum-free conditions (personal communication with Dr. Antje Danielczyk). One drawback of therapeutic IgA antibodies was the lack of established production systems, scale-up capabilities and purification strategies. Product heterogeneity might also arise due to the high number of glycosylation sites (Dechant et al. 2007). IgA productivity by GEX cell lines was high and clones could be selected within four to six months after stable transfection (Chapter 3.1). This allowed for fast generation of high yield monoclonal IgA antibody producing clones. In the past, specific production rates of up to 2.1 pg/cell/day (Brunke et al. 2013), 0.8 to5 pg/cell/day (Dechant et al. 2007; Beyer et al. 2010) or 0.17 to 16 pg/cell/day (Reinhart et al. 2012) were reported. Serum-free production of recombinant IgA antibodies has been described before (Beyer et al. 2009), maximal specific production rates were 2.2 pg/cell/day. Here much higher production rates were achieved using serum-free conditions, up to 53 pg/cell/day for hTM IgA2. Productivity differed between antibodies (Table 3), CM IgA2 clones showed maximal specific production rates of 3 pg/cell/day, which was the lowest among the IgA antibodies generated. Similarly, IgG antibody productivities can differ too, which indicates that variable domains or transfection events affect productivity. Chromosomal localization of the target genes affects expression levels and could be responsible for varying production levels (Yoshikawa et al. 2000; Kawabe et al. 2012). Using the ClonePix instrument to isolate single cell-derived colonies allowed pre-selection of high-producing clones, which is a reason for high abundance of clones with high and comparable specific production rates in following screenings. In standard 1 L spinner cultures high amounts of IgA antibody were produced (up to 56 mg). Productivities could probably be further increased by prolonged clone development

with additional amplifications and cloning rounds as usually done for therapeutic biologicals intended for GMP manufacture.

As shown for hTM IgA2 productivity could be remarkably increased by cultivation in a 2 L bioreactor. Due to the controlled environment (pH, oxygen saturation, temperature, metabolite analysis) and constant fresh media supply within the perfusion process much higher cell concentrations were reached as compared to spinner cultures. The bioreactor perfusion process with 1 L working volume greatly exceeded prior reported maximal yields of IgA production. On average over 35 days, 2,200 mg were produced per week as compared to 2.5 mg per roller bottle per week or 5.9 mg per CL1000 production flasks per week (Beyer et al. 2009; Beyer et al. 2010; Lohse et al. 2012). For the production of recombinant proteins, perfusion processes are advantageous compared to commonly used fed-batch processes due to better quality of the produced molecules with respect to more completely processed N-glycans (Lipscomb et al. 2008). In perfusion processes, product is constantly harvested from the reactor and does not accumulate during the duration of the process within the culture which contains metabolites and cell debris as in case of fed-batch processes (Goldman et al. 1998). This represents the first cultivation of IgA2 producing cells using a continues bioreactor process and confirms feasibility of high yield production as required for therapeutic antibodies intended for human use.

4.2 Highly stable recombinant IgA antibodies with specific antigen binding

Single-step affinity chromatography yielded clean IgA preparations as shown by SDS-PAGE, Western blots and SEC. In contrast to methods described before (Beyer et al. 2009; Reinhart et al. 2012), supernatants could be directly loaded onto the affinity column without the need for prior buffer exchange. This allowed for fast purification of monoclonal IgA1 and IgA2 antibodies in high purity and could be attributed to different production media. Monomer contents of affinity purified IgA antibodies lacking J chain co-expression and purity were comparable to literature (Beyer et al. 2009; Lohse et al. 2011).

As shown in Chapter 3.2.2 and by others (Oortwijn et al. 2006; Beyer et al. 2009; Pascal et al. 2012) using SEC, IgA antibodies in the absence of J chain form mainly monomers while dimers and higher order multimers are present in lower abundance. By co-expression of the J chain more dimers and multimers are formed. This was shown for all five IgA2 antibodies lacking J chain co-expression and all three IgA2J antibodies co-expressed with the J chain. At mucosal sites, dimeric IgA is transported through epithelial cells into the luminal site by pIgR

(Chapter 1.1.3). While the role of the J chain for pIgR binding is not clear (Hexham et al. 1999), it promotes the formation of dimers in IgA-producing cells and could thereby contribute to the transport of dimeric IgA to generate secretory IgA upon luminal release (Woof & Kerr 2006). The requirement of IgA multimerization for J chain association was confirmed by anti-J chain Western blots. J chain was exclusively detected in dimer and multimer preparations (Chapter 3.2.3). The association of J chain with multimers was also used for the isolation of multimers by affinity chromatography specific for His-tagged J chain (Lohse et al. 2011).

The generated IgA antibodies proved to be stable with respect to monomer contents or monomer/multimer distribution for the period tested of up to 2 years (Chapter 3.2.4). This was the case for monomer preparations as well as non-SEC-separated IgA1 and IgA2 antibodies. Hence, no aggregation or fragmentation occurred during long-time storage for monomers, dimers or multimers. This is in contrast to studies which showed dissociation and fragmentation of IgA2J dimers after 1 year storage (Lohse et al. 2012). J chain glycosylation is essential for correct dimer formation (Krugmann et al. 1997) and similarly IgA glycans could affect stable molecule assembly. Different glycosylation patterns of the J chain as well as IgA antibodies because of different expression systems used for production could be responsible for varying stabilities. The contribution of glycosylation for stability could be further elucidated by stability experiments using enzymatically deglycosylated IgA antibodies or testing differently produced IgA antibodies in parallel. Introduction of a single point mutation was shown to increase stability of an IgA2m(1) allotype (the same as used in this study). Mutated IgA2m(1) was not prone to fragmentation because inter-HC-LC disulfide bonds were formed. For IgA2 dimers, this resulted in better stability for the tested molecule (Lohse et al. 2012). In another approach, the stability of recombinant IgA2m(1) antibody was improved by deletion of the last two amino acids of the heavy chain, including the penultimate cysteine (Brunke et al. 2013). No biofunctional difference was observed but the mutation resulted in a decrease in sialylation and increase in terminal galactose which impairs pharmacokinetic behavior (Brunke et al. 2013). However, the IgA2m(1) allotypes generated in this study were stable and not prone to fragmentation during long time storage (Chapter 3.2.4) without stability-promoting sequence mutations while being highly sialylated as compared to CHO-derived recombinant IgA antibodies (Chapter 3.2.7) (Boross et al. 2013).

For the antibodies tested, comparable antigen binding for IgG and IgA antibodies was shown. This is consistent with data found in literature comparing anti-EGFR IgG and IgA antibodies (Dechant et al. 2007). Similar binding kinetics of IgG and IgA antibodies were observed by

others using a non-tumor-targeting IgA1 and corresponding IgG antibodies (Pleass et al. 2003). Using surface plasmon resonance, similar antigen binding kinetics for monomeric IgA and IgG antibodies were observed (Chapter 3.2.9). This was shown for non-tumor-targeting IgA antibodies before (Pleass et al. 2003; Tanikawa et al. 2008; Shi et al. 2011). Moreover, for the first time monomeric and dimeric IgA2 antibodies were compared in antigen binding kinetic analysis using surface plasmon resonance. As shown for CM, IgA2J dimers showed increased avidity compared to IgA2 monomers (Chapter 3.2.9). Most likely this can be attributed to increased avidity with two and four antigen binding sites for monomeric and dimeric IgA2, respectively. In sensorgrams, the main difference was the decreased dissociation for IgA2 dimers compared with IgA2 monomers. While clean dimers were successfully prepared, process development would be necessary to yield more homogenous dimeric product. Qualitatively comparable binding characteristics for IgA monomers and IgG antibodies were also confirmed by immunofluorescence (Chapter 3.2.8). Together, antigen binding experiments showed that binding characteristics and avidity is retained when switching form IgG to IgA isotype antibodies. However, compared to IgA monomers, IgA dimers with increased valence showed increased avidity (Chapter 3.2.9).

4.3 IgA antibodies as novel class for cancer immunotherapy – modes of action

In order to evaluate IgA isotype antibodies as potential novel class of tumor-specific immunotherapeutics, biofunctionalities against cancer cell lines were investigated. IgA antibodies inhibited the proliferation of cancer cells, mediated ADCC and ADCP.

Previously, recombinant IgA2 antibodies targeting EGFR were shown to require higher concentrations for similar binding signals in flow cytometry and about five times higher concentrations for similar proliferation inhibitions compared to IgG antibodies (Beyer et al. 2009; Lohse et al. 2012). However, comparable proliferation inhibition of IgG and IgA antibodies was shown for an antigen-transfected cell line (Dechant et al. 2007). As shown for hTM and CM IgA2 monomers here, switching the isotype from IgG to IgA2 did not change antigen binding kinetics (Chapter 3.2.9) or the potential to inhibit proliferation of target cells (Chapter 3.3.1). It can only be speculated why the reported anti-EGFR IgA antibodies behaved differently (Beyer et al. 2009; Lohse et al. 2012). Reasons could be different expression systems used for recombinant IgA production or the purity as well as stability of antibody preparations. For proliferation inhibition, potentially different target cells are more or less sensitive to IgG or IgA antibodies. Depending on the antigen presentation on the

surface of target cells, more flexibility in antigen binding might be required for some cell lines. Reduced structural flexibility of IgA compared to IgG antibodies might result in different potencies for those target cells (Furtado et al. 2004). CM IgA2 dimers were equally potent as monomer preparations when comparing same mass concentrations. The number of antigen binding sites was the same at equal mass concentrations and probably is the main factor affecting proliferation inhibition. Decreased dissociation rates for CM IgA2 dimers as compared to CM IgA2 monomers did not translate into more pronounced proliferation inhibition. As shown before for anti-EGFR IgA2 antibodies (Beyer et al. 2009; Lohse et al. 2012), IgA antibodies targeting Her2 inhibit the proliferation of cancer cell lines.

Cytotoxicity assays revealed potent lysis of target cells mediated by IgA antibodies when using granulocytes as source for effector cells. Granulocytes were chosen as effector cells because they are the most numerous leucocyte population in human blood, they express FcαRI and multiple studies have shown that IgA antibodies or FcαRI-engaging bispecific formats are more potent than IgG antibodies or FcγR-engaging bispecific formats (Valerius et al. 1997; Deo et al. 1998; Stockmeyer et al. 2000; van Egmond et al. 2001; Dechant et al. 2002; Dechant et al. 2007; Beyer et al. 2009; Lohse et al. 2012). Activation of granulocytes was successfully confirmed in the presence of target cells and IgA antibodies (Chapter 3.3.2). In ADCC assays, IgA2 antibodies were more effective than IgA1 antibodies, which is consistent with data found in literature for anti-human leukocyte antigen and anti-EGFR IgA antibodies (Dechant et al. 2002; Dechant et al. 2007). Binding experiments with IgA1 and IgA2 to FcαRI-transfected cells or primary granulocytes revealed increased binding for IgA2, which might be an explanation for more potent ADCC of this subclass (Dechant et al. 2007). Moreover, studies with differently sialylated IgA1 and IgA2 revealed differences in FcαRI binding depending on subclass as well as glycosylation (Basset et al. 1999). But the role of glycosylation for FcαRI binding remains controversial, while Basset et al. (Basset et al. 1999) found that glycosylation affects FcαRI binding Mattu et al. (Mattu et al. 1998) and Gomes et al. (Gomes et al. 2008) showed that IgA glycosylation is not important for binding this receptor. Here, IgA antibodies produced in GEX-Fuc$^-$ with reduced fucosylation do not differ in ADCC potency compared to IgA antibodies produced in GEX-H9D8. Considering studies that showed no difference between IgA antibodies of various sources or PNGase F-treated IgA antibodies in FcαRI binding (Gomes et al. 2008), it is not surprising that comparable ADCC potency was observed for IgA antibodies produced in expression systems resulting in varying glycosylation. Similarly, investigations using different recombinant IgA1 antibodies showed no dependency on glycosylation for FcαRI binding (Mattu et al. 1998). This is in

contrast to IgG-IgG receptor interactions, defucosylated IgG Fc glycans result in increased affinity towards FcγRIIIa. For defucosylated IgG, carbohydrate-carbohydrate interactions between receptor and antibody glycans are responsible for increased affinity and result in more potent FcγRIIIa-mediated ADCC (Ferrara et al. 2011). More potent ADCC for IgA2 over IgA1 antibodies and the lack of influence of glycosylation patterns were the reason for testing antibodies with other specificities in IgA2 format using the wild-type glycosylation cell line GEX-H9D8. As discussed before, IgA glycans may influence stability (Chapter 4.2) as well as be involved in interaction with microbes at mucosal sites (Arnold et al. 2007). Due to their surface exposed orientation, glycosylation effects on solubility and pharmacodynamics through interaction with glycan-specific receptors or lectins relevant for serum half-life and distribution could be expected to be more pronounced for IgA than for IgG antibodies. This highlights the importance of IgA glycosylation even though it does not directly affect FcαRI-mediated effector functions. In conclusion, ADCC was successfully shown as mode of action for all four IgA antibodies with targets of solid cancer indications (Chapters 3.3.3 and 3.3.4). However, as shown for hTM and CM IgA2 antibodies, ADCC potencies greatly differ depending on the cancer target cells used. Both, hTM and CM IgA2 were more potent against SK-BR-3 target cells than corresponding IgG antibodies which is consistent with literature comparing both isotypes (Huls et al. 1999; Beyer et al. 2009; Lohse et al. 2011; Lohse et al. 2012). Conversely, using other target cell lines IgA2 antibodies resulted in marginal or no specific target cell lysis while IgG antibodies mediated lysis. Hence, for each antibody several target cells should be tested to evaluate ADCC potential. One factor that could influence IgA or IgG potency differently is antigen density (Derer et al. 2012). IgG receptors might require not as dense antigen distribution on the surface of a target cell for efficient crosslinking and subsequent effector cell activation as compared to IgA-specific FcαRI. Additionally, the molecular environment in proximity to the antigen on the surface of target cells could affect FcγR or FcαRI activation differently. The combination of antigen density, antigen environment, antibody isotype and effector cell population could be relevant for ADCC activity against cancer cells (Valerius et al. 1997; Derer et al. 2012; Lohse et al. 2012).

In this study, the *in vitro* activity of IgA antibodies varied depending on the target and tested cancer cell lines (Chapter 3.3.4). In line with attempts to personalize medicinal treatments (Kalia 2015), it might be feasible to search for and define biomarkers which could indicate beneficial therapeutic potential of one or another isotype for a patient. Increasing the functional diversity of cancer therapeutics with isotypes other than IgG, could increase

therapeutic options for patients (Gravitz 2014; Henderson et al. 2014). Patients might benefit from IgA antibody therapy where IgG antibodies lack efficacy and thereby represent a promising strategy for cancer therapy.

As additional Fc-mediated mode of action, the potential of IgA antibodies to mediate phagocytosis of cancer cell lines was shown using monocyte-derived macrophages as effector cells. Before, FcαRI-mediated phagocytosis has been shown using a bispecific antibody directed against FcαRI and Her2 (Keler et al. 2000). Moreover, recombinant IgA2 directed against EGFR was investigated in macrophage-mediated ADCC assays (Lohse et al. 2012). In contrast, here phagocytosis was shown for recombinant anti-TA-MUC1 and anti-Her2 IgA2 antibodies. While maximal phagocytosis was similar or higher for IgG isotype antibodies, IgA2 concentration-dependent phagocytosis was shown using three cancer cell lines (Chapter 3.3.5). Hence, macrophages could represent another effector cell population for therapeutic IgA antibodies against cancer cells. A small subset of macrophages was cultivated under conditions promoting M2 type differentiation (Schmid & Varner 2010). Interestingly, anti-Her2 IgA2 antibody reached higher maximal lysis with M2-like as compared to M1-like macrophages. This is in contrast to ADCC assays using M1- and M2-like macrophages where both effector cell populations were comparable effective in ADCC assays with anti-EGFR IgA2 and IgG antibodies (Lohse et al. 2012). However, the experiments using M2-like macrophages were preliminary and need further elaboration. In tumors, M2 type macrophages are more prominent and possess a rather anti-inflammatory phenotype (Schmid & Varner 2010). As shown for different cancers, tumor-associated macrophages are involved in tumor vascularization (Nishie et al. 1999) and constitute up to 50% of the cell mass of a tumor (Lewis et al. 1995). Using therapeutic antibodies to mediate phagocytic activity of this lymphocyte population within the tumor microenvironment could represent a promising effector functionality for cancer therapy.

Evaluation of therapeutic IgA antibodies *in vivo* is difficult because mice do not express FcαRI (van Egmond et al. 1999). Hence, *in vitro* experiments using human effector cells and cancer cell lines might even be more relevant than efficacy experiments in mice. Nevertheless, studies were conducted to investigate *in vivo* pharmacokinetics and anti-tumor efficacy of IgA antibodies (Rifai et al. 2000; Boross et al. 2013). In human serum, IgA1 levels are much higher than IgA2 levels (Chapter 1.1.3). The half-life of recombinant IgA1 and IgA2 antibodies was investigated in mice and depended on asialoglycoprotein receptor (ASGP-R)-mediated clearance for IgA2. IgA2 clearance was faster than for IgA1 and could

be inhibited by free galactose. Interestingly, recombinant IgA1 lacking the O-glycosylated hinge region was cleared faster than wild-type IgA1, indicating that IgA1 O-glycans do not increase clearance in mice (Rifai et al. 2000). The higher number of N-glycans for IgA2 antibodies could also result in increased clearance mediated by the ASGP-R in case of incompletely sialylated N-glycans containing terminal glactose. Still, the relevance of the study by Rifai et al. (Rifai et al. 2000) for the IgA antibodies produced in the presented study is questionable since the half-life could be affected by the expression system used. Moreover, mice lack an FcαRI homologue which could affect clearance. Another study investigated IgA antibody clearance and anti-tumor efficacy in transgenic mice expressing FcαRI (Boross et al. 2013). While no effect of FcαRI expression on serum half-life was observed, blocking of the ASGP-R using asialofetuin resulted in decreased clearance within the first hours. In contrast to Rifai et al., clearance of IgA1 and IgA2 antibodies was comparable (Rifai et al. 2000). However, different glycosylation patterns might have affected clearance rates. In the study by Boross et al., sialylation of N-glycans was absent for IgA1 antibodies while 20% of IgA2 antibodies were sialylated (Boross et al. 2013). Compared to IgG, the anti-EGFR IgA2 antibody showed comparable and better anti-tumor efficacy in transgenic mouse xenograft models (Boross et al. 2013). Recently, protein and cell line engineering was used to decrease the number of glycosylation sites on IgA antibodies and increase the sialylation degree of glycans, respectively, and thereby improve pharmacokinetic properties and *in vivo* efficacy due to reduced terminal galactose (Meyer et al. 2015; Lohse et al. 2016; Rouwendal et al. 2016). Still, due to faster clearance, IgA2 antibodies were administered five to eleven times as compared to a single administration of IgG antibodies at equal doses. With more frequent administration and protein or cell line engineering, IgA2 antibodies reached comparable tumor growth inhibition like IgG antibodies (Lohse et al. 2016; Rouwendal et al. 2016). By the generation of non-engineered IgA antibodies with completely sialylated N-glycans, *in vivo* efficacy could potentially be further increased because of better pharmacokinetic behavior. In addition, while CHO-derived N-glycans exclusively possess α2,3-linked sialic acid, the majority of human serum IgA is linked in α2,6 configuration (Mattu et al. 1998; Jefferis 2009). This difference might also affect pharmacokinetic behavior of therapeutic IgA antibodies *in vivo* and could be overcome by using human expression systems.

4.4 Targeting hematological cancer indications with novel anti-CD20 IgA2 and IgG antibodies

hOM IgA2 and IgG were functional in target cell binding as well as B cell depletion. As seen for some antibodies directed against solid cancer targets, hOM IgG was more effective than IgA2 at lower concentrations. Moreover, hOM IgA2 antibodies did not reach the same maximal B cell depletion. Interestingly, at the highest hOM IgA2 concentration tested, a decrease of B cell depletion was observed. In molar excess of IgA over targets, this could indicate anti-inflammatory signaling during monovalent binding of free IgA antibodies to the FcαRI (Monteiro & Van De Winkel 2003; Bakema & van Egmond 2011; Ben Mkaddem et al. 2013) (Figure 2). However, similar effects at high antibody concentrations were observed for ofatumumab, a type I anti-CD20 IgG antibody (Herter et al. 2013). As described for type II anti-CD20 IgG antibodies, hOM IgG is much more potent than type I anti-CD20 Mabthera (rituximab) in mediating B cell depletion (Mossner et al. 2010; Herter et al. 2013). The reason for different potency of the two types of anti-CD20 IgG antibodies might be attributed to differently oriented target binding (Cragg 2011; Niederfellner et al. 2011). The effector mechanisms underlying B cell depletion were investigated and rather attributed to ADCC than CDC which could explain that type II anti-CD20 antibodies are more potent (Ferrara et al. 2006). Since B cell depletion using whole blood resembles the human situation for therapeutics better than other *in vitro* assays, other functionalities like lysosomal membrane permeabilization or homotypic adhesion of target cells were not investigated (Alduaij et al. 2011). Biofunctionality of the generated anti-CD20 IgA2 and IgG antibodies against target cells was shown. This indicates that IgA isotype antibodies could also be applicable for hematological cancer indications which was also shown using type I anti-CD20 antibody rituximab as parental antibody (Pascal et al. 2012).

4.5 Combining advantages of two isotypes by generating a mixed-isotype antibody targeting Her2

Mixed-isotype hTM IgG-Cα3 construct was successfully produced and biofunctionality was shown. Like IgA antibodies, mixed-isotype hTM IgG-Cα3 construct formed dimers and higher order multimers. The construct was designed by fusion of IgA1 Cα3 domain to the C terminus of full-length IgG heavy chain, including the tailpiece with penultimate cysteine (Figure 17). As for IgA antibodies (Chapter 3.2.3), J chain co-expression might further

increase mixed-isotype construct multimerization. This was shown for another construct consisting of IgG and IgA domains (VH, Cγ1, Cα2 and Cα3) which was recently generated. The mixed-isotype (termed hybrid-IgG/IgA) targets a bacterial toxin and dimerization was promoted by J chain co-expression (Iwata et al. 2014).

As expected, antigen binding was retained for the mixed-isotype construct. In biofunctional assays, hTM IgG-Cα3 was comparable with hTM IgG antibody in proliferation inhibition and reached similar maximal lysis in granulocyte ADCC and maximal phagocytosis in ADCP assays. Since mixed-isotype construct and IgG were comparable in biofunctional assays which rely on Fc receptor interactions, most likely FcγRs on the surface of effector cells were responsible for functionality of hTM IgG-Cα3 construct. Although hTM IgG-Cα3 construct is capable of FcαRI binding (Chapter 3.2.10), most likely this receptor did not functionally contribute in the effector cell-dependent assays tested. Blocking experiments with anti-FcγR and anti-FcαRI antibodies could further elucidate the role of individual Fc receptors. Since FcαRI binding of hTM IgG-Cα3 construct was low as compared to IgA antibodies, further mutations within the Cγ3 might be necessary for more affine binding to the FcαRI. IgA residues responsible for FcαRI binding mainly lye within Cα3 while only a small number of amino acids within Cα2 is involved (Bakema & van Egmond 2011) (Chapter 1.1.4). Indeed, Kelton et al. generated a mixed-isotype (termed cross-isotype) construct targeting Her2 by replacing IgG Cγ3 with Cα3 and introducing mutations in Cγ2. In biofunctional assays like granulocyte ADCC and ADCP using MDM, this construct was comparable to the corresponding IgA1 antibody while the corresponding IgG had only minor cytotoxic effects (Kelton et al. 2014).

4.6 Future prospective of therapeutic IgA antibodies

IgA antibodies against five targets were successfully generated and biofunctionality against cancer cell lines was shown. Large quantities and high quality monoclonal IgA antibodies were expressed. Hence, therapeutic IgA antibodies could be produced in sufficient amounts for potential application to treat cancer. However, weather *in vitro* activity translates into tumor growth inhibition or cytotoxicity against cancer *in vivo* remains to be elucidated. Animals might only be partly relevant to investigate the potential of IgA antibodies for cancer therapy due to differences in human and murine immune systems. Mice lack the Fc receptor responsible for cellular cytotoxicity mediated by IgA antibodies. In xenograft models, efficacy would be related to direct Fab-mediated effector functions or transgenic animals with

IgA-specific Fc receptors on the surface of immune effector cells would be required. Studies reported transgenic xenograft mouse models where IgA antibodies were administered more frequently than IgG antibodies *in vivo* to account for faster clearance rates (Boross et al. 2013; Lohse et al. 2016; Rouwendal et al. 2016). Glycan structures of the IgA2m(1) antibodies generated here possessed higher sialylation degrees, which could at least to some degree overcome ASGP-R-mediated clearance. Still, IgA antibodies do not bind the FcRn receptor which is responsible for the long half-life of IgG antibodies in circulation (Basset et al. 1999). Whether increased serum half-life of IgA antibodies translates into favorable tumor distribution remains to be elucidated. Protein engineering approaches might yield novel IgG antibody-based constructs which overcome fast clearance rates and bind to additional Fc receptors to mediate potent cellular cytotoxicity (Chapter 4.5).

The potential of IgA antibodies for cancer therapy is also supported by the fact that, upon other isotypes, production of IgA antibodies was induced after vaccination with recombinant carcinoembryonic antigen protein (Staff et al. 2012). Moreover, immunohistochemically staining of primary human breast cancer samples showed high abundance IgA1 antibodies on the membrane and in the cytosol (Welinder et al. 2013). Taken together, there are still challenges remaining to elucidate the potential of IgA antibodies *in vivo*, but involvement of IgA isotype antibodies in human cancer has been shown.

In other indications, fast clearance might be of advantage if clearance of soluble targets is desired. For example in case of tumor necrosis factor inhibitors like infliximab, etanercept, adalimumab, certolizumab, or golimumab which inhibits its function as inflammatory activator (Tanaka et al. 2014; Willrich et al. 2015). This might represent another attractive application of the IgA format as therapeutic for autoimmune disease by utilizing the increased clearance rates to inhibit and clear inflammatory activators. Monoclonal IgA antibodies could be also interesting for autoimmune disease through their inhibitory signaling within immune effector cells through FcαRI (Ivashkiv 2011). Upon monovalent binding, in the absence of immune complexes, IgA antibodies cause inhibitory signaling (Chapter 1.1.4). This could be an attractive strategy to improve current treatments like intravenous immunoglobulins (IVIg). IgA- or FcαRI-related treatment of autoimmune diseases could result in long-lasting inhibitory signals (Ben Mkaddem et al. 2013). In cases where B cell depletion could further contribute to efficacy, anti-CD20 hOM IgA2 generated here could simultaneously clear CD20-positive cells as well as inhibit inflammatory events by monovalent interaction with FcαRI on the surface of effector cells.

IgA antibodies were also investigated to treat infection diseases. One of the best known function of IgA antibodies is immune exclusion (Chapter 1.1.6, Figure 3). Indeed, IgA antibodies showed efficacy against tuberculosis (Balu et al. 2011) and in a murine malaria model (Shi et al. 2006). *In vitro* anti-human immunodeficiency virus type 1 IgA antibody inhibited epithelial viral transcytosis which indicates the potential of therapeutic IgA administration at mucosal sites (Wolbank et al. 2003). Targeting influenza virus hemagglutinin using IgG or IgA antibodies revealed higher potential to inhibit virus particle release from infected cells by IgA antibodies. This might have been caused by increased avidity since polymeric IgA antibodies were compared with monomeric IgG antibodies (Muramatsu et al. 2014). Together, these studies indicate that therapeutic IgA antibodies might be applied to sites where IgG antibodies cannot be administered or when bivalent binding of IgG antibodies is not sufficient for successful immune exclusion of pathogens. For vaccination strategies, IgA immune complexes could promote transcytosis of antigens across the epithelial barrier by intestinal microfold cells. On the basolateral site, dendritic cells subsequently internalize IgA-antigen complexes and present antigenic structures to initiate vaccination (Mantis et al. 2011; Rochereau et al. 2013).

In conclusion, the potential of IgA antibodies for cancer therapy was successfully shown for five heterogeneous targets. High yield production of monoclonal IgA antibodies using the human GEX expression system was established. To generate more affine dimeric IgA antibodies, J chain co-expression was successful to accomplish increased dimer association. Both, Fab- and Fc-mediated effector functions were shown against multiple cancer cell lines. This represents a thorough evaluation of IgA isotype antibodies for cancer therapy, highlighting the potential to use other formats than IgG antibodies. Hence, IgA antibodies could complement therapeutic options where patients do not benefit from IgG antibody therapy. However, beyond cancer therapy, the distinct characteristics of IgA antibodies could be beneficial in other indications too. As discussed above, therapeutic IgA administration might be considered at mucosal sites to prevent pathogen infection or to promote vaccination. Moreover, autoimmune diseases could be potentially treated with IgA antibodies which clear inflammatory activators or mediate anti-inflammatory responses through monovalent interaction with FcαRI.

5 Summary

In humans, IgA antibody production exceeds production of all other isotypes combined which highlights the importance of this isotype. However, approved cancer immunotherapeutics are restricted to IgG isotype antibodies. In order to improve the functional diversity of antibodies for cancer therapy, the potential of IgA isotype antibodies was elucidated. IgA antibodies mediate inflammatory responses through interaction with IgA receptors on the surface of immune effector cells like granulocytes and macrophages. Cellular activation results in the release of cytotoxic agents or phagocytosis of opsonized cells. Granulocytes represent the most numerous cell population in human blood and, like macrophages, are found within the tumor microenvironment. Thus, recruitment and activation of these effector cells represents a promising strategy for cancer immunotherapy.

Both IgA1 and IgA2 antibodies were expressed in human cell lines and multimerization was successfully enhanced by co-expression of the joining chain. High yields of IgA antibodies were achieved and 11 g IgA2 were produced by cultivation within 35 days in a one-liter perfusion bioreactor. Kinetic analysis revealed increased avidity antigen binding for IgA2J dimers as compared to monomeric IgA2 or IgG antibodies. An IgG-IgA mixed-isotype construct was generated to increased valence and allow interaction with both, IgG and IgA specific receptors.

IgA antibodies exhibited potent effector functions against cancer cell lines. IgA and IgG antibodies were comparable in Fab-mediated inhibition of target cell proliferation. IgA antibodies were effective in Fc-mediated antibody-dependent cellular cytotoxicity and phagocytosis where IgA2 antibodies were more potent than IgA1 in recruiting granulocytes against target cells. Activities of IgA and IgG antibodies in Fc-mediated effector functions differed depending on target and effector cells. This indicates that both, antigen density and antibody receptor expression on the surface of effector cells affect the potential of each isotype. The IgA antibody targeting CD20 was potent in B cell depletion.

Together, biofunctionality for the analyzed IgA antibodies directed against a heterogeneous group of targets for solid and hematological cancer indications was successfully shown. For patients who do not sufficiently benefit form therapeutic IgG antibodies, IgA antibodies may complement current regiment options and represent a promising strategy for cancer immunotherapy.

6 Zusammenfassung

Der humane Organismus produziert vom IgA Isotyp mehr als von allen anderen Isotypen zusammen, was die Bedeutung von IgA Antikörpern unterstreicht. Dennoch sind alle bislang zugelassenen Antikörper ausschließlich vom IgG Isotyp. Um die Diversität und Funktionalität von Antikörpern zur Krebstherapie zu erhöhen, wurde hier das Potential von IgA Antikörpern untersucht. IgA Antikörper können durch die Interaktion mit IgA-Rezeptoren, die auf der Oberfläche von Immun-Effektorzellen wie Granulozyten und Makrophagen lokalisiert sind, inflammatorische Reaktionen auslösen. Die zelluläre Aktivierung führt zur Ausschüttung von zytotoxischen Substanzen oder Phagozytose von opsonierten Zellen. Granulozyten repräsentieren die zahlreichste Zellpopulation im Blut und sind genau wie Makrophagen in der Tumormikroumgebung zu finden. Die Rekrutierung und Aktivierung dieser Zellpopulationen ist daher eine vielversprechende Strategie für die Krebstherapie.

IgA1 und IgA2 Antikörper wurden mit einer humanen Zelllinie exprimiert und mittels Co-Expression der J-Kette wurde die Multimerisierung erfolgreich gesteigert. Für alle IgA Antikörper wurden hohe Ausbeuten erzielt und innerhalb einer 35-tägigen Kultivierung im ein Liter Perfusionsbioreaktor konnten 11 g IgA produziert werden. In kinetische Analysen wurde gezeigt, dass IgA2J Dimere ihr Antigen mit höherer Avidität binden als IgA2 oder IgG Monomere. Ein Mix-Isotyp-Antikörperkonstrukt aus IgG und IgA wurde generiert, um erhöhte Valenz und Bindung von IgG- und IgA-Rezeptoren zu ermöglichen.

Alle IgA Antikörper zeigten potente Effektorfunktionen gegen Krebszelllinien. Die Fab-vermittelte Inhibition der Zielzellproliferation war zwischen IgA und IgG Antikörpern vergleichbar. Die IgA Antikörper waren effektiv in Fc-vermittelter Antikörper-abhängiger zellulärer Zytotoxizität und Phagozytose, wobei IgA2 effektiver Granulozyten gegen Zielzellen rekrutierten als IgA1. Die Aktivitäten der IgA und IgG Antikörper bei Fc-vermittelten Effektorfunktionen unterschied sich abhängig von Effektor- und Zielzellen. Sowohl die Antigenexpression auf der Oberfläche von Ziel-, als auch die Antikörper-Rezeptor-Expression auf der Oberfläche von Effektorzellen beeinflussten die Aktivtäten beider Isotypen. Der gegen CD20 gerichtete IgA Antikörper konnte effektiv B-Zellen depletieren.

Zusammenfassend konnte die Biofunktionalität von fünf IgA Antikörpern, die gegen eine heterogene Gruppe von Targets für solide und hämatologische Krebsindikationen gerichtet sind, erfolgreich gezeigt werden. Für Patienten, die von einer Therapie mit IgG Antikörpern nicht ausreichend profitieren, könnten IgA Antikörper vorhandene Behandlungsmöglichkeiten komplementieren und somit eine vielversprechende Strategie zur Krebstherapie darstellen.

7 References

Akewanlop, C. et al., 2001. Phagocytosis of breast cancer cells mediated by anti-MUC-1 monoclonal antibody, DF3, and its bispecific antibody. *Cancer research*, 61(10), pp.4061–5.

Alduaij, W. et al., 2011. Novel type II anti-CD20 monoclonal antibody (GA101) evokes homotypic adhesion and actin-dependent, lysosome-mediated cell death in B-cell malignancies. *Blood*, 117(17), pp.4519–4529.

Allen, a C. et al., 1999. Analysis of IgA1 O-glycans in IgA nephropathy by fluorophore-assisted carbohydrate electrophoresis. *Journal of the American Society of Nephrology : JASN*, 10(8), pp.1763–1771.

Amado, R.G. et al., 2008. Wild-type KRAS is required for panitumumab efficacy in patients with metastatic colorectal cancer. *Journal of Clinical Oncology*, 26(10), pp.1626–1634.

Arnold, J.N. et al., 2007. The impact of glycosylation on the biological function and structure of human immunoglobulins. *Annual review of immunology*, 25, pp.21–50.

Atkin, J.D. et al., 1996. Mutagenesis of the Human IgA1 Heavy Chain Tailpiece That Prevents Dimer Assembly. *The Journal of Immunology*, 157, pp.156–159.

Avery, O.T., 1944. Studies on the chemical nature of the substance inducing transformation of pneumococcal types: induction of transformation by a desoxyribonucleic acid fraction isolated from pneumococcus type III. *Journal of Experimental Medicine*, 79(2), pp.137–158.

Bafna, S., Kaur, S. & Batra, S.K., 2010. Membrane-bound mucins: the mechanistic basis for alterations in the growth and survival of cancer cells. *Oncogene*, 29(20), pp.2893–2904.

Bakema, J.E. et al., 2011. Targeting Fc alpha RI on Polymorphonuclear Cells Induces Tumor Cell Killing through Autophagy. *The Journal of Immunology*, 187(2), pp.726–732.

Bakema, J.E. & van Egmond, M., 2011. The human immunoglobulin A Fc receptor FcαRI: a multifaceted regulator of mucosal immunity. *Mucosal Immunology*, 4(6), pp.612–624.

Baldus, S.E. et al., 1998. Coexpression of MUC1 mucin peptide core and the thomsen-friedenreich antigen in colorectal neoplasms. *Cancer*, 82(6), pp.1019–1027.

Balu, S. et al., 2011. A Novel Human IgA Monoclonal Antibody Protects against Tuberculosis. *The Journal of Immunology*, 186(5), pp.3113–3119.

Baselga, J. & Swain, S.M., 2009. Novel anticancer targets: revisiting ERBB2 and discovering ERBB3. *Nature reviews. Cancer*, 9(7), pp.463–475.

Basset, C. et al., 1999. Glycosylation of immunoglobulin a influences its receptor binding. *Scandinavian Journal of Immunology*, 50(6), pp.572–579.

Beck, A. et al., 2010. Strategies and challenges for the next generation of therapeutic antibodies. *Nature reviews. Immunology*, 10(5), pp.345–352.

Beck, A. & Reichert, J.M., 2014. Antibody-drug conjugates. *mAbs*, 6(1), pp.15–17.

Beyer, T. et al., 2010. Expression of IgA Molecules in Mammalian Cells. In R. Kontermann & S. Dübel, eds. *Antibody Engineering*. Berlin, Heidelberg: Springer Berlin Heidelberg, pp. 471–486.

Beyer, T. et al., 2009. Serum-free production and purification of chimeric IgA antibodies. *Journal of Immunological Methods*, 346(1-2), pp.26–37.

Bibeau, F. et al., 2009. Impact of Fc RIIa-Fc RIIIa Polymorphisms and KRAS Mutations on the Clinical Outcome of Patients With Metastatic Colorectal Cancer Treated With Cetuximab Plus Irinotecan. *Journal of Clinical Oncology*, 27(7), pp.1122–1129.

Bitler, B.G. et al., 2009. Intracellular MUC1 Peptides Inhibit Cancer Progression. *Clinical Cancer Research*, 15(1), pp.100–109.

Boehm, M.K. et al., 1999. The fab and fc fragments of IgA1 exhibit a different arrangement from that in IgG: a study by X-ray and neutron solution scattering and homology modelling. *Journal of Molecular Biology*, 286(5), pp.1421–1447.

Bologna, L. et al., 2012. Ofatumumab Is More Efficient than Rituximab in Lysing B Chronic Lymphocytic Leukemia Cells in Whole Blood and in Combination with Chemotherapy. *The Journal of Immunology*, 190(1), pp.231–239.

Boross, P. et al., 2013. IgA EGFR antibodies mediate tumour killing in vivo. *EMBO Molecular Medicine*, 5(8), pp.1213–1226.

Boross, P. & Leusen, J.H.W., 2012. Mechanisms of action of CD20 antibodies. *American journal of cancer research*, 2(6), pp.676–90.

Bournazos, S. et al., 2009. Functional and clinical consequences of Fc receptor polymorphic and copy number variants. *Clinical and Experimental Immunology*, 157(2), pp.244–254.

Boveri, T., 1914. *Zur Frage der Entstehung maligner Tumoren*, Gustav Fischer.

Brandtzaeg, P., 2009. Mucosal immunity: induction, dissemination, and effector functions. *Scandinavian journal of immunology*, 70(6), pp.505–15.

Brandtzaeg, P., Baekkevold, E.S. & Morton, H.C., 2001. From B to A the mucosal way. *Nature Immunology*, 2(12), pp.1093–1094.

Brandtzaeg, P. & Johansen, F.E., 2005. Mucosal B cells: Phenotypic characteristics, transcriptional regulation, and homing properties. *Immunological Reviews*, 206(1), pp.32–63.

Brandtzaeg, P. & Prydz, H., 1984. Direct evidence for an integrated function of J chain and secretory component in epithelial transport of immunoglobulins. *Nature*, 311(5981), pp.71–73.

Breasted, J.H., 1930. *The Edwin Smith Surgical Papyrus*, Chicago, Illinois: The University of Chicago Press.

Brunke, C. et al., 2013. Effect of a tail piece cysteine deletion on biochemical and functional properties of an epidermal growth factor receptor-directed IgA2m(1) antibody. *mAbs*, 5(6), pp.936–45.

Bubien, J.K. et al., 1993. Transfection of the CD20 cell surface molecule into ectopic cell types generates a Ca2+ conductance found constitutively in B lymphocytes. *Journal of Cell Biology*, 121(5), pp.1121–1132.

Cao, Y. et al., 1995. Expression of Thomsen-Friedenreich-related antigens in primary and metastatic colorectal carcinomas: A reevaluation. *Cancer*, 76(10), pp.1700–1708.

Carayannopoulos, L., Max, E.E. & Capra, J.D., 1994. Recombinant human IgA expressed in insect cells. *Proceedings of the National Academy of Sciences*, 91(18), pp.8348–8352.

Carvajal-Hausdorf, D.E. et al., 2015. Measurement of Domain-Specific HER2 (ERBB2) Expression May Classify Benefit From Trastuzumab in Breast Cancer. *JNCI Journal of the National Cancer Institute*, 107(8), pp.djv136–djv136.

Celsus, A.C. & Spencer, W.G., 1935. *De medicina / with an English translation by W. G. Spencer.*, Harvard university press ; London : W. Heinemann, ltd, Cambridge, Mass.

Chintalacharuvu, K.R., Gurbaxani, B. & Morrison, S.L., 2007. Incomplete assembly of IgA2m(2) in Chinese hamster ovary cells. *Molecular Immunology*, 44(13), pp.3445–3452.

Chintalacharuvu, K.R., Raines, M. & Morrison, S.L., 1994. Divergence of human alpha-chain constant region gene sequences. A novel recombinant alpha 2 gene. *Journal of immunology (Baltimore, Md. : 1950)*, 152(l), pp.5299–304.

Chung, C.H. et al., 2008. Cetuximab-Induced Anaphylaxis and IgE Specific for Galactose-α-1,3-Galactose. *New England Journal of Medicine*, 358(11), pp.1109–1117.

Clark, R. & Kupper, T., 2005. Old meets new: The interaction between innate and adaptive immunity. *Journal of Investigative Dermatology*, 125(4), pp.629–637.

Clausen, H. et al., 1988. Monoclonal antibodies directed to the blood group A associated structure, galactosyl-A: specificity and relation to the Thomsen-Friedenreich antigen. *Molecular immunology*, 25(2), pp.199–204.

Coyne, R.S. et al., 1994. Mutational Analysis of Polymeric Immunoglobulin ReceptorLigand Interactions. *The Journal of Biological Chemistry*, 269(50), pp.31620–31625.

Cragg, M.S., 2011. CD20 antibodies: Doing the time warp. *Blood*, 118(2), pp.219–220.

Cragg, M.S. et al., 2005. The biology of CD20 and its potential as a target for mAb therapy. *Current directions in autoimmunity*, 8, pp.140–174.

Danielczyk, A. et al., 2006. PankoMab: A potent new generation anti-tumour MUC1 antibody. *Cancer Immunology, Immunotherapy*, 55(11), pp.1337–1347.

Deans, J.P., Li, H. & Polyak, M.J., 2002. CD20-mediated apoptosis: Signalling through lipid rafts. *Immunology*, 107(2), pp.176–182.

Dechant, M. et al., 2002. Chimeric IgA antibodies against HLA class II effectively trigger lymphoma cell killing. *Blood*, 100(13), pp.4574–4580.

Dechant, M. et al., 2007. Effector Mechanisms of Recombinant IgA Antibodies against Epidermal Growth Factor Receptor. *The Journal of Immunology*, 179(5), pp.2936–2943.

Deo, Y.M. et al., 1998. Bispecific molecules directed to the Fc receptor for IgA (Fc alpha RI, CD89) and tumor antigens efficiently promote cell-mediated cytotoxicity of tumor targets in whole blood. *The Journal of Immunology*, 160, pp.1677–1686.

Derer, S. et al., 2012. Impact of epidermal growth factor receptor (EGFR) cell surface expression levels on effector mechanisms of EGFR antibodies. *The Journal of Immunology*, 189(11), pp.5230–9.

DeVita, V.T. & Rosenberg, S. a, 2012. Two Hundred Years of Cancer Research. *New England Journal of Medicine*, 366(23), pp.2207–2214.

Dhodapkar, K.M. et al., 2002. Antitumor monoclonal antibodies enhance cross-presentation ofcCellular antigens and the generation of myeloma-specific killer T cells by dendritic cells. *The Journal of experimental medicine*, 195(1), pp.125–133.

Van Dijk, T.B. et al., 1996. Cloning and characterization of Fc alpha Rb, a novel Fc alpha receptor (CD89) isoform expressed in eosinophils and neutrophils. *Blood*, 88(11), pp.4229–4238.

Dumitru, C. a., Lang, S. & Brandau, S., 2013. Modulation of neutrophil granulocytes in the tumor microenvironment: Mechanisms and consequences for tumor progression. *Seminars in Cancer Biology*, 23(3), pp.141–148.

Van Egmond, M. et al., 2001. Enhancement of polymorphonuclear cell-mediated tumor cell killing on simultaneous engagement of fcgammaRI (CD64) and fcalphaRI (CD89). *Cancer research*, 61(10), pp.4055–4060.

Van Egmond, M. et al., 1999. Human immunoglobulin A receptor (FcalphaRI, CD89) function in transgenic mice requires both FcR gamma chain and CR3 (CD11b/CD18). *Blood*, 93(12), pp.4387–4394.

Van Egmond, M. et al., 2001. IgA and the IgA Fc receptor. *Trends in Immunology*, 22(4), pp.205–211.

Favre, L., Spertini, F. & Corthésy, B., 2005. Secretory IgA possesses intrinsic modulatory properties stimulating mucosal and systemic immune responses. *The Journal of Immunology*, 175(5), pp.2793–2800.

Ferrara, C. et al., 2006. Modulation of therapeutic antibody effector functions by glycosylation engineering: Influence of Golgi enzyme localization domain and co-expression of

heterologous β1, 4-N-acetylglucosaminyltransferase III and Golgi α-mannosidase II. *Biotechnology and Bioengineering*, 93(5), pp.851–861.

Ferrara, C. et al., 2011. Unique carbohydrate-carbohydrate interactions are required for high affinity binding between FcgammaRIII and antibodies lacking core fucose. *Proceedings of the National Academy of Sciences of the United States of America*, 108(31), pp.12669–12674.

Field, M.C. et al., 1994. Structural analysis of the N-glycans from human immunoglobulin A1: comparison of normal human serum immunoglobulin A1 with that isolated from patients with rheumatoid arthritis. *The Biochemical journal*, 299 Pt 1, pp.261–275.

Franklin, R.E. & Gosling, R.G., 1953. Molecular Configuration in Sodium Thymonucleate. *Nature*, 171(4356), pp.740–741.

Furtado, P.B. et al., 2004. Solution structure determination of monomeric human IgA2 by X-ray and neutron scattering, analytical ultracentrifugation and constrained modelling: A comparison with monomeric human IgA1. *Journal of Molecular Biology*, 338(5), pp.921–941.

Fuster, M.M. & Esko, J.D., 2005. The sweet and sour of cancer: glycans as novel therapeutic targets. *Nature reviews. Cancer*, 5(7), pp.526–542.

Gasteiger, E. et al., 2005. Protein Identification and Analysis Tools on the ExPASy Server. *The Proteomics Protocols Handbook*, pp.571–607.

Gerdes, C. a. et al., 2013. GA201 (RG7160): A novel, humanized, glycoengineered anti - EGFR antibody with enhanced ADCC and superior in vivo efficacy compared with cetuximab. *Clinical Cancer Research*, 19(5), pp.1126–1138.

Ghumra, A. et al., 2009. Structural requirements for the interaction of human IgM and IgA with the human Fc α/μ receptor. *European Journal of Immunology*, 39(4), pp.1147–1156.

Golay, J. et al., 2013. Glycoengineered CD20 antibody obinutuzumab activates neutrophils and mediates phagocytosis through CD16B more efficiently than rituximab. *Blood*, 122(20), pp.3482–91.

Goldman, M.H. et al., 1998. Monitoring recombinant human interferon-gamma N-glycosylation during perfused fluidized-bed and stirred-tank batch culture of CHO cells. *Biotechnology and Bioengineering*, 60(5), pp.596–607.

Goletz, S. et al., 2003. Thomsen-Friedenreich antigen: the "hidden" tumor antigen. *Advances in experimental medicine and biology*, 535, pp.147–62.

Gomes, M.M. et al., 2008. Analysis of IgA1 N -Glycosylation and Its Contribution to FcαRI Binding. *Biochemistry*, 47(43), pp.11285–11299.

Gravitz, L., 2014. Therapy: This time it's personal. *Nature*, 509, pp.S52–S54.

Hajdu, S.I., 2011. A note from history: Landmarks in history of cancer, part 1. *Cancer*, 117(5), pp.1097–1102.

Hanahan, D. & Coussens, L.M., 2012. Accessories to the Crime: Functions of Cells Recruited to the Tumor Microenvironment. *Cancer Cell*, 21(3), pp.309–322.

Hanahan, D. & Weinberg, R. a., 2011. Hallmarks of cancer: The next generation. *Cell*, 144(5), pp.646–674.

Hanahan, D. & Weinberg, R. a., 2000. The hallmarks of cancer. *Cell*, 100, pp.57–70.

Hang, H.C. & Bertozzi, C.R., 2005. The chemistry and biology of mucin-type O-linked glycosylation. *Bioorganic and Medicinal Chemistry*, 13(17), pp.5021–5034.

Henderson, D. et al., 2014. Personalized medicine approaches for colon cancer driven by genomics and systems biology: OncoTrack. *Biotechnology Journal*, 9(9), pp.1104–1114.

Herr, A.B., White, C.L., et al., 2003. Bivalent binding of IgA1 to FcαRI suggests a mechanism for cytokine activation of IgA phagocytosis. *Journal of Molecular Biology*, 327(3), pp.645–657.

Herr, A.B., Ballister, E.R. & Bjorkman, P.J., 2003. Insights into IgA-mediated immune responses from the crystal structures of human FcalphaRI and its complex with IgA1-Fc. *Nature*, 423(6940), pp.614–620.

Herter, S. et al., 2013. Preclinical activity of the type II CD20 antibody GA101 (obinutuzumab) compared with rituximab and ofatumumab in vitro and in xenograft models. *Molecular cancer therapeutics*, 12(10), pp.2031–42.

Hexham, J.M. et al., 1999. A human immunoglobulin (Ig)A calpha3 domain motif directs polymeric Ig receptor-mediated secretion. *The Journal of experimental medicine*, 189(4), pp.747–752.

Hiki, Y. et al., 1999. Underglycosylation of IgA1 hinge plays a certain role for its glomerular deposition in IgA nephropathy. *Journal of the American Society of Nephrology*, 10(4), pp.760–769.

Hudis, C.A., 2007. Trastuzumab — Mechanism of Action and Use in Clinical Practice. *The New England Journal of Medicine*, 357, pp.39–51.

Huls, G. et al., 1999. Antitumor immune effector mechanisms recruited by phage display-derived fully human IgG1 and IgA1 monoclonal antibodies. *Cancer Research*, 59(22), pp.5778–5784.

Ivashkiv, L.B., 2011. How ITAMs inhibit signaling. *Science signaling*, 4(169), pp.20.

Iwata, K. et al., 2014. Stable expression and characterization of monomeric and dimeric recombinant hybrid-IgG/IgA immunoglobulins specific for Shiga toxin. *Biological & pharmaceutical bulletin*, 37(9), pp.1510–1515.

Jaehne, J. et al., 1992. Expression of Her2/neu oncogene product p185 in correlation to clinicopathological and prognostic factors of gastric carcinoma. *Journal of Cancer Research and Clinical Oncology*, 118(6), pp.474–479.

Jefferis, R., 2009. Glycosylation as a strategy to improve antibody-based therapeutics. *Nature reviews. Drug discovery*, 8(3), pp.226–234.

Johansen, F.-E. & Kaetzel, C.S., 2011. Regulation of the polymeric immunoglobulin receptor and IgA transport: new advances in environmental factors that stimulate pIgR expression and its role in mucosal immunity. *Mucosal Immunology*, 4(6), pp.598–602.

Ju, T., Otto, V.I. & Cummings, R.D., 2011. The Tn antigena-structural simplicity and biological complexity. *Angewandte Chemie - International Edition*, 50(8), pp.1770–1791.

Juarez, P. et al., 2013. Combinatorial Analysis of Secretory Immunoglobulin A (sIgA) Expression in Plants. *International Journal of Molecular Sciences*, 14(3), pp.6205–6222.

Kalia, M., 2015. Biomarkers for personalized oncology: recent advances and future challenges. *Metabolism: clinical and experimental*, 64(3 Suppl 1), pp.S16–21.

Karapetis, C.S. et al., 2008. K-ras mutations and benefit from cetuximab in advanced colorectal cancer. *The New England journal of medicine*, 359(17), pp.1757–1765.

Karsten, U. et al., 1995. A new monoclonal antibody (A78-G/A7) to the Thomsen-Friedenreich pan-tumor antigen. *Hybridoma*, 14(1), pp.37–44.

Karsten, U. & Goletz, S., 2013. What makes cancer stem cell markers different? *SpringerPlus*, 2(1), p.301.

Kawabe, Y. et al., 2012. Repeated integration of antibody genes into a pre-selected chromosomal locus of CHO cells using an accumulative site-specific gene integration system. *Cytotechnology*, 64(3), pp.267–279.

Keler, T. et al., 2000. Differential effect of cytokine treatment on Fc alpha receptor I- and Fc gamma receptor I-mediated tumor cytotoxicity by monocyte-derived macrophages. *The Journal of Immunology*, 164(11), pp.5746–5752.

Kelton, W. et al., 2014. IgGA: A "Cross-Isotype" Engineered Human Fc Antibody Domain that Displays Both IgG-like and IgA-like Effector Functions. *Chemistry & Biology*, 21(12), pp.1603–1609.

Kerr, M.A., 1990. The structure and function of human IgA. *Human cell official journal of Human Cell Research Society*, 271(2), pp.285–296.

Khambata-Ford, S. et al., 2007. Expression of epiregulin and amphiregulin and K-ras mutation status predict disease control in metastatic colorectal cancer patients treated with cetuximab. *Journal of Clinical Oncology*, 25(22), pp.3230–3237.

Köhler, G. & Milstein, C., 1975. Continuous cultures of fused cells secreting antibody of predefined specificity. *Nature*, 256(5517), pp.495–497.

Kokubo, T. et al., 1997. Evidence for involvement of IgA1 hinge glycopeptide in the IgA1-IgA1 interaction in IgA nephropathy. *Journal of the American Society of Nephrology : JASN*, 8(6), pp.915–9.

Kondoh, H. et al., 1986. Jacalin, a jackfruit lectin, precipitates IgA1 but not IgA2 subclass on gel diffusion reaction. *Journal of immunological methods*, 88(2), pp.171–173.

Krawczyk, P.A. & Kowalski, D.M., 2014. Review Genetic and immune factors underlying the efficacy of cetuximab and panitumumab in the treatment of patients with metastatic colorectal cancer. *Współczesna Onkologia*, 1(1), pp.7–16.

Krugmann, S. et al., 1997. Structural requirements for assembly of dimeric IgA probed by site-directed mutagenesis of J chain and a cysteine residue of the alpha-chain CH2 domain. *The Journal of Immunology* , 159 (1), pp.244–249.

Lamkhioued, B. et al., 1995. Human eosinophils express a receptor for secretory component. Role in secretory IgA-dependent activation. *European journal of immunology*, 25(1), pp.117–125.

Larrick, J.W. et al., 2001. Production of secretory IgA antibodies in plants. *Biomolecular Engineering*, 18(3), pp.87–94.

Leget, G.A. & Czuczman, M.S., 1998. Use of rituximab, the new FDA-approved antibody. *Current opinion in oncology*, 10(6), pp.548–551.

Lemmon, M. a, Schlessinger, J. & Ferguson, K.M., 2014. The EGFR Family: Not So Prototypical Receptor Tyrosine Kinases. *Cold Spring Harbor Perspectives in Biology*, 6(4), pp.a020768–a020768.

Lewis, C.E. et al., 1995. Cytokine regulation of angiogenesis in breast cancer: the role of tumor-associated macrophages. *Journal of leukocyte biology*, 57(5), pp.747–751.

Lim, S.H. et al., 2010. Anti-CD20 monoclonal antibodies: Historical and future perspectives. *Haematologica*, 95(1), pp.135–143.

Lipscomb, M.L. et al., 2008. Effect of Production Method and Gene Amplification on the Glycosylation Pattern of a Secreted Reporter Protein in CHO Cells. *Biotechnology Progress*, 21(1), pp.40–49.

Lohse, S. et al., 2016. An Anti-EGFR IgA That Displays Improved Pharmacokinetics and Myeloid Effector Cell Engagement In Vivo. *Cancer Research*, 76(2), pp.403–417.

Lohse, S. et al., 2012. Characterization of a mutated IgA2 antibody of the m(1) allotype against the epidermal growth factor receptor for the recruitment of monocytes and macrophages. *Journal of Biological Chemistry*, 287(30), pp.25139–25150.

Lohse, S. et al., 2011. Recombinant Dimeric IgA Antibodies against the Epidermal Growth Factor Receptor Mediate Effective Tumor Cell Killing. *The Journal of Immunology*, 186(6), pp.3770–3778.

Loupakis, F. et al., 2009. PTEN expression and KRAS mutations on primary tumors and metastases in the prediction of benefit from cetuximab plus irinotecan for patients with metastatic colorectal cancer. *Journal of Clinical Oncology*, 27(16), pp.2622–2629.

Lycke, N., 2012. Recent progress in mucosal vaccine development: potential and limitations. *Nature Reviews Immunology*, 12(8), pp.592–605.

Majumdar, S. et al., 1991. Protein kinase C isotypes and signaling in neutrophils. Differential substrate specificities of a translocatable calcium-and phospholipid-dependent beta-protein kinase. *Journal of Biological Chemistry*, 266(14), pp.9285–9294.

Mall, A.S., 2008. Analysis of mucins: role in laboratory diagnosis. *Journal of clinical pathology*, 61(9), pp.1018–1024.

Mantis, N.J. et al., 2002. Selective adherence of IgA to murine Peyer's patch M cells: evidence for a novel IgA receptor. *Journal of immunology (Baltimore, Md. : 1950)*, 169(4), pp.1844–1851.

Mantis, N.J., Rol, N. & Corthésy, B., 2011. Secretory IgA's complex roles in immunity and mucosal homeostasis in the gut. *Mucosal Immunology*, 4(6), pp.603–611.

Mattu, T.S. et al., 1998. The glycosylation and structure of human serum IgA1, Fab, and Fc regions and the role of N-glycosylation on Fc alpha receptor interactions. *Journal of Biological Chemistry*, 273(4), pp.2260–2272.

Meyer, S. et al., 2015. Improved in vivo anti-tumor effects of IgA-Her2 antibodies through half-life extension and serum exposure enhancement by FcRn targeting. *mAbs*, 0862(December), pp.1–12.

Ben Mkaddem, S. et al., 2013. Anti-inflammatory role of the IgA Fc receptor (CD89): From autoimmunity to therapeutic perspectives. *Autoimmunity Reviews*, 12(6), pp.666–669.

Moldt, B. et al., 2014. Simplifying the synthesis of SIgA: Combination of dIgA and rhSC using affinity chromatography. *Methods*, 65(1), pp.127–132.

Monteiro, R.C., Cooper, M.D. & Kubagawa, H., 1992. Molecular heterogeneity of Fc alpha receptors detected by receptor-specific monoclonal antibodies. *Journal of immunology (Baltimore, Md. : 1950)*, 148(6), pp.1764–1770.

Monteiro, R.C., Kubagawa, H. & Cooper, M.D., 1990. Cellular distribution, regulation, and biochemical nature of an Fc alpha receptor in humans. *The Journal of experimental medicine*, 171(3), pp.597–613.

Monteiro, R.C. & Van De Winkel, J.G.J., 2003. IgA Fc receptors. *Annual review of immunology*, 21, pp.177–204.

Morton, H.C. et al., 1993. Purification and characterization of chimeric human IgA1 and IgA2 expressed in COS and Chinese hamster ovary cells. *The Journal of Immunology*, 151(9), pp.4743–4752.

Morton, H.C. & Brandtzaeg, P., 2001. CD89: the human myeloid IgA Fc receptor. *Archivum immunologiae et therapiae experimentalis*, 49(3), pp.217–229.

Mossner, E. et al., 2010. Increasing the efficacy of CD20 antibody therapy through the engineering of a new type II anti-CD20 antibody with enhanced direct and immune effector cell-mediated B-cell cytotoxicity. *Blood*, 115(22), pp.4393–4402.

Mostov, K.E., 1994. Transepithelial Transport of Immunoglobulins. *Annual Review of Immunology*, 12(1), pp.63–84.

Moura, I.C. et al., 2001. Identification of the transferrin receptor as a novel immunoglobulin (Ig)A1 receptor and its enhanced expression on mesangial cells in IgA nephropathy. *The Journal of experimental medicine*, 194(4), pp.417–425.

Mukherjee, P. et al., 2001. MUC1-specific CTLs are non-functional within a pancreatic tumor microenvironment. *Glycoconjugate Journal*, 18(11-12), pp.931–942.

Muramatsu, M. et al., 2014. Comparison of Antiviral Activity between IgA and IgG Specific to Influenza Virus Hemagglutinin: Increased Potential of IgA for Heterosubtypic Immunity G. P. Kobinger, ed. *PLoS ONE*, 9(1), p.e85582.

Murphy, K.M., 2011. *Janeway's Immunobiology*, Garland Science.

Narimatsu, Y. et al., 2010. Effect of glycosylation on cis/trans isomerization of prolines in IgA1-hinge peptide. *Journal of the American Chemical Society*, 132(16), pp.5548–5549.

Narita, I. et al., 2001. Genetic polymorphisms in the promoter and 5' UTR region of the Fc alpha receptor (CD89) are not associated with a risk of IgA nephropathy. *Journal of Human Genetics*, 46(12), pp.694–698.

Nath, S. & Mukherjee, P., 2014. MUC1: A multifaceted oncoprotein with a key role in cancer progression. *Trends in Molecular Medicine*, 20(6), pp.332–342.

Niederfellner, G. et al., 2011. Epitope characterization and crystal structure of GA101 provide insights into the molecular basis for type I/II distinction of CD20 antibodies. *Blood*, 118(2), pp.358–367.

Nilson, B.H.K. et al., 1992. Protein L from Peptostreptococcus magnus binds to the κ light chain variable domain. *Journal of Biological Chemistry*, 267(4), pp.2234–2239.

Nimmerjahn, F. & Ravetch, J. V., 2006. Fcγ receptors: Old friends and new family members. *Immunity*, 24(1), pp.19–28.

Nirenberg, M.W. & Matthaei, J.H., 1961. The dependence of cell-free protein synthesis in E. coli upon naturally occurring or synthetic polyribonucleotides. *Proceedings of the National Academy of Sciences of the United States of America*, 47(10), pp.1588–1602.

Nishie, A. et al., 1999. Macrophage Infiltration and Heme Oxygenase-1 Expression Correlate with Angiogenesis in Human Gliomas. *Clinical Cancer Research* , 5 (5), pp.1107–1113.

Novak, J. et al., 2001. Heterogeneity of O-glycosylation in the hinge region of human IgA1. *Molecular Immunology*, 37(17), pp.1047–1056.

Odani, H. et al., 2000. Direct evidence for decreased sialylation and galactosylation of human serum IgA1 Fc O-glycosylated hinge peptides in IgA nephropathy by mass spectrometry. *Biochemical and biophysical research communications*, 271(1), pp.268–274.

Oortwijn, B.D. et al., 2006. Differential glycosylation of polymeric and monomeric IgA: a possible role in glomerular inflammation in IgA nephropathy. *Journal of the American Society of Nephrology : JASN*, 17(12), pp.3529–3539.

Otten, M. a et al., 2005. Immature neutrophils mediate tumor cell killing via IgA but not IgG Fc receptors. *Journal of immunology (Baltimore, Md. : 1950)*, 174(9), pp.5472–5480.

Pabst, O., 2012. New concepts in the generation and functions of IgA. *Nature Reviews Immunology*, 12(12), pp.821-832.

Pascal, V. et al., 2012. Anti-CD20 IgA can protect mice against lymphoma development: evaluation of the direct impact of IgA and cytotoxic effector recruitment on CD20 target cells. *Haematologica*, 97(11), pp.1686–1694.

Patel, D. et al., 2007. Monoclonal antibody cetuximab binds to and down-regulates constitutively activated epidermal growth factor receptor vIII on the cell surface. *Anticancer Research*, 27(5 A), pp.3355–3366.

Pedrali-Noy, G. et al., 1982. Inhibition of DNA replication and growth of several human and murine neoplastic cells by aphidicolin without detectable effect upon synthesis of immunoglobulins and HLA antigens. *Cancer research*, 42(9), pp.3810–3.

Peipp, M., Dechant, M. & Valerius, T., 2009. Sensitivity and resistance to EGF-R inhibitors: Approaches to enhance the efficacy of EGF-R antibodies. *mAbs*, 1(6), pp.590–599.

Pfirsch-Maisonnas, S. et al., 2011. Inhibitory ITAM signaling traps activating receptors with the phosphatase SHP-1 to form polarized “inhibisome” clusters. *Science signaling*, 4(169), p.ra24.

Phillips, G.D.L. et al., 2014. Dual targeting of HER2-positive cancer with trastuzumab emtansine and pertuzumab: Critical role for neuregulin blockade in antitumor response to combination therapy. *Clinical Cancer Research*, 20(2), pp.456–468.

Pirker, R. et al., 2012. EGFR expression as a predictor of survival for first-line chemotherapy plus cetuximab in patients with advanced non-small-cell lung cancer: analysis of data from the phase 3 FLEX study. *The Lancet Oncology*, 13(1), pp.33–42.

Piscano, a et al., 1993. Glycosylation sites identified by solid-phase Edman degradation: O-linked glycosylation motifs on human glycophorin A. *Glycobiology*, 3(5), pp.429–435.

Pleass, R.J. et al., 1999. Identification of Residues in the CH2/CH3 Domain Interface of IgA Essential for Interaction with the Human Fc Receptor (Fc R) CD89. *Journal of Biological Chemistry*, 274(33), pp.23508–23514.

Pleass, R.J. et al., 2003. Limited role of charge matching in the interaction of human immunoglobulin A with the immunoglobulin A Fc receptor (Fc alpha RI) CD89. *Immunology*, 109(3), pp.331–5.

Polyak, M.J. & Deans, J.P., 2002. Alanine-170 and proline-172 are critical determinants for extracellular CD20 epitopes; heterogeneity in the fine specificity of CD20 monoclonal antibodies is defined by additional requirements imposed by both amino acid sequence and quaternary structure. *Blood*, 99(9), pp.3256–3262.

Pouria, S. et al., 2004. Glycoform composition profiling of O-glycopeptides derived from human serum IgA1 by matrix-assisted laser desorption ionization-time of flight-mass spectrometry. *Analytical Biochemistry*, 330(2), pp.257–263.

Ravetch, J. V, 1997. Fc receptors. *Current Opinion in Immunology*, 9(1), pp.121–125.

Reinhart, D., Weik, R. & Kunert, R., 2012. Recombinant IgA production: Single step affinity purification using camelid ligands and product characterization. *Journal of Immunological Methods*, 378(1-2), pp.95–101.

Reth, M., 1992. Antigen receptors on B lymphocytes. *Annual review of immunology*, 10, pp.97–121.

Rifai, a et al., 2000. The N-glycans determine the differential blood clearance and hepatic uptake of human immunoglobulin (Ig)A1 and IgA2 isotypes. *The Journal of experimental medicine*, 191(12), pp.2171–2182.

Rochereau, N. et al., 2013. Dectin-1 Is Essential for Reverse Transcytosis of Glycosylated SIgA-Antigen Complexes by Intestinal M Cells. *PLoS Biology*, 11(9), p.e1001658.

Roock, W. De et al., 2011. KRAS, BRAF, PIK3CA, and PTEN mutations: implications for targeted therapies in metastatic colorectal cancer. *The Lancet Oncology*, 12(6), pp.594–603.

Roque-Barreira, M.C. & Campos-Neto, a, 1985. Jacalin: an IgA-binding lectin. *Journal of immunology (Baltimore, Md. : 1950)*, 134(3), pp.1740–1743.

Rous, P., 1911. A Sarcoma of the Fowl Transmissible By an Agent Separable From the Tumor Cells. *The Journal of experimental medicine*, 13(4), pp.397–411.

Rouwendal, G.J. et al., 2016. A comparison of anti-HER2 IgA and IgG1 in vivo efficacy is facilitated by high N-glycan sialylation of the IgA. *mAbs*, 8(1), pp.74–86.

Royle, L. et al., 2003. Secretory IgA N- and O-glycans provide a link between the innate and adaptive immune systems. *Journal of Biological Chemistry*, 278(22), pp.20140–20153.

Rudd, P.M. et al., 1994. A human T-cell receptor recognizes “O”-linked sugars from the hinge region of human IgA1 and IgD. *Immunology*, 83(1), pp.99–106.

Sakamoto, N. et al., 2001. A novel Fc receptor for IgA and IgM is expressed on both hematopoietic and non-hematopoietic tissues. *European Journal of Immunology*, 31(5), pp.1310–1316.

Sambrook, J. & Russell, D.W., 2001. *Molecular Cloning: A Laboratory Manual, Volume 1*, CSHL Press.

Schlessinger, J., 2002. Ligand-induced, receptor-mediated dimerization and activation of EGF receptor. *Cell*, 110(6), pp.669–672.

Schmid, M.C. & Varner, J. a., 2010. Myeloid Cells in the Tumor Microenvironment: Modulation of Tumor Angiogenesis and Tumor Inflammation. *Journal of Oncology*, 2010, pp.1–10.

Schroeder, J. a et al., 2003. MUC1 alters beta-catenin-dependent tumor formation and promotes cellular invasion. *Oncogene*, 22(9), pp.1324–1332.

Scott, A.M., Allison, J.P. & Wolchok, J.D., 2012. Monoclonal antibodies in cancer therapy. *Cancer immunity*, 12, p.14.

Scott, A.M., Wolchok, J.D. & Old, L.J., 2012. Antibody therapy of cancer. *Nature Reviews Cancer*, 12(4), pp.278–287.

Shi, J. et al., 2011. The generation and evaluation of recombinant human IgA specific for Plasmodium falciparum merozoite surface protein 1-19 (PfMSP119). *BMC Biotechnology*, 11(1), p.77.

Shi, J., Mcintosh, R.S. & Pleass, R.J., 2006. Antibody- and Fc-receptor-based therapeutics for malaria. *Clinical Science*, 110(1), pp.11–19.

Shibuya, a et al., 2000. Fc alpha/mu receptor mediates endocytosis of IgM-coated microbes. *Nature immunology*, 1(5), pp.441–446.

Sijtsema, N.M. et al., 2000. Intracellular reactions in single human granulocytes upon phorbol myristate acetate activation using confocal Raman microspectroscopy. *Biophysical journal*, 78(5), pp.2606–2613.

Slamon, D.J. et al., 1987. Human breast cancer: correlation of relapse and survival with amplification of the HER-2/neu oncogene. *Science (New York, N.Y.)*, 235(4785), pp.177–182.

Smith, H.O. & Welcox, K.W., 1970. A Restriction enzyme from Hemophilus influenzae. *Journal of Molecular Biology*, 51(2), pp.379–391.

Springer, G.F., 1984. T and Tn, general carcinoma autoantigens. *Science (New York, N.Y.)*, 224(4654), pp.1198–206.

Springer, G.F. & Desai, P.R., 1975. Increase in anti-T titer scores of breast-carcinoma patients following mastectomy. *Die Naturwissenschaften*, 62(12), p.587.

Staff, C. et al., 2012. Induction of IgM, IgA and IgE Antibodies in Colorectal Cancer Patients Vaccinated with a Recombinant CEA Protein. *Journal of Clinical Immunology*, 32(4), pp.855–865.

Stockert, R.J. et al., 1982. IgA interaction with the asialoglycoprotein receptor. *Proceedings of the National Academy of Sciences of the United States of America*, 79(20), pp.6229–6231.

Stockmeyer, B. et al., 2000. Triggering Fc alpha-receptor I (CD89) recruits neutrophils as effector cells for CD20-directed antibody therapy. *Journal of immunology (Baltimore, Md. : 1950)*, 165, pp.5954–5961.

Sutherland, D.B. & Fagarasan, S., 2012. IgA synthesis: A form of functional immune adaptation extending beyond gut. *Current Opinion in Immunology*, 24(3), pp.261–268.

Swenson, C.D. et al., 1998. Human T cell IgD receptors react with O-glycans on both human IgD and IgA1. *European Journal of Immunology*, 28(8), pp.2366–2372.

Tanaka, T., Hishitani, Y. & Ogata, A., 2014. Monoclonal antibodies in rheumatoid arthritis: comparative effectiveness of tocilizumab with tumor necrosis factor inhibitors. *Biologics: Targets and Therapy*, 8, p.141.

Tanikawa, T. et al., 2008. Characterization of Monoclonal Immunoglobulin A and G Against Shiga Toxin Binding Subunits Produced by Intranasal Immunization. *Scandinavian Journal of Immunology*, 68(4), pp.414–422.

Tedder, T.F. & Engel, P., 1994. CD20: A regulator of cell-cycle progression of B lymphocytes. *Immunology Today*, 15(9), pp.450–454.

Thie, H. et al., 2011. Rise and fall of an anti-MUC1 specific antibody. *PLoS ONE*, 6(1), pp.e15921.

Tomasi, T.B. et al., 1965. Characteristics of an Immune System Common To Certain External Secretions. *The Journal of experimental medicine*, 121, pp.101–124.

Trivedi, S. et al., 2014. Immune biomarkers of anti-EGFR monoclonal antibody therapy. *Ann. Oncol.*, pp.1–8.

Umaña, P. et al., 1999. Engineered glycoforms of an antineuroblastoma IgG1 with optimized antibody-dependent cellular cytotoxic activity. *Nature biotechnology*, 17(2), pp.176–180.

Vagelpohl, U., 2014. *Galeni In Hippocratis Epidemiarum librum I commentariorum I-III versio Arabica*, De Gruyter.

Valerius, T. et al., 1997. FcalphaRI (CD89) as a novel trigger molecule for bispecific antibody therapy. *Blood*, 90(11), pp.4485–4492.

Varki, A. et al., 2009. *Essentials of Glycobiology*, Cold Spring Harbor Laboratory Press.

Virchow, R.L.K., 1863. *Cellular pathology as based upon physiological and pathological histology ... / by Rudolf Virchow. Translated from the 2d ed. of the original by Frank Chance. With notes and numerous emendations, principally from MS. notes of the author*, Philadelphia: J. B. Lippincott.

Walsh, G., 2014. Biopharmaceutical benchmarks 2014. *Nature biotechnology*, 32(10), pp.992–1000.

Watson, J. & Crick, F.H.F., 1953. Molecular structure of nucleic acids. *Nature*, 171(4356), pp.737–8.

Weiner, L.M., Surana, R. & Wang, S., 2010. Monoclonal antibodies: versatile platforms for cancer immunotherapy. *Nature reviews. Immunology*, 10(5), pp.317–327.

Welinder, C. et al., 2013. Primary Breast Cancer Tumours Contain High Amounts of IgA1 Immunoglobulin: An Immunohistochemical Analysis of a Possible Carrier of the Tumour-Associated Tn Antigen. *PLoS ONE*, 8(4), p.e61749.

Wilkins, M.H.F., Stokes, A.R. & Wilson, H.R., 1953. Molecular structure of deoxypentose nucleic acids. *Nature*, 171(4356), pp.738–740.

Willrich, M.A.V., Murray, D.L. & Snyder, M.R., 2015. Tumor necrosis factor inhibitors: clinical utility in autoimmune diseases. *Translational Research*, 165(2), pp.270–282.

Wines, B.D. et al., 1999. Identification of residues in the first domain of human Fc alpha receptor essential for interaction with IgA. *The Journal of Immunology*, 162(4), pp.2146–2153.

Wolbank, S. et al., 2003. Characterization of Human Class-Switched Polymeric Immunoglobulin M [IgM] and IgA Anti-Human Immunodeficiency Virus Type 1 Antibodies 2F5 and 2G12. *Journal of Virology*, 77(7), pp.4095–4103.

Woof, J.M., 2002. The human IgA-Fc α receptor interaction and its blockade by streptococcal IgA-binding proteins. *Biochemical Society Transactions*, 30(4), pp.491–494.

Woof, J.M. & Burton, D.R., 2004. Human antibody-Fc receptor interactions illuminated by crystal structures. *Nature reviews. Immunology*, 4(2), pp.89–99.

Woof, J.M. & Kerr, M. a., 2004. IgA function - Variations on a theme. *Immunology*, 113(2), pp.175–177.

Woof, J.M. & Kerr, M.A., 2006. The function of immunoglobulin A in immunity. *Journal of Pathology*, 208(2), pp.270–282.

Woof, J.M. & Russell, M.W., 2011. Structure and function relationships in IgA. *Mucosal Immunology*, 4(6), pp.590–597.

Wu, J. et al., 2007. FcalphaRI (CD89) alleles determine the proinflammatory potential of serum IgA. *The Journal of Immunology*, 178, pp.3973–3982.

Xue, J. et al., 2010. Deglycosylation of FcαR at N58 increases its binding to IgA. *Glycobiology*, 20(7), pp.905–915.

Xue, J., Zhu, L.P. & Wei, Q., 2013. IgG-Fc N-glycosylation at Asn297 and IgA O-glycosylation in the hinge region in health and disease. *Glycoconjugate Journal*, 30(8), pp.735–745.

Yarden, Y., 2001. The EGFR family and its ligands in human cancer. signalling mechanisms and therapeutic opportunities. *European journal of cancer*, 37 Suppl 4, pp.S3–S8.

Yarden, Y. & Sliwkowski, M.X., 2001. Untangling the ErbB signalling network. *Nature Reviews. Molecular Cell Biology*, 2(2), pp.127–137.

Yoo, E.M. et al., 2010. Differences in N-glycan structures found on recombinant IgA1 and IgA2 produced in murine myeloma and CHO cell lines. *MAbs*, 2(3), pp.320–334.

Yoshikawa, T. et al., 2000. Amplified Gene Location in Chromosomal DNA Affected Recombinant Protein Production and Stability of Amplified Genes. *Biotechnology Progress*, 16(5), pp.710–715.

Yu, L.G., 2007. The oncofetal Thomsen-Friedenreich carbohydrate antigen in cancer progression. *Glycoconjugate Journal*, 24(8), pp.411–420.

Yuasa, N. et al., 2013. Expression and structural characterization of anti-T-antigen single-chain antibodies (scFvs) and analysis of their binding to T-antigen by surface plasmon resonance and NMR spectroscopy. *Journal of Biochemistry*, 154(6), pp.521–529.

Van Zandbergen, G. et al., 1999. Crosslinking of the human Fc receptor for IgA (FcalphaRI/CD89) triggers FcR gamma-chain-dependent shedding of soluble CD89. *Journal of Immunology*, 163(11), pp.5806–5812.

Zhang, W. et al., 2007. FCGR2A and FCGR3A Polymorphisms Associated With Clinical Outcome of Epidermal Growth Factor Receptor Expressing Metastatic Colorectal Cancer Patients Treated With Single-Agent Cetuximab. *Journal of Clinical Oncology*, 25(24), pp.3712–3718.

8 Curriculum Vitae

For reasons of data protection, the curriculum vitae is not published in the electronic version.

9 Annex

9.1 List of abbreviations

aa	amino acid(s)
ADCC	antibody-dependent cellular cytotoxicity
ADCP	antibody-dependent cellular phagocytosis
AGP	asialoglycophorin
ASGP-R	asialoglycoprotein receptor
Asn	asparagine
bp	base pair
CD	cluster of differentiation
CDC	complement-dependent cytotoxicity
CDR	complementary-determining region
CHO	chinese hamster ovary
CID	collision-induced dissociation
CM	cetuximab
Cys	cysteine
d	day(s)
DLS	dynamic light scattering
DNA	deoxyribonucleic acid
EGF	epidermal growth factor
EGFR	epidermal growth factor receptor ErbB1
ELISA	enzyme-linked immunosorbent assay
ESI-qTOF	electrospray ionization-quadrupole time-of-flight mass spectrometry
Fab	fragment antigen binding
FBS	fetal bovine serum
Fc	fragment crystallizable
FcR	Fc receptor
FcRn	neonatal Fc receptor
FcαRI	Fc alpha receptor I or CD89
FcγR	Fc gamma receptor
FPLC	fast protein liquid chromatography
Fuc	fucose
Fv	Fab variable fragment
Gal	galactose
GalNAc	N-acetylgalactoseamine

GALT	gut-associated lymphoid tissue
GEX	GlycoExpress
GlcNAc	N-acetylglucosamine
Gly	glycine
HC	heavy chain
Her2	epidermal growth factor receptor ErbB2
HILIC	hydrophilic interaction liquid chromatography
hKM	KaroMab
hOM	obinutuzumab
hPM	PankoMab
hTM	trastuzumab
Ig	immunoglobulin
ITAM	immunoreceptor tyrosine-based activation motifs
ITAMi	inhibitory immunoreceptor tyrosine-based activation motifs
J chain	joining chain
kDa	kilo Dalton
LB	Luria-Bertani broth
LC	light chain
LP	lamina propria
M	mol/L
Man	mannose
MWCO	molecular weight cutoff
Neu5Ac	N-acetylneuraminic acid
Neu5Gc	N-glycolylneuraminic acid
pI	isoelectric point
pIgA	polymeric IgA
pIgR	polymeric immunoglobulin receptor
PP	molecular weight marker
RNA	ribonucleic acid
SC	secretory component
SCR	secretory component receptor
SDS-PAGE	sodium dodecyl sulfate polyacrylamide gel electrophoresis
Ser	serine
SIgA	secretory IgA
TF	Thomsen-Friedenreich antigen
Thr	threonine
Tris	tris(hydroxymethyl)aminomethane
UDP	uridine diphosphate

9.2 List of chemicals

Aqua-Poly/Mount	18606	Polysciences (Warrington, USA)
Cytochalasin D	BML-T109-0001	Enzo (Farmingdale, USA)
Easycoll solution	L6145	Biochrom
Enhancement solution	1244-105	PerkinElmer (Waltham, USA)
GelRed Nucleic Acid Stain	41003	Biotrend
Guava ViaCount	4000	Merck Millipore
PBS	1825	Biochrom
Pharm Lyse	555899	BD Biosciences
TAE buffer system	1610743	Bio-Rad (Hercules, USA)
TMB One Component HRP Substrate	TMBS100	Tebu-bio

If not purchased from Biochrom, PBS was prepared as follows: 154 mM sodium chloride, 1.06 mM potassium dihydrogen phosphate, 2.97 mM disodiumhydrogen phosphate, pH 7.4

9.3 Amino acid sequences of generated antibodies

	Uniprot ID/reference
Ig alpha-1 chain C region	P01876
Ig alpha-2 chain C region	P01877
Joining chain	P01591
Ig kappa chain C region	P01834
Ig gamma-1 chain C region	P01857
hPM variable domains	(Danielczyk et al. 2006)
hTM variable domains	www.drugbank.ca (Acession Number DB00072)
CM variable domains	www.drugbank.ca (Acession Number DB00002)
hKM variable domains	(Goletz et al. 2003), humanized Nemod-TF2
hOM variable domains	www.drugbank.ca (Acession Number DB08935)

9.4 Eukaryotic cell lines – media composition, sources and media supplements

Cell lines, media composition	*Source*
A-431, DMEM, 10% FBS, 4 mM L-glutamine	DSMZ no. ACC 91 (Brunswick, Germany)
BT-474, HybriCare, 10% FBS, 2 mM L-glutamine	DSMZ no. ACC 64
GlycoExpess H9D8, Glycotope medium	Glycotope, Berlin, Germany
GlycoExpress Fuc$^-$, Glycotope medium	Glycotope, Berlin, Germany
KG-1, DMEM, 10% FBS, 4 mM L-glutamine	DSMZ no. ACC 14
Ls174T, RPMI 1640, 10% FBS, 2 mM L-glutamine	DSMZ no. ACC 759
Panc-1, DMEM, 10% FBS, 4 mM L-glutamine	DSMZ no. ACC 783
Raji, RPMI 1640, 10% FBS, 2 mM L-glutamine	DSMZ no. ACC 319
SK-BR-3, McCoy's 5A, 10% FBS	Cell Line Service No 300333
T47D, RPMI 1640, 10% FBS, 2 mM L-glutamine	ECACC No 85102201
ZR-75-1, RPMI 1640, 10% FBS, 2 mM L-glutamine	ATCC No CRL 1500

Media, supplements and additives

Accutase	L11-007, GE Healthcare (Little Chalfont, UK)
Dulbecco's MEM (DMEM)	F0415, Biochrom (Berlin, Germany)
Fetal Bovine Serum (FBS)	S0115, Biochrom
G 418 Sulfate	345812, Merck Millipore (Billerica, USA)
Glycotope medium	custom formulation, Biochrom
HybriCare	50188277FP, Fisher Scientific (Pittsburgh, USA)
L-glutamine, 200 mM	K0283, Biochrom
McCoy's 5A (Modified) Medium	26600, Thermo Fisher Scientific (Waltham, USA)
Methotrexate hydrate	M8407, Sigma-Adrich
Puromycin	631306, Clontech (Mountain View, USA)
RPMI 1640	F1215, Biochrom
Trypsin-EDTA	25200, Thermo Fisher Scientific (Waltham, USA)

9.5 Detailed method description for N-glycan profiling

Enzymatically liberated N-glycans were fluorescently labeld at the reducing end and separated by hydrophilic interaction liquid chromatography with subsequent electrospray ionization-quadrupole time-of-flight mass spectrometry (ESI-qTOF) with collision-induced dissociation (CID) for structure identification.

Two hundred µg of dried antibody were dissolved in 28 µL deionized water. For denaturation of the protein, 8 µL sample buffer (2% (w/v) sodium dodecyl sulfate, 63 mM Tris) and 4 µL 5 M dithiothreitol were added. Subsequent to mixing and incubation at 65 °C for 30 minutes, 4 µL 0.5 M iodoacetamide were added and samples were incubated for 30 minutes at room temperature.

Four aliquots of 11 µL of the sample were pipetted into flat bottom 96-well polypropylene plates. For gel block formation, 22.5 µL ProtoGel (National Diagnostics, cat. no. EC-890), 11.25 µL 1.5 M Tris pH 8.8, 1 µL 10% (w/v) sodium dodecyl sulfate and 2 µL ammonium persulfate were added. Subsequent to mixing, 1 µL tetramethylethylenediamine was added and the plate was incubated at room temperature for 20 minutes. After polymerization, gel blocks were transferred into a 96-well filter plate (VWR, cat. no. 734-1146) which was placed on top of a 2 mL deep well collector plate. Gel blocks were incubated for 10 minutes with 1 mL acetonitrile while shaking the plate. By application of vacuum, this wash solution was transferred into the deep well collector plate and discarded. Next, gel blocks were washed twice according to the same procedure alternating with 1 mL PNGase F buffer (20 mM sodium bicarbonate, pH 7.0) and 1 mL acetonitrile.

The flat bottom 96-well plate was transferred onto a new deep well collector plate and 30 µL enzyme solution (15 µL PNGase F buffer and 15 µL PNGase F in deionized water containing 1 unit/µL PNGaseF) were added per gel block and incubated for 15 minutes at room temperature. Then 100 µL of PNGase F buffer were added and the plate was incubated at 37 °C overnight.

For extraction of the liberated glycans, three times 200 µL deionized water were added followed by addition of 200 µL acetonitrile, 200 µL deionized water and 200 µL acetonitrile. Each solvent addition was followed by shaking for 10 minutes at room temperature and subsequent transfer into the deep well collection plate by vacuum. The whole glycan liberation procedure was repeated three times and filtrates were collected. Aliquots for each sample ware pooled and lyophilized overnight.

Glycans were dissolved in 20 µL 1% (v/v) formic acid and incubated for 40 min at room temperature in order to transform the initially formed 1-amino sugar into the corresponding hydroxyl form. This rearrangement of the reducing end is essential for the following labeling reaction.

Glycans were fluorescently labeled using the LudgerTag 2-AB (2-aminobenzamide) Glycan Labeling Kit (Ludger, cat. no. LT-KAB-A2) and LudgerClean S Glycan Cleanup Cartridges (Ludger, cat LC-S-A6) according to the manufacturer's instructions. Labeled and cleaned glycans were stored at -20 °C until analysis.

Samples derived from 50 µg antibody were dissolved in 100 mM ammonium formate/acetonitrile 40/60% (v/v) and subsequently injected on an ACQUITY UPLC Glycan BEH Amide Column, 130Å, 1.7 µm, 2.1 mm x 100 mm (Waters, cat. no. 186004741; Milford, USA) using an Acquity UPLC (Waters) instrument coupled to ESI-qTOF with CID on an Impact HD45 instrument (Bruker; Billerica, USA). A linear gradient form 22% to 44% eluent A (100 mM aqueous ammonium formate buffer, pH 4.5) was run within 54 minutes at a flow rate of 0.5 mL/min and the column temperature was set to 60 °C. Eluent B was acetonitrile. For fluorescence detection, excitation and emission wavelength were 330 nm and 420 nm, respectively. Glycan structures of each peak were identified by a combination of MS and CID fragmentation data using the Compass DataAnalysis software 4.3 (Bruker). Quantification was based on fluorescence signals using the Empower 3 software (Waters). In case of co-eluting compounds, quantification was based on relative abundances of MS signals.